

2005

# Experimental investigation of dynamic interfacial interactions at reservoir conditions

Wei Xu

*Louisiana State University and Agricultural and Mechanical College, wxu4@lsu.edu*

Follow this and additional works at: [https://digitalcommons.lsu.edu/gradschool\\_theses](https://digitalcommons.lsu.edu/gradschool_theses)



Part of the [Petroleum Engineering Commons](#)

---

## Recommended Citation

Xu, Wei, "Experimental investigation of dynamic interfacial interactions at reservoir conditions" (2005). *LSU Master's Theses*. 968.  
[https://digitalcommons.lsu.edu/gradschool\\_theses/968](https://digitalcommons.lsu.edu/gradschool_theses/968)

This Thesis is brought to you for free and open access by the Graduate School at LSU Digital Commons. It has been accepted for inclusion in LSU Master's Theses by an authorized graduate school editor of LSU Digital Commons. For more information, please contact [gradetd@lsu.edu](mailto:gradetd@lsu.edu).

**EXPERIMENTAL INVESTIGATION OF DYNAMIC INTERFACIAL  
INTERACTIONS AT RESERVOIR CONDITIONS**

A Thesis

Submitted to the Graduate Faculty of the  
Louisiana State University and  
Agricultural and Mechanical College  
In partial fulfillment of the  
requirements for the degree of  
Master of Science in Petroleum Engineering

in

The Craft and Hawkins Department of Petroleum Engineering

by

Wei Xu

B.S in Petroleum Geology, University of Petroleum, East China, June 1993

M.S in Petroleum Geology& Exploration, University of Petroleum, China, June 1996

May 2005

## **DEDICATION**

This work is dedicated to my wife, Min Zhang, and my beloved family ...

## **ACKNOWLEDGEMENTS**

I am deeply indebted to my esteemed professor Dr. Dandina N. Rao for his able guidance, encouragement and support throughout this work. I am also thankful to Dr. Julius P. Langlinais and Dr. Christopher D. White who served as members on the examination committee.

The financial support of this project from the Louisiana Board of Regents through the fund contract LEQSF (2000-03-RD-B-06) and Marathon Oil Company is greatly appreciated. I sincerely thank the Department of Petroleum Engineering, LSU, for the partial research assistantship.

I am grateful to Dr. Ed Overton, Dr. Roberto L. Wong, Mr. Scott Miles and Ms. Buffy M. Ashton, Department of Environmental Studies, LSU, for their help in using rotary evaporator and de-asphalting procedures. I would like to thank Ms. Min Zhang, Electrical Engineering (LSU), for her help in using SEM at CAMD (LSU) for characterizing the roughness of rock samples, Madhav Kulkarni and Daryl Sequeira, Petroleum Engineering, for preparing live crude oil, and all the people who once worked on the fabrication and assembly of High-Pressure-High-Temperature Dual-Drop-Dual-Crystal Optical System.

I would also like to specially thank Subhash C. Ayirala for his valuable help during this study, Lynne Adrienne Estrada for her help on manuscripts.

I would like to express my sincere thanks to all the faculty members and graduate students in the Department of Petroleum Engineering for their constant encouragement and help in every possible way. My heartfelt thanks to my family and all my friends for their spiritual support to finish this project.

## TABLE OF CONTENTS

DEDICATION .....	ii
ACKNOWLEDGEMENTS .....	iii
LIST OF TABLES .....	vi
LIST OF FIGURES .....	vii
NOMENCLATURE .....	x
ABSTRACT .....	xi
CHAPTER 1. INTRODUCTION AND OBJECTIVES.....	1
CHAPTER 2. LITERATURE REVIEW .....	4
2.1 Interfacial Tension Measurements .....	4
2.1.1 Wilhelmy Plate Technique .....	5
2.1.2 Du Nouy Ring Method .....	6
2.1.3 Measurement of Capillary Pressure .....	6
2.1.4 Analysis of the Balance Between Capillary and Gravity Forces.....	7
2.1.5 Spinning Drop Technique.....	8
2.1.6 Analysis of Gravity-Distorted Drops.....	8
2.1.7 Drop Shape Analysis Method.....	8
2.2 Dynamic Interfacial Tension.....	10
2.2.1 Numerical Models.....	11
2.2.2 Experimental Models.....	13
2.2.3 Effects of Temperature and Pressure on Interfacial Tension .....	17
2.3 Wettability and Contact Angles.....	18
2.3.1 Definition.....	18
2.3.2 Dynamic Contact Angles.....	19
2.3.3 Contact Angle Measurements.....	20
2.3.4 Effects of Temperature and Pressure.....	21
2.3.5 Effects of Crude Oil Composition.....	22
2.3.6 Effects of Brine Composition.....	24
2.3.7 Summary.....	25
2.4 Surfactants.....	26
2.4.1 Surfactant Types.....	27
2.4.2 Surfactant-induced wettability alteration.....	28
CHAPTER 3. EXPERIMENTAL APPRATUS AND PROCEDURES.....	30
3.1 High-Pressure High-Temperature Dual-Drop-Dual-Crystal Apparatus .....	30
3.2 Ambient Dual-Drop-Dual-Crystal Apparatus .....	30
3.3 DSA Technique and Dynamic IFT Measurement Procedure.....	32

3.4 DDDC Contact Angle Measurement Procedure.....	33
3.5 Surfactant-Injection Simulation Procedure.....	33
3.6. Other Miscellaneous Procedures.....	35
CHPATER 4. RESULTS AND DISCUSSIONS .....	38
4.1 Dynamic Interfacial Tension in Crude Oil – Brine System .....	38
4.1.1 Effect of Crude Oil Composition .....	39
4.1.2 Effect of Brine Composition .....	43
4.1.3 Effect of Temperature and Pressure .....	46
4.1.4 Effect of Surfactant .....	49
4.1.5 Dynamic IFT Model of Crude Oil.....	51
4.2 Wettability and Dynamic Contact Angles.....	56
4.2.1 Effect of Rock Characteristics .....	56
4.2.2 Effect of Brine Composition .....	59
4.2.3 Effect of Crude Oil Composition.....	61
4.2.4 Effect of Pressure and Temperature.....	62
4.2.5 Wettability of Subsurface Reservoir.....	64
4.3 Surfactant Injection.....	66
4.3.1 Stocktank Oil at Reservoir Conditions.....	66
4.3.2 Live oil at Reservoir Conditions.....	74
4.3.3 Surfactant-induced Wettability Alteration Mechanism.....	80
4.4 Enhanced Oil Recovery.....	84
CHAPTER 5. CONCLUSIONS AND DISCUSSIONS .....	88
5.1 Summary and Conclusions.....	88
5.2 Recommendations.....	89
REFERENCES.....	91
VITA .....	98

## LIST OF TABLES

1. Accuracy and Suitability of Classical Techniques Used in Interfacial Tension Measurements .....	10
2. Composition and properties of Yates Live Oil .....	36
3. Interfacial Tension of Different Oil Components .....	40
4. Effect of Surfactants on Dynamic Interfacial Tension of Yates Live Oil / Yates Brine at Reservoir Conditions (82°F & 700 psi) .....	51
5. Dynamic Contact Angles of Yates Live Oil at Reservoir Conditions .....	59
6. Dynamic Contact Angles of Different Oil Components at Ambient Conditions ..	61
7. Interfacial Tension and Dynamic Contact Angle Measurements for Yates Stocktank oil / Brine / Dolomite System at Reservoir Conditions (700psi and 82°F) .....	66

## LIST OF FIGURES

1. Classification of Techniques for Interfacial Tension Measurements .....	5
2. Definition of dimensions and coordinates describing the sessile drop .....	9
3. Diffusion-Limited Adsorption of a Variety of Non-ionic Surfactants .....	14
4. Stages of interfacial tension change with time .....	14
5. Dynamic Mathematical Model of Transient IFTs .....	16
6. Contact Angle at Oil/Water/Solid Interfaces .....	18
7. Schematic Representation of the Structure of an Aqueous Micelle .....	28
8. Flowchart of High Pressure High Temperature Dual-Drop Dual-Crystal System at LSU.....	31
9. High Pressure High Temperature Dual-Drop Dual-Crystal System .....	31
10. Ambient Dual-Drop-Dual-Crystal (DDDC) Apparatus at LSU.....	32
11. Schematic Depiction of the New Dual-Drop-Dual-Crystal (DDDC) Contact Angle Technique .....	33
12. Monitoring TPCL Movement .....	34
13. Dynamic Interfacial Tension of Yates Live Oil/Yates Brine at Reservoir Conditions (82°F and 700 psi, over a time period of 10 days) .....	39
14. Dynamic Interfacial Tension of Different Oil Components in Deionized Water at Ambient Conditions using the Ambient Optical Cell.....	41
15. Dynamic Interfacial Tension of Different Oil Components in Yates Brine using HTHP Optical Cell (700psi & 71°F) .....	41
16. Comparison of Time-dependent behavior of Interfacial Tension (Yates Live Oil and Yates Stocktank Oil) .....	43
17. Dynamic Interfacial Tension of Yates Live Oil and Different Brine at Reservoir Conditions (82°F & 700 psi) .....	44
18. Optimal salinity in oil recovery .....	44



19. Effect of brine dilution on Interfacial Tension between Yates Reservoir brine and Yates stocktank oil at Ambient Conditions .....	45
20. Effect of Pressure on Dynamic Interfacial Tension of Yates Live Oil and Yates Brine at 136°F .....	46
21. Influence of Pressure on Interfacial Tension of Yates Live Oil and Yates Brine at 136°F .....	47
22. Effect of Pressure on Dynamic Interfacial Tension of Yates Live Oil and Yates Brine at 74°F .....	47
23. The Effect of Pressure on Interfacial Tension of Yates Live Oil against Yates Brine at 74°F .....	48
24. The Effect of Temperature on Interfacial Tension of Yates Live Oil against Yates Brine at 3000 psi .....	48
25. The Effect of Nonionic Surfactant on Interfacial Tension of Yates Live Oil against Yates Brine at Reservoir Conditions (82°F & 700 psi).....	49
26. The Effect of Anionic Surfactant on Interfacial Tension of Yates Live Oil against Yates Brine at Reservoir Conditions (82°F & 700 psi) .....	50
27. $IFT \sim 1/\sqrt{t}$ (Yates Live Oil against Yates brine at 82°F and 700psi) .....	53
28. Dynamic Interfacial Tension, IFT versus $\sqrt{t}$ (Yates Live Oil against Yates Brine at 82°F and 700 psi) .....	53
29. $F(IFT) \sim \log(t)$ Model(Yates Live Oil against Yates brine, 700psi and 82°F) ....	54
30. Multi-stage Model for Dynamic Interfacial Tension of Yates Live Oil against Yates Brine at Reservoir Conditions .....	54
31. Rock Surface Roughness Analysis Using SEM (Magnified 150 times).....	57
32. DDDC Contact Angle Measurements and Three Phase Contact Line Movement (Yates Stocktank Oil/Brine/Dolomite System Before Surfactant Injection at Reservoir Conditions of 700 psi and 82 °F) .....	67
33. Depiction of Drop Movement During and After Surfactant Injection (Nonionic Surfactant A at 3500 ppm, 700 psi and 82 °F, Yates stocktank oil) .....	68

34. Depiction of Drop Movement During Surfactant Injection (Nonionic Surfactant A at 1000 ppm, 700 psi and 82°F, Yates stocktank oil) .....	69
35. Dynamic Contact Angle Measurements and Three Phase Contact Line Movement in Yates Stocktank Oil/Brine/Dolomite System During 500 ppm Anionic Surfactant B Injection at Reservoir Conditions of 700 psi and 82 °F .....	70
36. Depiction of Drop Movement During and After Surfactant Injection (Anionic Surfactant B at 500 ppm, 700 psi and 82 °F, Yates stocktank oil) .....	71
37. Depiction of Drop Movement During Surfactant Injection (Anionic Surfactant B at 3500 ppm, 700 psi and 82 °F, Yates stocktank oil) .....	72
38. DDDC Contact Angle Measurements and Three Phase Contact Line Movement in Yates Stocktank Oil/Brine/Dolomite System, 16 hours after 500 ppm Anionic Surfactant B Injection at Reservoir Conditions of 700 psi and 82 °F .....	74
39. Depiction of Drop Movement During Surfactant Injection (Nonionic Surfactant A at 500 ppm, 700 psi and 82 °F, Yates Live Oil/Brine/Dolomite) .....	76
40. Depiction of Drop Movement During Surfactant Injection (Nonionic Surfactant A at 1500 ppm, 700 psi and 82 °F, Yates Live oil/Brine/Dolomite) .....	77
41. Depiction of Drop Movement During Surfactant Injection (Nonionic Surfactant A at 3500 ppm, 700 psi and 82 °F, Yates Live oil/Brine/Dolomite) .....	78
42. Depiction of Drop Movement During Surfactant Injection (Anionic Surfactant B at 500 ppm, 700 psi and 82 °F, Yates Live oil/Brine/Dolomite) .....	78
43. Depiction of Dynamic Contact angle at Anionic Surfactant B Solution (900 ppm, 700 psi and 82 °F, Yates Live oil/Brine/Dolomite) .....	79
44. Depiction of Drop Movement During Surfactant Injection (Anionic Surfactant B at 1500 ppm, 700 psi and 82 °F, Yates Live oil/Brine/Dolomite) .....	79
45. Depiction of Drop Movement During Surfactant Injection (Anionic Surfactant B at 500 ppm, 700 psi and 82 °F, Yates Live oil/Brine/Dolomite) .....	80
46. The Effect of Surfactant Concentrations on Water-Advancing Angles (Anionic Surfactant B, Yates Live oil/Brine/Dolomite System, 82°F & 700 psi.) .....	81
47. Schematic representation of the growth of aggregates for various regions of the adsorption isotherm .....	82
48. The Effect of Surfactant Concentrations on Water-Advancing Angles (Nonionic Surfactant A, Yates Live oil/Brine/Dolomite System, 82°F & 700 psi.) .....	83

## NOMENCLATURE

$N_c$  = Capillary number

$v$  = Velocity

$\mu$  = Viscosity

$\sigma$  = Interfacial tension

$\theta$  = Contact angle

$\gamma$  = Surface (Interface) tension

$F$  = Force

$p$  = Perimeter of the three phase contact line

$\Delta P$  = Pressure difference

$\Delta \rho$  = Density difference of two immiscible fluids

$R_1, R_2$  = Principal radii of curvature

$r$  = Inner radius of tube or ring

$W$  = Weight of drop

$V$  = Drop volume

$\omega$  = Rotational velocity

$\Gamma(t)$  = Surface concentration at time  $t$

$\Gamma(t)D$  = Diffusion coefficient

$\gamma_e$  = Surface (Interfacial) tension at equilibrium

$\gamma_t$  = Surface (Interfacial) tension at time  $t$

$\gamma_o$  = First contact surface (Interfacial) tension

$IFT_e$  = Interfacial tension at equilibrium

$IFT_o$  = First contact interfacial tension

$\theta_a$  = Water-advancing contact angle

$\theta_r$  = Water-receding contact angle

$t$  = Time

$S_{o/s}$  = Spreading coefficient

$\sigma_{os}$  = Oil/ Solid interfacial tension

$\sigma_{ow}$  = Oil/water interfacial tension

$\sigma_{ws}$  = Water/solid interfacial tension

## ABSTRACT

Much of the research on wettability in the existing literature has been done using stocktank oils and at ambient conditions. The main objective of this study is therefore to examine the validity of ambient measurements in inferring in-situ reservoir wettability. For this purpose, Drop-Shape-Analysis for interfacial tension and Dual-Drop-Dual-Crystal (DDDC) contact angle measurements have been carried out using dolomite rock, Yates reservoir stocktank and live crude oils and Yates synthetic brine at Yates reservoir conditions of 82° F and 700 psi. Two types of surfactants (nonionic and anionic) in varying concentrations have been used to study the effect of surfactants on wettability alteration in Yates reservoir.

Dynamic behavior of interfacial tension (IFT) of crude oil - brine are mainly caused by the polar components or surfactants in the liquids. The oil composition especially light ends, and brine composition also have effect on it. A four-staged model was adapted from the literature to explain this time-dependent behavior of IFT.

An advancing contact angle of 156° measured for dolomite rock, Yates stocktank oil and Yates synthetic brine in the absence of surfactants showed the strongly oil-wet nature. Experiments with Yates live oil at reservoir conditions indicated weakly water-wet behavior with a water-advancing angle of 55°. For oil-wet stocktank oil system, the anionic surfactant was able to alter wettability from strongly oil-wet (156°) to less oil-wet (135°). No significant wettability alterations were observed with the nonionic surfactant in the stocktank oil containing system. However, for water-wet live oil system, the nonionic surfactant injection altered the wettability to intermediate-wet and the anionic surfactant altered it into strong oil-wet. The oil-wet behavior observed with Yates live oil due to anionic surfactant indicates the ability to this surfactant to form continuous oil-wet paths for mixed-wettability development.

These experiments clearly indicate the need to use live crude oils at reservoir conditions for in-situ reservoir wettability determination. Furthermore, these experiments provided clear evidence that the surfactants used altered wettability to either intermediate-wet or mixed-wet, which could result in potential oil recovery enhancements in field applications.

## CHAPTER 1. INTRODUCTION AND OBJECTIVES

A large amount of oil is still trapped in reservoirs after the traditional primary and secondary oil recovery processes. To recover these huge amounts of residual oil, the true understanding of subsurface characteristics especially the interfacial interactions between crude oil, brine and rock is essential. The surface chemistry involved in the equilibrium of capillary, viscous and gravitational forces is very important in oil recovery enhancement.

The interfacial properties such as wettability (contact angle) and interfacial tension, and the fluid flow characteristics of velocity and viscosity are correlated to the oil production through the capillary number ( $N_c$ ),

$$N_c = \frac{v\mu}{\sigma \cos \theta} \dots\dots\dots(1)$$

where  $v$  is the velocity,  $\mu$  is the viscosity,  $\theta$  is contact angle and  $\sigma$  is interfacial tension. The greater the capillary number, the lower the residual oil saturation in the reservoir and hence higher the oil recovery.

Addition of surfactants can lower the interfacial tension between oil and water and alter wettability of the rock-oil-brine system and hence enhance oil recovery. However, the high costs and high concentrations of chemical surfactants required rendered this process uneconomical due to the loss of chemicals by adsorption and precipitation on reservoir rock. Therefore this study aims to use relatively inexpensive surfactants at dilute concentrations to study the effects of surfactants on interfacial tension (IFT) and wettability alteration. From the Kilns plot (Kilns, 1984), it can be seen that four to six orders of magnitude reduction is required for significant oil recovery enhancements. At the same time, it can be seen from Equation (1) that slight wettability alteration to intermediate-wet (about  $90^\circ$ ) can result in infinite capillary numbers and thereby leading to very high oil recoveries. Hence wettability alteration mechanism can be considered more effective for improving oil recovery when compared to IFT reduction.

There exist several experimental methods to determine contact angle and IFT. Most of the existing measurement techniques have limited application in complex high

pressure, high temperature multi-component multi-phase reservoir systems. Furthermore, very few attempts have been made to study the dynamic behavior of IFT, which can better express the dynamic rock – fluid interactions taking place in a reservoir during production.

The following are some of the shortcomings existing in this research area, which serve as the basis for this study.

- Most of the interfacial tension and contact angle measurements have been made at ambient conditions. The neglect of temperature and pressure effects has rendered the results non-applicable to real reservoir fluids.
- Pure hydrocarbons and stocktank oils have been widely used in much of the previous work, which do not represent real reservoir live oil. The light ends in the live oil may have significant influence on wettability and IFT. Compositional effects of crude oil on dynamic IFT and contact angles at reservoir conditions have so far been largely ignored.

Furthermore, some fundamental theoretical uncertainties existing in this area which also need to be explored during this experimental study. It is generally difficult to study the interfaces of an undisturbed oil reservoir in laboratory. The restoration of the native wettability of core samples is also difficult due to changes in temperature, pressure, fluids, influence of cleaning processes and the uncertainty of aging times. The widely used approach so far has been the use of producing or synthetic fluids on outcrop rock samples and minerals in the laboratory experiments. There is also no widely accepted measurement technique for reservoir wettability. The accuracy of different methods is largely influenced by experimental environments.

The dynamic behavior of IFT and wettability alteration by surfactants is more important than static behavior in enhanced oil recovery applications. However, the studies of dynamic behavior of IFT and contact angles have been largely ignored in the existing literature due to experimental complexities. The existing dynamic IFT models, which were developed for pure or binary component systems and at ambient conditions cannot be used for complex crude oil systems at elevated pressures and temperatures. Therefore, there still exists a need to explore the long time behavior of the system and

build time-dependence models. The components of crude oil which are responsible for the time-dependent behavior of IFT and wettability are also need to be identified.

The wettability alteration by surfactants is not only dependant on the type of surfactants but also on the initial wettability of the rock-fluid system, temperature, pressure, and compositions of oil, brine and rock characteristics. Higher surfactant concentration may not result in better wettability alteration due to multilayered structures that they can assume.

This study attempts to draw a relatively complete picture of interfacial properties of underground oil reservoir by conducting fundamental experiments. The main objectives of this study are therefore to experimentally determine the influence of surfactant and oil composition on oil-water interfacial tension (IFT) and dynamic contact angles in rock-oil-brine systems at reservoir conditions. Experimental design includes selecting the best measurement techniques for IFT and contact angle, simulating the reservoir temperature and pressure, using live crude oil, reservoir brine and reservoir rock in the experiments. The data analysis involves comparison of the results between ambient versus reservoir conditions, live oil versus stocktank oil, brine versus water and dolomite versus other rock surfaces.

## CHAPTER 2. LITERATURE REVIEW

This project focuses on the interfacial properties and their measurements in rock-oil-brine systems and their surfactant-induced dynamic behavior. Therefore, the related literature is thoroughly reviewed and reported in the following sections.

### 2.1 Interfacial Tension Measurements

The Interfacial tension (IFT) is the surface tension at the surface separating two immiscible liquids. By the definition of Webster's 1913 Dictionary, surface tension is that "property, due to molecular forces, which exists in the surface film of all liquids and tends to bring the contained volume into a form having the least superficial area. The thickness of this film, amounting to less than a thousandth of a millimeter, is considered to equal the radius of the sphere of molecular action, that is, the greatest distance at which there is cohesion between two particles. It is a phenomenon at the surface of a liquid caused by intermolecular forces".

The net effect of this interfacial situation is the presence of free energy at the surface. The common units for surface tension are dynes/cm or mN/m. These units are equivalent. This excess energy exists at the interface of two fluids. Solids also may be described to have a surface free energy at their interfaces but direct measurement of this value is not possible through techniques used for liquids. Polar liquids, such as water, have strong intermolecular interactions and thus high surface tensions. Any factor that decreases the strength of this interaction will lower surface tension. Any contamination, especially by surfactants, will lower surface tension [1]. Since lower interfacial tension will have lower capillary force between oil and brine, it is possible to improve oil recovery by lowering interfacial tension (IFT).

For more than a century, a variety of techniques have been used to measure interfacial tensions between immiscible fluid phases. A recent monograph by Rusanov and Prokhorov (1996) provided a broad review of the technical literature on the interfacial tension techniques with detailed discussion of the theoretical bases and instrumentation. More than 40 methods have been introduced. The most common techniques used in interfacial tension measurements were summarized by Drelich et al. (2002) and are



shown in Figure 1.

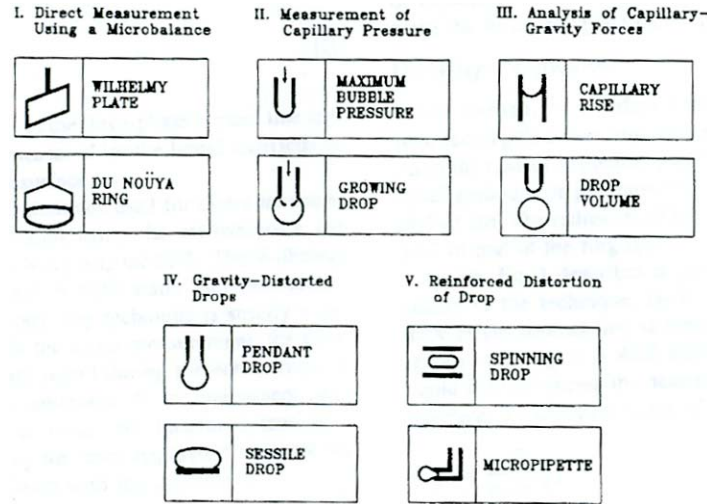


**Figure 1: Classification of Techniques for Interfacial Tension Measurements**  
(Drelich et al., 2002)

The selection of a measurement technique depends on the purpose and experimental environment. The most commonly used measurement techniques and the principles involved are discussed in detail below.

### 2.1.1 Wilhelmy Plate Technique

The two principal techniques used for direct measurement of interfacial tension using the microbalance are the Wilhelmy plate and Du Nouÿ ring methods. The Wilhelmy plate technique is used in both static and detachment modes, whereas du Nouÿ ring technique is strictly a detachment technique. In the static measurement, the plate remains in contact with liquid during the entire cycle of interfacial tension measurement. If the instrument operates in the detachment mode, the interfacial tension is measured by measuring the force required to separate the ring or plate from contact with the interface.

A vertical thin platinum plate is used in the Wilhelmy technique. The plate is put in a fixed position relative to the horizontal surface of the liquid. Then, the force ( $F$ ) vertically acting on the plate by the liquid meniscus is measured by using a microbalance. The force applied to the plate is equal to the weight of the liquid meniscus uplifted over the horizontal surface. By measuring this force, the interfacial tension can be calculated by using the following equation,

$$\gamma = \frac{F}{p \cos \theta} \dots \dots \dots (2)$$

where  $p$  is the perimeter of the three phase contact line. Adsorption of organic compounds from the laboratory environment or test solutions can be a major source of experimental error when measuring surface tensions using the Wilhelmy plate method.

### 2.1.2 Du Nouy Ring Method

In this method, the interfacial tension relates to the force required to pull a wire ring off the interface. As in the case of the Wilhelmy plate, the ring is usually made up of platinum or a platinum-iridium alloy. The radius ( $r$ ) of the wire ranges from 1/30 to 1/60 of that of the ring.

Equation (2) describes in general the calculation procedure of the technique. The perimeter ( $p$ ) of the three-phase contact line is equal to twice the circumference of the ring;  $p = 4\pi R$ . Because additional volume of liquid is lifted during the detachment of the ring from the interface, a correction factor ( $f$ ) is added to Equation (2) on the right hand side.

The high-accuracy measurements from the ring method require that the plane of the ring remain parallel to the interface. The major error in this technique is caused by deformation of the ring, which is a very delicate probe and subject to inadvertent deformation during handling and cleaning. It is also important that perfect wettability of the ring surface by the denser fluid be maintained. If perfect wetting is not achieved, additional correction of the instrument reading is needed.

### 2.1.3 Measurement of Capillary Pressure

Interfacial tension is defined as the work required to create a unit area of interface at a constant temperature, pressure, and chemical potential. It always tends to decrease the area of interface. This tendency gives rise to a pressure difference between fluids on either side of a curved interface, with the higher pressure on the concave side of the interface. This pressure difference results in phenomena such as a capillary rise, bubble and drop formation, etc. A formula describing the pressure difference ( $\Delta P$ ) across the curved interface is known as the Young-Laplace equation:

$$\Delta P = \gamma \left( \frac{1}{R_1} + \frac{1}{R_2} \right) \dots\dots\dots(3)$$

Where  $R_1$  and  $R_2$  are the radii of curvature.

The pressure difference can be measured in a number of ways (e.g. using a pressure

sensor or observing a capillary rise). One common method is based on measuring the maximum pressure to force a gas bubble out of a capillary into a liquid. The measured pressure is the sum of the capillary pressure caused by the interfacial tension and the hydrostatic pressure caused by the liquid column above the orifice of the capillary.

#### 2.1.4 Analysis of the Balance Between Capillary and Gravity Forces

Methods based on analysis of capillary effects, other than the shape of a drop or meniscus, such as capillary rise and drop volume or weight, are among the oldest surface tension measurement methods in use.

- Capillary Rise Method

The basis for the capillary rise method is to measure the height  $h$  of the meniscus in a round glass tube having the known inner radius  $r$ . The shape of the meniscus is spherical, and the surface tension can be calculated by using the following equation:

$$\gamma = \frac{\Delta\rho g h r}{2 \cos \theta} \dots\dots\dots(4)$$

The capillary rise method can be one of the most accurate techniques used to make surface tension measurements. It is one of the oldest methods but now it has seldom been used because it is hardly commercial. Technical problems with the technique are related to fabrication of a uniform bore capillary tube and precise determination of its inside diameter.

- Drop Volume or Weight Method

In this method, the weight or volume of a drop falling from a capillary with a radius  $r$  is measured. The weight ( $W$ ) of the drop falling off the capillary correlated with the interfacial tension using the following equation:

$$W = V\Delta\rho g = 2\pi r\gamma\left(\frac{r}{\sqrt[3]{V}}\right) \dots\dots\dots(5)$$

where  $V$  is the drop volume,  $r$  is the radius of the capillary, and  $f$  is the correction factor required because only a portion of the drop volume is released from the capillary during detachment.

The measurements of interfacial tension with the drop weight or volume technique are very simple, but unfortunately, sensitive to vibrations on the other side. Vibrations of the apparatus can cause premature separation of the drop.

### 2.1.5 Spinning Drop Technique

This technique relies on the fact that gravitational acceleration has little effect on the shape of a fluid drop suspended in a liquid, when the drop and the liquid are contained in a horizontal tube spun about its longitudinal axis. At low rotational velocities ( $w$ ), the fluid drop will take on an ellipsoidal shape, but when  $w$  is sufficiently large, it will become cylindrical. Under this latter condition, the radius ( $r$ ) of the cylindrical drop is determined by the interfacial tension, the density difference between the drop and the surrounding fluid, and the rotational velocity of the drop. As a result, the interfacial tension is calculated from the following equation:

$$\gamma = \frac{1}{4} r^3 \Delta \rho \omega^2 \dots\dots\dots (6)$$

The spinning drop method has been very successful in the measurement of ultralow interfacial tensions down to  $10^{-6} \text{ mN/m}$  (by its Manual). This method is specially used for low IFT measurements such as in the surfactant systems. The accuracy of measuring results under high-pressure and high-temperature (HPHT) conditions has not been found in literature but HPHT spinning drop instruments have recently become commercial (Ruska Company).

### 2.1.6 Analysis of Gravity-Distorted Drops

Interfacial tension causes interfaces to behave as elastic membranes that always tend to compress the liquid. In the absence of other forces (e.g., at zero gravity), the liquid surface has a natural tendency to form spherical shapes to minimize the interfacial area per unit volume of liquid and thus minimizes the excess energy of the interface. The shape of an interface in a gravitational field depends on the competition between the capillary and gravitational forces and can be described by the Bashforth-Adams equation:

$$\gamma \left( \frac{\sin \phi}{x} + \frac{1}{R} \right) = \frac{2\gamma}{b} + \Delta \rho g z \dots\dots\dots (7)$$

Where  $\Delta \rho = D_1 - D_2$  (Density difference),  $R$  is the radius of the curvature at point P,  $b$  is the radius of the apex of the curvature (Figure 2).

### 2.1.7 Drop Shape Analysis Method

For this study, the IFT measurement technique should be able to use in a liquid-liquid system at high temperature and high pressure. According to the accuracy and suitability

of classic techniques used in interfacial tension measurements (Table 1), the pendant drop method is the best one suited for this project. Commercial software, so called Drop Shape Analysis for IFT calculation, is introduced here.

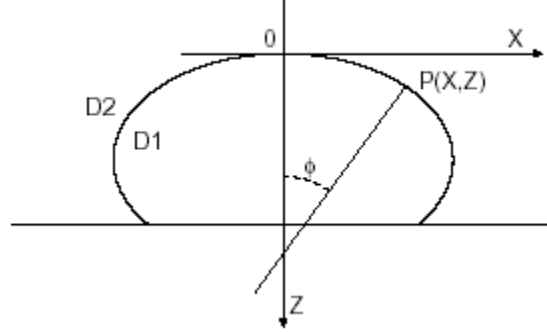


**Figure 2: Definition of dimensions and coordinates describing the sessile drop**  
(Busoni, 2003)

The drop shape is a function of  $\gamma$  and other parameters and is easily to be measured, as showing in the following Young-Laplace equation

$$\gamma\left(\frac{1}{R_1} + \frac{1}{R_2}\right) = C + gz\Delta\rho \quad \dots\dots\dots(8)$$

Where  $R_1$  and  $R_2$  are the radii of the surface at point  $P$  of height  $Z$ ,  $C$  is the pressure difference across the interphase in  $Z = 0$ ,  $g$  is the gravity acceleration, and  $\Delta\rho$  is the density difference between the drop and the surrounding fluid. For an axisymmetric system, this equation reduces to the Bashforth and Adams equation (Equation 7).

The analysis of the profile of an axisymmetric drop of liquid – either a sessile or a pendant drop – immersed in a second fluid phase, has always been considered as the most reliable and accurate method to measure interfacial tension at the liquid-fluid interphase. But the technical requirement of high quality image and computing prevented it from becoming popular in the past. The experimental setup requires a camera with a low-magnification lens to record the shape of the drop. The interfacial tension can be easily calculated from the dimensions of the pendant drop, sessile drop, or liquid meniscus taken from the photographic picture and by using numerical solutions to the above equations. Modern instruments use image analysis software whose role is to match the entire drop profile to the best fit of the theoretical curve (e.g., the Bashforth-Adams equation) in describing the shape of the drop. These advances significantly improved the

precision of these techniques and reduced the time of the measurement, providing an opportunity for examination of the interface aging process. The DSA –2 software from Kruss Company is used in this study.

**Table 1: Accuracy and Suitability of Classic Techniques Used in Interfacial Tension Measurements**

(Main Sources: Drelich et al., 2002, Dukhin, et al.,1995 and Schramm, 2000)

Method	Accuracy [mN/m]	Suitability				Time Range	Commercial Availability
		Surfactant Solutions	Two-liquid Systems	Gas-liquid	High Temperature and High Pressure		
Wilhelmy plate	0.1	Limited	Good	Good	No	>10s	Yes
Du NoUy ring	0.1	Limited	Reduced accuracy	Good	No	>30s	Yes
Maximum bubble pressure	0.1-0.3	Very good	Very good	Good	No	1ms-100s	Yes
Capillary rise	«0.1	Very good	Very good, experimentally difficult	Good	No*		No
Drop volume	0.1-0.2	Limited	Good	Good	Yes	1s-20min	Yes
Pendant drop	0.1	Very good	Very good	Good	Yes	10s-24h	Yes
Sessile drop	>0.1	Good	Very good	Possible	Yes		No
Laser Scattering	<0.1	-	possible	Good	Yes		Yes
Spinning drop	0.0001	Good	Good (small range)	Possible	No**		Yes

\* Currently performed at LSU at reservoir conditions

\*\* Recently available from Ruska Company

## 2.2 Dynamic Interfacial Tension

For the static interfacial tension measurement of two immiscible fluids, the compositional equilibrium status is required. Normally the equilibrium is reached by mixing two liquids together and aging the mixture for a certain time. However, in many interfacial processes such as high-speed wetting, foaming or surfactant injection, this equilibrium cannot easily or ever be reached and dynamic behavior plays a major role in these processes. In such applications it is important to measure the dynamic interfacial tensions.

The study of time-dependent interfacial tension remains largely unexplored. Most of the previous studies measure a single IFT value by assuming the equilibrium status of two fluids. Several of them focused on the time needed to attain an equilibrium value. For the pendant drop method, 10 seconds after the formation of a drop is believed to be the

best time for equilibrium IFT (Jennings, 1967). The results between different measurement techniques in some cases are significantly different. Table 1 provides a characteristic time range available for the selected interfacial tension measurement techniques.

The dynamic behavior of interfacial tension is believed to be caused by the adsorption kinetics of interfacially active molecules at liquid interfaces. This adsorption kinetics of molecules to a liquid interface is controlled by transport processes in the bulk and the transfer of molecules from a solution state into an adsorbed state or vice versa. These adsorption and desorption reactions at the interface area as well as the diffusive movement inside the two fluids are controlled by many factors. Hence, the complete mathematical model to accurately describe the dynamic interfacial tensions is difficult to build, leading to some confusion in the published literature. Even for the general agreement of diffusion theory, whether the time dependent behavior of IFT is a linear function of  $t^{1/2}$ ,  $1/t^{1/2}$ ,  $\exp(t)$ ,  $\log(t)$  or combination of them, is still unclear.

### 2.2.1 Numerical Models

There are two general perceptions to describe the dynamics of adsorption at liquid interfaces. (Dukhin et al., 1995, Diamant et al., 1996, He et al., 2002) The diffusion controlled model assumes the diffusional transport of interfacially active molecules from the bulk to the interface to be the rate-controlling process, while the so-called kinetic controlled model is based on transfer mechanisms of molecules from the solution to the adsorbed state and vice versa, in other words, the attachment of the molecules onto the interface due to high adsorption activation energy barriers. Dukhin et al. (1995) described qualitative and quantitative models of adsorption kinetics of surfactants and polymers. Evans et al. (2002) analyzed the combined dynamic effects of the adsorption kinetics using the mass transfer, micellisation equilibria and random sequential adsorption theory.

The pioneering theoretical work of Ward and Tordai (1946) formulated a time-dependent relationship between the surface density of surfactants adsorbed at an interface and their concentration at the sub-surface layer of solution, assuming a diffusive transport from the bulk solution.

$$\Gamma(t) = 2c_0 \left( \frac{Dt}{\pi} \right)^{\frac{1}{2}} - \int_0^{\sqrt{t}} 2 \left( \frac{D}{\pi} \right)^{\frac{1}{2}} c_s(t-\lambda) d(\lambda) \frac{1}{2} \dots\dots\dots(9)$$

where  $\Gamma(t)$  (g/m<sup>2</sup>) is the surface concentration at time t(s),  $c_o$  and  $c_s$  (g/m<sup>3</sup>) are the bulk concentration and subsurface concentration,  $D$  (m<sup>2</sup>/s) is the diffusion coefficient and  $\lambda$  is a dummy variable.

If the adsorption was limited by the activation energy barrier, on the other hand, Breen and Lankveld and Lyklema (He et al., 2002) proposed that the change of interfacial tension could be fitted to a simple exponential decay as

$$\frac{\gamma_t - \gamma_e}{\gamma_0 - \gamma_e} = Ae^{-Bt} \dots\dots\dots(10)$$

where  $\gamma_e$  is the interfacial tension at equilibrium,  $\gamma_0$  and  $\gamma_t$  are the interfacial tension at the beginning and time t,  $A$  and  $B$  are constants.

Diamant and Andelman (1996, 1997)) summarized that diffusion theories have been quite successful in describing the experimentally observed adsorption of common non-ionic surfactants but they have several drawbacks: i) The closure relationship between the surface density and sub-surface concentration, which expresses the kinetics taking place just at the interface, is introduced as an *external* boundary condition, and does not uniquely arise from the model itself; ii) the calculated dynamic surface tension relies on an *equilibrium* equation of state, and assumes that it also holds out of equilibrium; iii) similar theories cannot be successfully extended to describe more complicated, *ionic* surfactant solutions. They also introduced the models to present an alternative approach for the kinetics of non-ionic and ionic surfactant adsorption at fluid/fluid interfaces.

For a non-ionic surfactant,

$$\phi_0(t) = (1/a)\sqrt{D/\pi} \left[ 2\phi_b\sqrt{t} - \int_0^t \phi_1(\tau)(t-\tau)^{-1/2} d\tau \right] + 2\phi_b - \phi_1 \dots\dots\dots(11)$$

This relationship is similar to the classical Ward and Tordai equation, except for the term  $2\phi_b - \phi_1$ , where  $\phi_0$  and  $\phi_b$  are the surfactant volume fraction at the interface and in the bulk solution. The  $a$  denotes the surfactant molecular dimension.

This equation represents the diffusive transport from the bulk solution. It can be simplified as

$$\begin{aligned} \phi_1(t)/\phi_b &\cong 1 - \sqrt{\tau_d/t}; & t &\rightarrow \infty \\ \tau_d &\equiv (\alpha^2/\pi D)(\phi_{0,eq}/\phi_b)^2, \end{aligned} \dots\dots\dots(12)$$

where  $\phi_{0,eq}$  denotes the equilibrium surface coverage.



The kinetics at the interface itself is described as

$$\partial \phi_0 / \partial t = \phi_1 D (\mu_1 - \mu_0) / a^2 T = (D / a^2) \phi_1 \{ \ln [\phi_1 (1 - \phi_0) / \phi_0] + \alpha / T + \beta \phi_0 / T \}$$

or

$$\phi_0(t) / \phi_{0,eq} \cong 1 - e^{-t/\tau_k} \quad t \rightarrow \infty$$

$$\tau_k \equiv (\alpha^2 / D) (\phi_{0,eq} / \phi_b)^2 e^{-(\alpha + \beta \phi_{0,eq}) / T} \dots\dots\dots(13)$$

The kinetics of the system has been separated into two coupled kinetic processes. 1) *Diffusion-limited adsorption* applies when the process inside the solution is much slower than the one at the interface. One can then assume that the interface is in constant equilibrium with the adjacent solution, which is described by equation (12).  $\Phi_0$  responds to changes in  $\Phi_1$ . ii) *Kinetically limited adsorption* takes place when the kinetic process at the interface is the slower one. In this case, the solution is assumed to be in constant equilibrium with the bulk reservoir.  $\Phi(x > 0) = \Phi_b$  and  $\Phi_0$  changes with time according to Equation (13). Normally, the kinetics component is much smaller than the diffusive component, so the adsorption of common non-ionic surfactants is expected to be diffusion-limited.

England and Berg (1971) also presented a kinetic IFT model to describe the transfer of normal and isobutyric acids from oil to water. Trujillo (1983) used the same model to explain the increasing IFT with time in crude oil and caustic systems.

## 2.2.2 Experimental Models

- Surfactant Systems

It is a general notion that if IFT is plotted versus  $t^{-1/2}$ , resulting straight line signifies that the process is diffusion controlled. Some have plotted log of IFT versus log t, the slope is supposed to be -0.5 for diffusion controlled process. A complex explanation is also given in several papers. A typical approach can be found in the papers of Taylor et al. (1996), Hunsel et al. (1989), Diamant et al. (2001), Touhami et al. (1998), Gao and Rosen (1994), Hua and Rosen (1988, 1991) etc. (see Figure 3)

Hua and Rosen (1988) proposed a generalized dynamic surface tension model,  $\gamma_t$  versus log time (Figure 4). They divided the total response into four regions: (I) induction region; (II) rapid fall region; (III) meso-equilibrium region and (IV) equilibrium region. The first three regions were described by using the equation,

$$\gamma_t - \gamma_m = \frac{\gamma_0 - \gamma_m}{1 + (t/t^*)^n} \quad \dots\dots\dots (14)$$

where  $\gamma_m$  is the meso-equilibrium surface tension and  $t^*$  and  $n$  are constants, with  $t^*$  having the dimensions of time in the same units as  $t$ , and  $n$  being dimensionless. This equation is in a form similar to the Fourier transform of a correlation function, often used in relaxation theory. By using the log form of this equation, a straight line with a slope of  $n$  is expected for  $\log[(\gamma_0 - \gamma_t)/(\gamma_t - \gamma_m)]$  versus  $\log t$ .

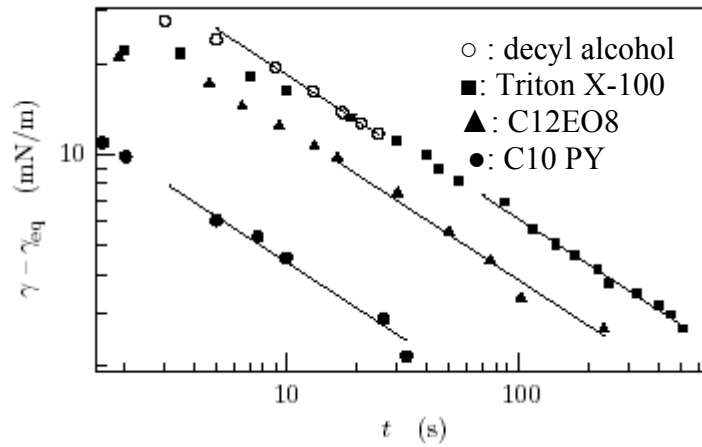


**Figure 3 Diffusion-Limited Adsorption of a Variety of Non-ionic Surfactants** (Diamant and Andelman 1996) Note the asymptotic behavior with slope of  $-0.5$

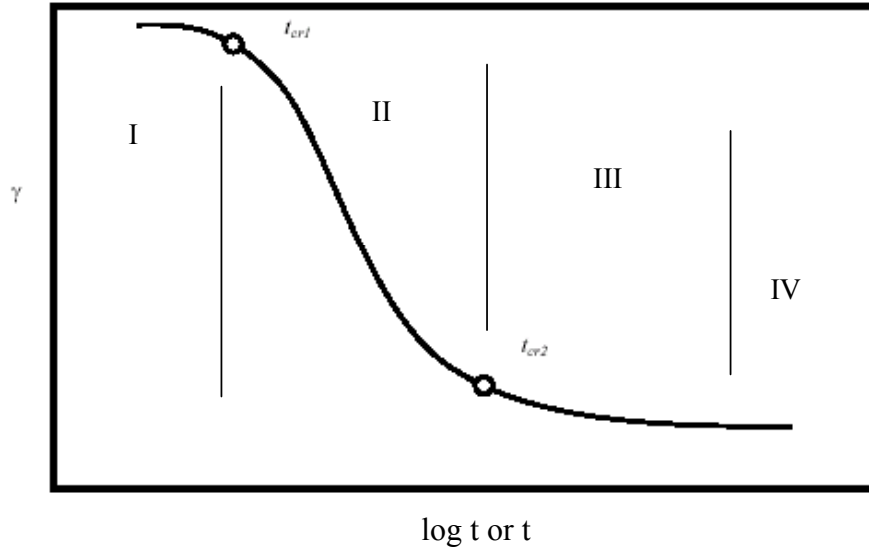


**Figure 4: Stages of interfacial tension change with time** (from Hua and Rosen, 1988 ( $\log t$ ), and He 2002 ( $t$ ))

- Crude Oil – Caustic Solution Systems

One popular method used for enhanced oil recovery is alkaline waterflood. The wettability alteration and IFT reduction are the main mechanisms behind the oil recoveries with caustic. The IFT was lowered by about three orders of magnitude with a 0.5% NaOH solution (Reisberg and Doscher, 1956) or with 0.05 to 0.5% NaOH solutions (Jennings et al., 1974). It was also found that the existence of calcium ions increased the IFT between caustic and crude oil considerably. Sodium chloride reduced the amount of caustic required for maximum surface activity. Cooke et al. (1974) concluded that sodium chloride is beneficial but calcium is detrimental for enhanced oil recovery. Taylor et al. (1996) reported that the effect of surfactant on IFT depends on the alkali (sodium carbonate) concentration.

Several investigators have studied the reaction of caustic with crude oils and they reported that the IFT between crude oil and caustic or alkaline solutions increases with time (summarized by Trujillo, 1983). The reaction between the natural surfactant in the crude and the caustic in a solution creates a surface-active agent, and the amount of surface activity depends on the pH and calcium-ion concentration (Trujillo, 1983). Trujillo also proposed a graphical model from England and Berg's equation (Figure 5). The main observation here is that the IFT decreases initially to a minimum and then increases. Rubin and Radke (1980) and Brown and Radke (1980) used a modified version of England and Berg's model to describe dynamic IFT's with caustic. They accounted for the finite volume of the two phases and found that the rise in IFT with time is related to the ratio of the phase volumes. Therefore, the time dependency observed in the laboratory may not be representative of that in the field.

Five physical constants can be seen in Figure 5: the molecular diffusion constants for the transporting species in both the oil and water phases,  $D_1$  and  $D_2$ ; the distribution or partition coefficient,  $m$ ; the adsorption coefficient,  $c$ ; and the desorption-rate constant,  $k_2$ .

Radke and coworkers (1980) have suggested that the IFT minimum for acidic crude oils, as measured with the spinning drop tensiometer, is indicative of the lowest achievable reservoir equilibrium value. Taylor et al. (1996) also demonstrated that experimental surfactant-enhanced alkaline flooding in sandstone cores correlates better

with the minimum dynamic IFT. They examined in detail the effect of a surfactant on the dynamic IFT of crude oil / alkali / polymer systems. A linear relationship was observed between IFT and  $t^{-1/2}$ , both before and after minimum IFT was reached, indicating that the dynamic IFT was diffusion controlled. The rate limiting diffusion process occurs in the aqueous phase before the minimum IFT and in the oil phase after the minimum IFT.

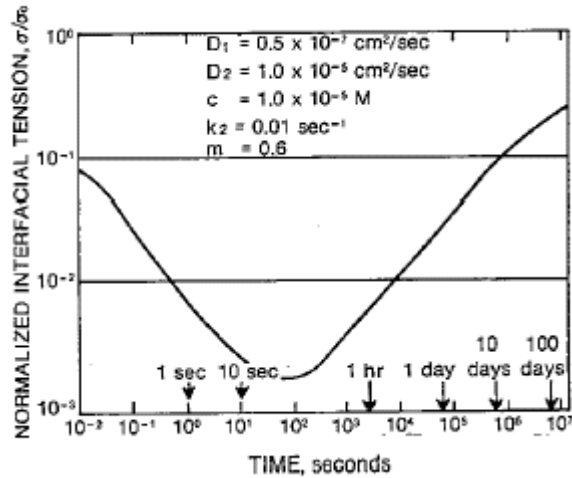


**Figure 5: Dynamic Mathematical Model of Transient IFTs (Trujillo, 1983)**

- Crude Oil –Water System

Freer and Radke (2004) employed a model oil system consisting of asphaltenes precipitated from a heavy crude oil and dissolved in toluene. The dynamic interfacial tension (ADSA method) for this system was similar to that observed for the original crude oil from which the asphaltenes were extracted. After aging the interface for 24 hours, an interfacial skin was observed visually upon compression of the model crude oil/water interface. They found that the linear viscoelastic response fits a combination of a modified form of the LDVT (Lucassen and van den Tempel, 1972) diffusion-exchange model and a Maxwell surface-relaxation model (Monroy et al., 1999). Upon washout by toluene, the IFT increased only by 1.5 mN/m, indicating that the majority of asphaltenes are irreversibly adsorbed and that only a small fraction desorbs into the fresh toluene. The relaxation time of the interface after washout increased by an order of magnitude, suggesting that the reversibly adsorbed species disrupt asphaltene aggregation at the interface, resulting in a more tenuous and weaker network structure.

It is interesting to note that all the literature that reported the continuous decrease of IFT with time was based on experiments in surfactants system and used pendent drop

method. The studies that reported the decreasing and then increasing of IFT with time involved the caustic/alkaline and used the spinning drop method. Since spinning drop method is used for low IFT measurement and pendent drop is used for relatively high IFT measurement, the dynamic differences caused by different mechanisms of the measuring techniques need to be noticed. The variation of phase volume ratios in different measurement methods might be a reason for these differences observed.

### **2.2.3 Effects of Temperature and Pressure on Interfacial Tension**

Hocott (1938) reported that the IFT between water and subsurface oil samples increased with pressure until a saturation pressure is reached, and then slowly decreased with pressure.

Hough et al. (1951) reported that for the water-methane system, IFT decreases and then increases with pressure at high temperature or decreases with pressure at room temperature.

Jennings (1967) investigated the effect of temperature and pressure on the IFT of benzene-water and n-decane–water using the pendent drop method and reported that IFT increased with the increasing pressure and decreased with increasing temperature, respectively.

Hjelmeland and Larrondo's (1986) investigation of the IFT between crude oil and brine showed that IFT increased with the increase in temperature under anaerobic conditions, whereas at aerobic conditions, IFT decreased with the increase of temperature.

Ziegler (1988) conducted the high temperature surfactant flooding experiments. He found that temperature and brine salinity significantly affected the IFT between solutions of alkylaryl sulfonates and heavy crude oil (14.5° API). Here, increasing temperature increased the salinity needed to obtain ultralow IFT's.

Drelich et al. (1994) reported that the surface tension of bitumens decreases linearly with increase in temperature.

Yang et al. (2005) studied dynamic IFT of the reservoir brine-CO<sub>2</sub> system by the pendant drop method. They reported that the equilibrium IFT generally decreased as the pressure increases, whereas it increased as the temperature increased.

The effects of temperature and pressure on IFT were not well studied due to the experimental difficulties. In most cases, the IFT between water/oil decreased with

temperature because the solubility of water in oil increases exponentially with the temperature, thus reducing the free energy between these two immiscible fluids. The change of IFT with pressure is largely influenced by the composition of fluids especially the light ends present in crude oils.

## 2.3 Wettability and Contact Angles

### 2.3.1 Definition

Wettability is defined as the tendency of one fluid to spread on or adhere to a solid surface in the presence of other immiscible fluids. Changes in the wettability of cores have been shown to affect electrical properties, capillary pressure, waterflood behavior, relative permeability, dispersion and simulated EOR (Anderson, 1986).

For oil/water/rock system, Young's equation is employed by considering equilibrium between force factors at the three-phase-contact:

$$\sigma_{so} = \sigma_{sw} + \sigma_{wo} \cos \theta \quad \dots\dots\dots(14)$$

where  $\theta$  is the contact angle at the oil/water/solid contact line.

Three-phase contact line is defined as the intersection of a solid surface with the interface between two immiscible fluids. When one fluid displaces another immiscible fluid along a solid surface, the process is called *dynamic wetting* and a "moving" contact line (one whose position relative to the solid changes in time) often appears. The corresponding contact angle is called *dynamic contact angle*.

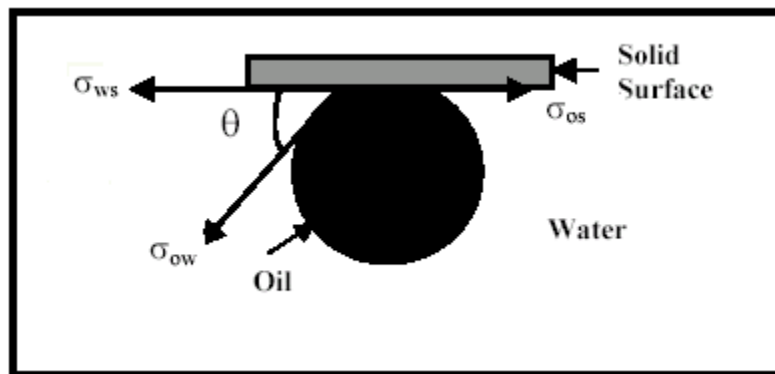


**Figure 6: Contact Angle at Oil/Water/Solid Interfaces** (Rao and Girard, 1996)

From Figure 6, it can be seen that the contact angle is a direct measure of the surface wettability. A contact angle of  $0^\circ$  indicates total hydrophilicity, which means completely water-wet, whereas an angle of  $180^\circ$  means the surface is totally hydrophobic, completely

oil-wet. If the angle is less than  $90^\circ$  the water is said to wet the solid. If it is greater than  $90^\circ$  it is said to be oil-wet. Since the measurement techniques influence the value of contact angle, the angles measured by different techniques may not be comparable. The generally accepted wetting classification is (Anderson, 1986):  $0^\circ\sim 75^\circ$ , water-wet;  $75^\circ\sim 115^\circ$ , intermediate-wet;  $115^\circ\sim 180^\circ$ , oil-wet. In this study,  $55^\circ - 75^\circ$  was defined as weakly water-wet and  $115^\circ - 135^\circ$  was defined as weakly oil-wet.

Various experimental techniques have been developed to measure the wettability of a surface. These techniques include contact angle measurement, two-phase separation, bubble pickup, microflotation, and vacuum flotation, and are based on the fact that the water wetting process is essentially an oil displacement phenomenon on a solid surface (Somnasundaran and Zhang, 2004). Other generally used methods are the Amott method (imbibition and forced displacement) and USBM method. The contact angle measures the wettability of a specific surface, while the Amott and USBM methods measure the average wettability of a core sample.

### **2.3.2 Dynamic Contact Angles**

The measurement of a single static contact angle to characterize an interaction is no longer thought to be adequate. For any given solid/ liquid interaction there exists a range of contact angles that may be found. The values of static contact angles are found to depend on the recent history of the interaction. When the drop has recently expanded, the angle is said to represent the ‘advanced’ contact angle. When the drop has recently contracted, the angle is said to represent the ‘receded’ contact angle. These angles fall within a range, with advanced angles approaching a maximum value and receded angles approaching a minimum value. The conditions which produce advanced and receded angles are sometimes difficult to reproduce. Although drops in motion can produce data on dynamic contact angles, the velocity of motion cannot be controlled [2].

If the three-phase (liquid/solid/vapor) boundary is in actual motion, the angles produced are called *Dynamic Contact Angles* and are referred to as ‘*advancing*’ and ‘*receding*’ angles. The difference between ‘advanced’ and ‘advancing’, ‘receded’ and ‘receding’ is that in the static case, motion is incipient whereas in the dynamic case, motion is actual. Dynamic contact angles may be assayed at various rates of speed. Dynamic contact angles measured at low velocities should be equal to properly measured

static angles. The difference between the maximum (advanced/advancing) and minimum (receded/receding) contact angle values is called the *contact angle hysteresis*. A great deal of research has gone into the analysis of the significance of hysteresis. It has been used to help characterize surface heterogeneity, roughness and mobility.

### 2.3.3 Contact Angle Measurements

Two different approaches are commonly used to measure contact angles of non-porous solids, goniometry and tensiometry [3].

*Goniometry* involves the observation of a sessile drop of test liquid on a solid substrate. The basic elements of a goniometer include a light source, sample stage, lens and image capture. Contact angle can be assessed directly by measuring the angle formed between the solid and the tangent to the drop surface.

Limitations: The assignment of the tangent line which will define the contact angle is a factor which can limit the reproducibility of contact angle measurements. Conventional goniometry relies on the consistency of the operator in the assignment of the tangent line. This can lead to significant error, especially a subjective error between multiple users.

The *tensiometric method* for measuring contact angles measures the forces that are present when a sample of a solid is brought into contact with a test liquid. If the forces of interaction, geometry of the solid and surface tension of the liquid are known, the contact angle may be calculated using the following equation:

$$F_{\text{total}} = \text{wetting force} + \text{weight of probe} - \text{buoyancy}$$

Limitations: There are two major limitations for the application of this technique. Firstly, the user must have enough of the liquid being tested available so that he can immerse a portion of his solid in it. Secondly the solid in question must be available in samples that meet the following constraints: i) The sample must be formed or cut in a regular geometry such that it has a constant perimeter over a portion of its length. Rods, plates or fibers of known perimeter are ideal. ii) The sample must have the same surface on all sides that contact the liquid. iii) The sample must also be small enough so that it can be hung on the microbalance

In the case of porous solids, powders and fabrics another approach is commonly used. This technique involves using a tensiometer and the Washburn method. It is the method of choice when your sample contains a porous architecture that absorbs the wetting liquid



[4]. This method is chosen when the solid sample to be tested contains a porous architecture that leads to absorption of the wetting liquid. The solid is brought into contact with the testing liquid and the mass of liquid absorbed into the solid is measured as a function of time. The amount absorbed is a function of the viscosity, density and surface tension of the liquid, the material constant of the solid, and the contact angle of the interaction. If the viscosity, density and surface tension of the liquid are known, the material constant and contact angle can be solved. According to this theory when a porous solid is brought into contact with a liquid, the rise of the liquid into the pores of the solid will obey the following relationship:

$$T = [h / C r^2 g \cos\theta] M^2 \dots\dots\dots(15)$$

The terms are defined as follows:

T = time after contact; h = viscosity of liquid; C = material constant characteristic of solid sample; r = density of liquid; g = surface tension of liquid;  $\theta$  = contact angle; M = mass of liquid adsorbed on solid.

The methods that are widely used in the petroleum industry for contact angle measurements are the sessile drop method and a modified sessile drop method. In both methods, the mineral crystal to be tested is mounted in a test cell composed entirely of inert materials to prevent contamination. The sessile drop method uses a single flat, polished mineral crystal. The modified sessile drop method uses two flat, polished mineral crystals that are mounted parallel to each other on adjustable posts.

### **2.3.4 Effects of Temperature and Pressure**

Anderson (1986) summarized the effect of temperature on wettability using the earlier literature. He concluded that changing the temperature has two different effects, both of which tend to make the core more water-wet at higher temperatures: first, an increase in temperature tends to increase the solubility of wettability-altering compounds. Some of these compounds will even desorb from the surface as the temperature increases. Second, the IFT and the contact angle measured through the water will decrease as the temperature increases. This effect has been noted in experiments with cleaned cores, mineral oil, and brine, where it was found that cores at higher temperatures were more water-wet even though there were no compounds that could adsorb and desorb.

Hjelmeland and Larrondo (1986) reported that a predominantly oil-wet system at a lower temperature altered to a predominantly water-wet system at a high temperature but pressure along has little effect on the wettability of system.

Wang and Gupta (1995) developed an experimental method for the measurements of contact angle at the elevated temperature and pressure in which a Pendant Drop Interracial Tension Cell was modified. They reported that the contact angle for the systems studied increased with pressure, increased with temperature for the sandstone system and decreased with temperature for the carbonate system.

Rao (1999) investigated the effect of temperature on contact angles on a quartz surface using DDDC technique, and reported that both advancing and receding angles increased with temperature.

Al-Hadhrami and Blunt (2001) summarized the thermally induced wettability alteration in fractured reservoirs. They pointed out that experiments on core from fields in Oman and elsewhere have indicated that rock will undergo a transition from oil-wet to water-wet as the temperature increases.

### **2.3.5 Effects of Crude Oil Composition**

Buckley et al. (1997) summarized the effect of oil composition especially asphaltenes on oil wetting. They stated that asphaltenes and other high molecular weighted polar components of crude oils are responsible for altering the wetting of reservoir rocks. However, the concentration of asphaltenes in oil is not a good predictor of rock/oil interactions. The composition of the remainder of the oil phase is equally important, particularly with regard to its properties as a solvent for some of its largest constituents. Organic liquids can be classified as solvents or precipitants on the basis of their effect on the solubility and aggregate size of asphaltenes.

Kaminsky and Radke (1997) summarized three basic assumptions that are now widely accepted. The first and most significant of these was discovered by Salathiel (1973). Salathiel hypothesized a mixed-wet condition with large pores being oil-wet and smaller pores being water-wet, and with the oil-wet and water-wet regions continuously connected. Mixed-wet rock exhibits very low residual oil saturations and slow oil production rates at these low saturations. The second assumption, consistent with Salathiel's vision of continuous oil and water phases, is that configurations of oil in pores

involve either direct contact between oil and rock, or separation of the oil phase from the solid by aqueous films. The third basic assumption is that in a given pore, when a critical capillary pressure is exceeded, water films destabilize and rupture to an adsorbed molecular film of up to several water monolayers. Crude oil now contacts rock directly, allowing polar oil species to adsorb and/or deposit onto the rock. It is this process that locally reverses the wettability of the rock from water-wet to oil-wet.

Basu and Shama (1999) investigated the role of crude-oil components on wettability alteration using atomic force microscopy. They concluded that the surface force vs. distance curves for asphaltenes and resins follow the trends predicted by DLVO theory where the critical disjoining pressure decreases with increasing brine salinity and decreasing pH, which suggested that for the polar fractions of the crude oil electrostatic interactions play a dominant role. In the presence of nonpolar oil, however, hydrophobic interactions (attractive) become important and the brine film is more unstable. It is not explainable on the basis of DLVO theory.

Two interaction mechanisms related to wettability alteration have been demonstrated by Al-Maamari and Buckley (2003). First mechanism is ionic interactions that involve ionization of acids and bases at the oil/water and solid/water interfaces (acid/base, ion-binding, and other specific interactions are included in this category). These interactions dominate in oil mixtures in which asphaltenes are in stable dispersion. The other mechanism is surface precipitation interactions that depend mainly on crude-oil-solvent properties with respect to their asphaltenes that produce more oil-wet conditions. If the pressure decreases below the bubblepoint, the lightest components begin to separate into another phase, leaving the remaining oil phase a better solvent for its asphaltenes and returning rock/fluid interactions to the region of ionic mechanisms.

Kokal et al. (2004) pointed out that asphaltene precipitation and deposition increase with increasing GORs. Asphaltenes comprise the heaviest and most polar fraction of crude oils. Asphaltenes exist in the form of colloidal dispersions and are stabilized in solution by resins and aromatics that act as peptizing agents. Asphaltene precipitation is a function of pressure, temperature and live crude oil composition. Asphaltenes have a tendency to precipitate as the pressure is reduced, especially near the bubble point (precipitation can occur even at pressures higher than the bubble point, depending on the

crude oil). Another important reason for precipitation is the stripping of crude oil by gas. When gas is added to the crude oil, the composition changes and this may lead to precipitation.

Wang et al. (2004) found that asphaltenes can separate from some oils during depressurization. In other cases, the addition of lift or injection gas can destabilize asphaltenes.

Zhang and Austad (2005) summarized that the charge of the oil-water interface is usually negative due to the content of carboxylic acid in the crude oil, while the charge on the water-rock interface is positive due to  $\text{pH} < 9.5$  and a high content of  $\text{Ca}^{2+}$  in the brine. The water film then becomes unstable, and the oil contacts the carbonate surface. The carboxylic group that is usually present in large molecules (resins and asphaltenes), adsorbs strongly onto the carbonate surface by displacement of water. Thus, the acid number (AN) of the crude oil has been shown to be a crucial factor for the wetting state of carbonates, and it was observed that the water wetness decreases as the AN increases.

Kumar et al. (2005) investigated the mechanisms of wettability alteration by crude oil components and surfactants by contact angle measurements as well as atomic force microscopy (AFM). They concluded that the wettability is controlled by the adsorption of asphaltenic components. The force of adhesion for minerals aged with just the asphaltene fraction is similar to that of the whole oil. The force of adhesion for the minerals aged with just the resin fraction is highest of all the SARA (Saturates, Aromatics, Resins and Asphaltenes) fractions. They also reported that greater wettability alteration is possible with the anionic surfactants than the cationic surfactant and that the water imbibition rate does not increase monotonically with an increase in the surfactant concentration.

### **2.3.6 Effects of Brine Composition**

Tang et al. (1999) summarized that cation valence is of specific importance to crude oil/brine/rock interactions as follows: i) When the salinity is high, an increase in cation valence tends to decrease water-wetness, but the corresponding oil recovery by waterflooding tends to increase. The effect of cation valence on wetting and oil recovery was much less when the salinity was low. ii) A decrease in NaCl and  $\text{CaCl}_2$  brine concentration can result in wettability transitions towards increased water-wetness and an increase in waterflooding recovery. However, for  $\text{AlCl}_3$  brine, a decrease in salinity can

result in increased water-wetness and decreased oil recovery. iii) For a given connate brine composition (both reservoir brine or single cation brine), injection of dilute single cation brine (no matter what the cation valence) always resulted in increased oil recovery. iv) Switching the injection brine from a high salinity brine to a dilute brine at high water-cut can also result in increased oil recovery by waterflooding. However, earlier injection of dilute brine is of benefit with respect to both increased breakthrough and final oil recovery.

Sharma and Filoco (2000) found that imbibition ~ waterflooding experiments show a strong salinity dependence. Higher oil recoveries are obtained for lower connate brine salinities by using three oil samples. For the nonpolar mineral oils no salinity dependence was detected. They attribute this salinity dependence to alteration of the wettability to mixed-wet conditions from water-wet conditions.

Zekri et al. (2003) observed a significant reduction of the oil/water contact angle (from  $48^\circ$  to  $29^\circ$ ) at intermediate salinity of 10,000 ppm. The results indicate that an optimum salinity does exist for the studied system and altering the salinity of the reservoir during water injection will result in changing the contact angle of the flooded area and consequently the performance of the flooding process. What he measured is the receded angle by the definition above.

Rao (2003) and Vijapurapu (2002) reported that using a mixture containing 75% Yates brine and 25% deionized water, the oil drop spreaded completely on the dolomite surface as indicated by a receding contact angle of about  $173^\circ$ . They correlated this spreading behavior observed as an effect of changing brine dilution against the oil-brine interfacial tension and found that if the interfacial tension between the fluid pairs falls below the critical spreading tension (CST), then the drop-phase would spread on the solid surface with a large water-receding angle. The dilution of Yates brine caused an initial decrease and a later increase in interfacial tension, having a minimum interfacial tension at the 50-50 mixture composition.

### **2.3.7 Summary**

Historically, all petroleum reservoirs were believed to be strongly water-wet. However, this assumption came to be increasingly challenged as numerous investigators showed that wettability actually ranged from strongly water-wet to strongly oil-wet, with

many possible intermediate stages (Rao, 2002). Recently, some reservoir rocks are believed to be mixed-wet. Polar components in the crude oil have been found to alter wettability. The real wettability of a reservoir and its sensitivity to alteration are difficult to predict by its geological properties.

No single industry-wide accepted method for wettability determination for all situations exists. Most widely used methods have some limitations of their own.

The differences in the definition of contact angle used by several researchers have caused confusion while comparing their works.

In order to measure the native state wettability of a subsurface reservoir, the same conditions as in the reservoir must be simulated in the laboratory. Unfortunately, due to inherent limitations, most basic wettability studies reported in the literature used one or more simplifications, such as decane or toluene instead of live crude oil, water instead of brine, and pure mica or quartz instead of reservoir rock, ambient pressure and temperature instead of reservoir pressure and temperature. These simplifications may lead to wrong conclusions. The actual reservoir conditions must include the reservoir temperature, pressure, reservoir brine, reservoir rock and live crude oil. To meet these requirements, a high-pressure high-temperature Dual-Drop-Dual-Crystal Optical System has been set up for this study. This is the primary aspect of this project to evaluate reservoir wettability and its alterations at actual reservoir conditions of pressure, temperature and fluids composition.

## **2.4 Surfactants**

A surfactant is a polar compound, consisting of an amphiphilic molecule, with a hydrophilic part (anionic, cationic, amphoteric or nonionic) and a hydrophobic part. As a result, the addition of a surfactant to an oil-water mixture would lead to a reduction in the interfacial tension.

In the past time, the surfactants were used to increase oil recovery by lowering IFT. Later on, due to the difficulty of initiating imbibition process in oil-wet carbonate rocks, many researchers have focused on how to alter the oil-wet carbonate to water-wet by using surfactants. The most successful method reported is the surfactant flooding in the presence of alkaline.

There are a number of mechanisms for surfactant adsorption such as electrostatic attraction/repulsion, ion-exchange, chemisorption, chain-chain interactions, hydrogen bonding and hydrophobic bonding. The nature of the surfactants, minerals and solution conditions as well as the mineralogical composition of reservoir rocks play a governing role in determining the interactions between the reservoir minerals and externally added reagents (surfactants/polymers) and their effect on solid-liquid interfacial properties such as surface charge and wettability (Somasundaran and Zhang, 2004).

### 2.4.1 Surfactant Types

Depending upon the nature of the hydrophilic group, the surfactants are classified as (Rosen, 1978):

1. Anionic – the surface active portion of the molecule bears a negative charge, for example,  $\text{RC}_6\text{H}_4\text{SO}_3^-\text{Na}^+$  (alkyl benzene sulphonates)
2. Cationic – the surface active portion bears a positive charge, for example  $\text{RNH}_3^+\text{Cl}^-$  (salt of long chain amine)
3. Amphoteric or Zwitterionic – both positive and negative charges may be present in the surface active portion, for example  $\text{RN}^+\text{H}_2\text{CH}_2\text{-COO}^-$  (long chain amino acid)
4. Nonionic – the surface active portion bears no apparent ionic charge, for example,  $\text{RCOOCH}_2\text{CHOHCH}_2\text{OH}$  (monoglyceride of long chain fatty acid )

When a surfactant is injected into a reservoir, it disperses into oil and water and thus creates a low IFT zone, in which the capillary number increases greatly. As a result, more of the residual oil becomes mobile. Also, it is believed that some surfactants can alter wettability too. From Equation (1), if chemicals change the contact angle somehow to near 90 degrees, the capillary number would be significantly increased. To identify such kind of surfactant, an accurate measuring technique for contact angle is essential because it is very difficult to get the contact angle at low IFT status.

The main properties of surfactants are the effect of hydrophobic and hydrophilic behavior and micelle formation. At high concentrations, the formation of organized aggregates of large numbers of molecules called micelles. Figure 7 shows the illusion presented by Hiemenz and Rajagopalan (1997). The formation of micelles in aqueous solution is generally viewed as a compromise between the tendency for alkyl chains to

avoid energetically unfavorable contacts with water, and the desire for the polar parts to maintain contact with the aqueous environment (Schramm, 2000).

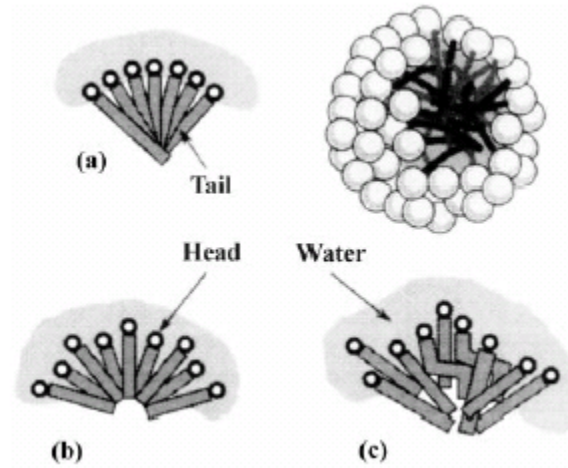


**Figure 7: Schematic Representation of the Structure of an Aqueous Micelle**  
 (a) overlapping tails in the center; (b) water penetrating to the center and (c) chains protruding and bending. (Hiemenz and Rajagopalan, 1997)

#### 2.4.2 Surfactant-induced wettability alteration

Although the surfactants are widely used in other areas, surfactant-induced EOR has been limited in the oil industry due to uneconomical field applications. Hence the relative studies related to its application in the oil industry are not adequate in comparison with the other areas.

Babadagli (2003) compared the oil recovery for four different rock types (sandstone, limestone, dolomite and chalk), a wide variety of oils (light and heavy-crude, kerosene, and engine oil) and different types (non-ionic and anionic) and concentrations of surfactants in laboratory tests. He found that except for light oil, the same non-ionic surfactant solution yielded a higher ultimate recovery and faster recovery rate. When an anionic surfactant was used in chalks, a higher surfactant concentration yielded higher recovery but lower surfactant concentration resulted in even lower recovery than the brine case. The ultimate oil recovery is correlated with the inverse bond number.

Hirasaki and Zhang (2004) reported that an alkaline-anionic solution altered the calcite plate to preferentially water-wet (intermediate) conditions.

According to Seethepalli et al. (2004), anionic surfactants have been identified that can change the wettability of the calcite to an intermediate/water-wet condition as well or



better than a cationic surfactant with a West Texas crude oil. The adsorption of the sulphonate surfactants can be suppressed significantly by the addition of the  $\text{Na}_2\text{CO}_3$ .

The adsorption of surfactants certainly has influence on the stability of thin water film between oil and rock. The EOR by surfactant flooding is a function of initial and altered wettability as well as the initial and changed interfacial tension. The injection concentration of surfactant is also important.

## **CHAPTER 3. EXPERIMENTAL APPARATUS AND PROCEDURES**

Two widely used experimental techniques namely Dual Drop Dual Crystal (DDDC) technique (Rao and Girard, 1996; Rao, 2002) for contact angle measurements and Drop Shape Analysis (DSA) for IFT measurements (Kruss Manual, 2002) have been chosen. The experiments were carefully planned using a newly built apparatus and chosen experimental techniques in order to complete the research objectives of this study.

### **3.1 High Pressure High Temperature Dual Drop Dual Crystal Apparatus**

A high pressure and high temperature apparatus has been built to measure IFT and contact angles at elevated pressures and temperatures at LSU. This system was built with the financial support from Louisiana Board of Regents and Marathon Oil Company. The fabrication and assembly of the setup were completed in summer, 2004. Most experiments of this study are conducted using this unique system.

The core part of this system is an optical cell that was fabricated by the Petroleum Recovery Institute, Canada. It has a design rating of 20,000 pisa at 200°C (Figure 8, Figure 9).

Four adjustable arms make this cell unique. The top one and a side one are used to hold rock crystals, the other side arm is used to hold a calibration ball, and the bottom arm has a needle tip which can form a pendent drop and place the oil drop on a rock surface. All these arms can rotate as well as move in and out.

The other accessories include an oven which is used to adjust temperature, some high-pressure vessels and valves to hold and transport fluids, and an imaging capture system. The imaging capture system includes a high-quality digital camera and a light source. It is connected to the computer, monitor and video recorder. Computer software can capture the image and calculate interfacial tension.

### **3.2 Ambient Dual-Drop-Dual-Crystal Apparatus**

The ambient Dual-Drop-Dual-Crystal (DDDC) cell and the associated apparatus for carrying out the contact angle tests at ambient conditions are shown in Figure 10. It has the same functions as a high-pressure high-temperature cell but it has a larger volume and can operate only at ambient conditions.

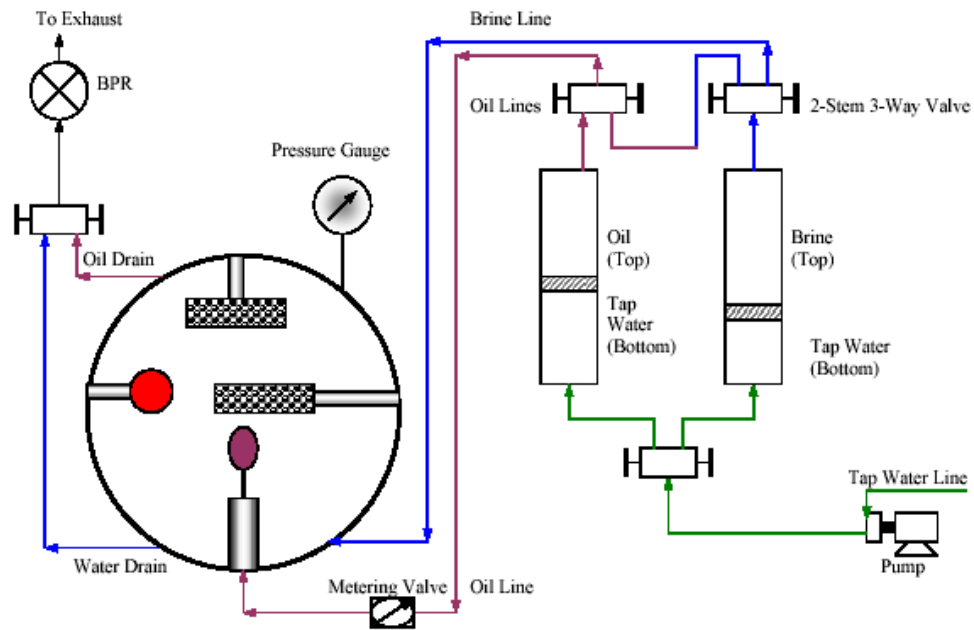


**Figure 8: Flowchart of High Pressure High Temperature Dual-Drop Dual-Crystal System at LSU (Rao et al, 2004)**

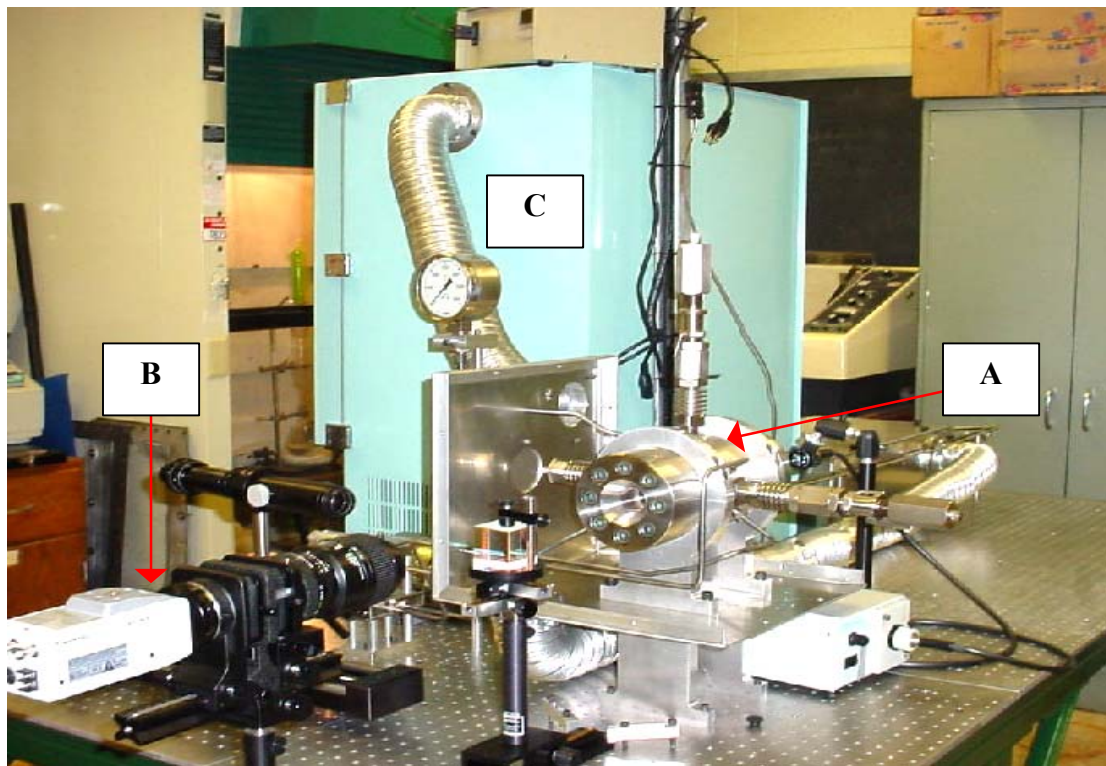


**Figure 9: High Pressure High Temperature Dual-Drop Dual-Crystal System (Rao et al, 2004)A: High Pressure Optical Cell; B: Digital Camera; C: Oven**

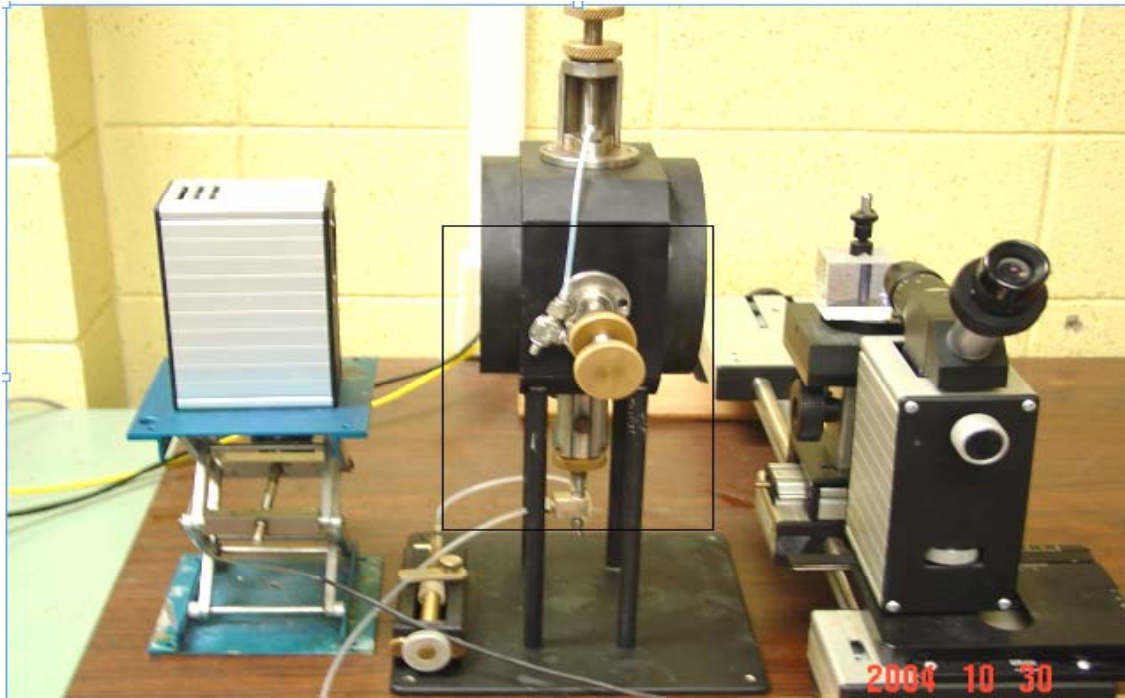


**Figure 10: Ambient Dual-Drop-Dual-Crystal (DDDC) Apparatus at LSU**

### **3.3 DSA Technique and Dynamic IFT Measurement Procedure**

According to the accuracy and suitability of classical techniques used in interfacial tension measurements (Table 1), the pendant drop method is identified as the best one for this study. Commercial software, called Drop Shape Analysis (DSA), has been used to calculate interfacial tensions.

Pendant oil drops are injected into a DDDC cell (ambient or HTHP) that is already filled with brine. Pre-equilibration of oil and brine is required before the measurement. As soon as the pendant drop reaches the maximum volume, close the valve. The computerized software program begins to record and calculate the IFT at the rate of 3 seconds per value. Without the influence of other environments, the pendant drop can stay for a long time on the tip. The density of liquids and temperature are the required inputs to the calculation procedure. The system can automatically run as long as the drop stays in view. Normally measurements of about ten drops are made to obtain the average value of IFT.

### 3.4 DDDC Contact Angle Measurement Procedure

The detailed procedure of this measurement technique can be found elsewhere (Rao and Girard, 1996; Rao, 2002). In this technique, both oil drops on the two crystal surfaces are aged as sessile drops with buoyancy forces acting upwards, producing oil contacted rock surface. It also can save a lot of aging time in comparison with the traditional modified sessile drop method. By turning the lower crystal upside down and mingling the two oil drops, the advancing and receding contact angles can be measured by shifting the lower crystal laterally, which also helps in monitoring, without any ambiguity, of the solid-oil-water three phases contact line (TPCL) movements within the areas previously exposed to crude oil (Figure 11, 12). The measurement is reproducible by moving the oil drop back to the original position.

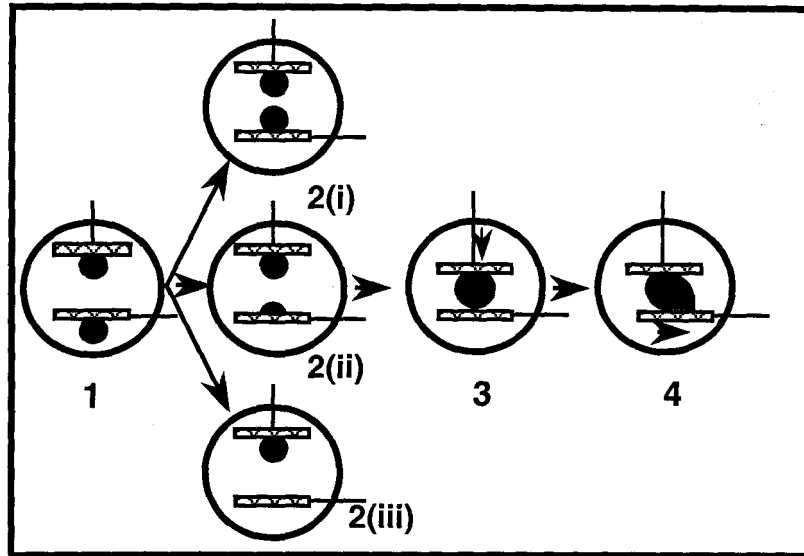


**Figure 11: Schematic Depiction of the New Dual-Drop-Dual-Crystal (DDDC) Contact Angle Technique (Rao and Girard, 1996)**

### 3.5 Surfactant-Injection Simulation Procedure

A high-pressure high-temperature (HPHT) optical cell and a related operational process system have been set up for Dual-Drop-Dual-Crystal (DDDC) dynamic contact angle and oil-water interfacial tension measurements. A new experimental procedure was developed in which crude oil equilibrated with reservoir brine in the rock matrix has been

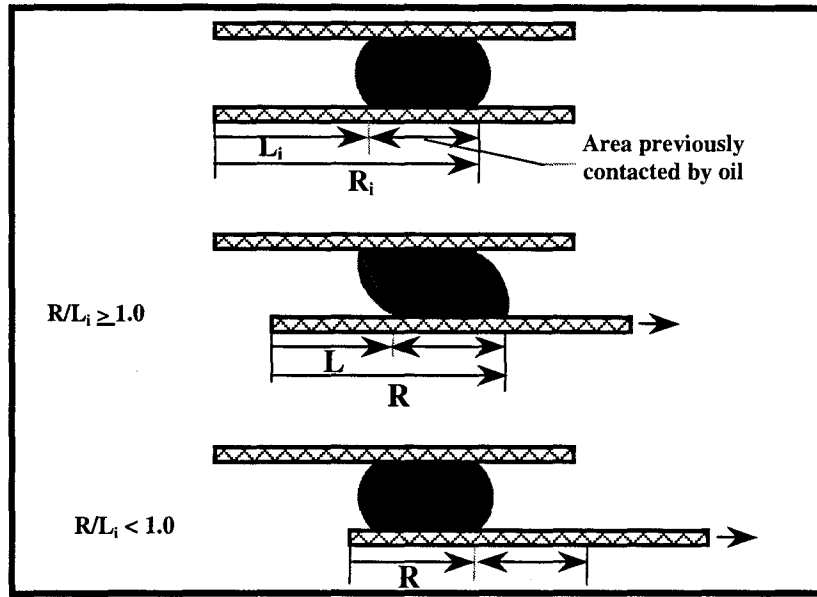


**Figure 12: Monitoring TPCL movement** (Rao and Girard, 1996)

exposed to surfactant injection to simulate the matrix-fracture interactions at reservoir conditions of temperature and pressure. This new procedure involves the following steps:

- Load crystals, pre-aged in brine, into the HPHT cell. Open all valves along the brine line. Pump the brine into the cell to fill and continue to pump brine to increase the pressure to reservoir pressure using a backpressure regulator.
- Check for leaks. Start the oven and set temperature to reservoir temperature (82-83 °F).
- Let 10-12 oil drops float at the top in brine for fluid equilibration. Then, capture the image of a pendant oil drop and measure the interfacial tension (IFT) between brine and crude oil by using the Drop Shape Analysis (DSA) technique. Repeat the measurements for at least 10 images of the oil drops to obtain an average value and the standard deviation.
- Place a drop of oil on each of the two crystals and measure the sessile drop water-receding angles.
- Close all the valves of the system and let the two drops on the two crystal surfaces age for 24 hours under reservoir pressure and temperature.
- Measure the equilibrium receding angles on both the surfaces after aging.

- Measure the  $L_i$  and  $R_i$  (Figure 11) of the drop on the lower crystal surface. Turn the lower crystal surface upside down and mingle the drop with the drop on the upper surface. Shift the lower crystal sideways. Measure the advancing and receding angles and TPCL movement.

- Repeat the above step, to make sure that the contact angles are reproducible.

- Bring the drop back to the equilibrium position between the two crystal surfaces. Switch the brine tank to surfactant tank and pump the surfactant containing brine into the cell from the bottom. Maintain the same reservoir temperature and pressure.

- Pump enough surfactant containing brine to make sure that all the normal brine in the cell is replaced with surfactant containing brine (Since the volume of the cell is 70 ml, at least about 1000 ml, 12 times the volume of the cell is pumped to assure that the brine in the cell contains the desired concentration of the surfactant).

- Record the entire injection process using a video camera. Especially, pay attention to the times when the oil drop begins to move. The data recorded can be used later for further analysis of drop diameter and TPCL movements.

- After injection, two crystals are moved closer to mingle the oil drops. The time required for mingling the two drops varies for different surfactant concentrations. If able to mingle the drops, measure the advancing contact angles.

- Measure the IFT between the crude oil and the surfactant containing brine.

- Try to place another oil drop on the other surface of lower crystal not previously exposed to oil to measure the receding angles. Age overnight to attain equilibrium. Measure the advancing contact angle by shifting the lower crystal, if possible. Turn the lower crystal upside down to observe the behavior of the oil drop placed on it.

### **3.6 Other Miscellaneous Procedures**

*Live oil* is prepared according to the Yates live oil composition (Table 2). This is done by adding a certain volume of gas ( $C_1$  to  $C_5$ ) to Yates stocktank oil at high pressure and

shaking for long periods. The measured bubblepoint pressure of this synthetic live oil is about the same as Yates reservoir bubblepoint (650-680 psi).

**Table 2: Compositions and properties of Yates Live Oil (Rao et al., 2004)**

Component	Molecular Weight	Live Oil Mole fraction	Z Factor	Density g/cc	Pressure		Volume Added cc gas/mol Live Oil
					kPa	psig	
N <sub>2</sub>	28.000	0.012013	0.9873	---	3500	508	8.521
CO <sub>2</sub>	44.100	0.053261	---	0.7399	6895	1000	3.174
C <sub>1</sub>	16.010	0.092727	0.7993	---	20685	3000	9.010
C <sub>2</sub>	30.100	0.035863	---	0.3644	6206	900	2.962
C <sub>3</sub>	44.090	0.021439	---	0.5277	1400	203	1.808
C <sub>4</sub>	58.120	0.035741	---	0.6084	700	102	3.414
C <sub>5</sub>	72.146	0.027104	---	0.6262	89	13	3.123
C <sub>6+</sub>	245.141*	0.721846	---	0.8779	3447	500	201.565**
Total		1.000000					233.577
* Analyzed by a commercial laboratory. ** Volume of Stock Tank Oil per Mole of Live Oil.							

*Deasphalting procedure* is the standard ASTM recommended procedure (ASTM D2007-80). 40 times higher the volume of pentane was added into the Stocktank oil and shaken well for two days, and then filtrated with 0.22 um membrane filter paper. Pentane solvent is removed from the deasphalted oil by a standard rotary evaporator. De-resining (SARA) is done by an open-column liquid chromatography method (Silica Gel).

*Rock substrates* are cut into pieces and then polished by different sized diamonds or sandpaper. All crystals need to be polished and cleaned again before using for contact angle measurements. The rock roughness is analyzed using the Scanning Electron Microscopy at CAMD, LSU.

*Yates Synthetic Brine* is prepared using the composition provided by Marathon Company. Certain weights of salts were added into deionized water. After mixing, the brine is deaerated by a vacuum pump before use.



The rock substrates are obtained from Ward's Company. All chemicals are from Fisher Scientific. Stocktank oil and dolomite cores are supplied by Marathon Oil Company.

## **CHPATER 4. RESULTS AND DISCUSSIONS**

Reduction of interfacial tension and alteration of wettability are the two main mechanisms behind the use of surfactants for enhancing oil recovery. To study these two mechanisms, the accurate and dynamic measurements of IFT and contact angle at reservoir conditions are necessary. As summarized in literature review, most of previous study were done at ambient conditions and used stocktank oil. In this chapter, the results obtained from live crude oil experiments at reservoir temperature and pressure are presented and discussed.

The dynamic behavior of interfacial tension is caused by the surfactants in both fluids hence it is a good indicator to evaluate the interfacial interactions in chemical flooding. The restoration of initial reservoir wettability and its alteration mechanism by different surfactants have troubled the oil industry for a long time. The effect of fluids composition, rock characteristics, temperature and pressure on both IFT and wettability also need further investigations. These issues are discussed in this chapter according to related experimental results.

### **4.1 Dynamic Interfacial Tension in Crude oil – Brine System**

It is widely believed that two immiscible liquids can be brought to mutual saturation easily. If this is true, the interfacial tension between two liquids at this stage should remain unchanged. However, in all our IFT measurements of Yates crude oil – brine, it is found that the IFT is time-dependent. The ambient experiments were conducted after allowing oil and brine to pre-equilibrate by mixing with a stirrer for more than 24 hours. The high-pressure high-temperature experiments were conducted after pre-equilibrating 25-volume% oil and 75-volume% brine together for more than one week. In order to explain the time-dependent behavior of IFT with pre-equilibrated fluids, several experiments were conducted.

To determine the time needed for equilibrium, the high-pressure high-temperature cell was filled with 75-volume% Yates brine and 25-volume% Yates live oil under Yates reservoir temperature and pressure (82°F and 700 psi). After aging for two weeks, a pendant drop was formed inside the cell. The changes in IFT were continuously

monitored and recorded for nearly a month using the DSA software program. The recording time interval was 3 seconds at the beginning, and then 1 minute after 2 hours. The first contact IFT (at 0 second) was 31.7 mN/m. The average equilibrium IFT of Yates fluids system was about 23.77 mN/m in the third day, 23.6 mN/m from the fourth to the eighth day, and 23.54 mN/m in the eleventh day. From this long duration experiment, it was concluded that the equilibrium status of crude oil and brine could be finally reached in several days (Figure 13). It was also found that most of the decrease of IFT was happened at the first one hour.

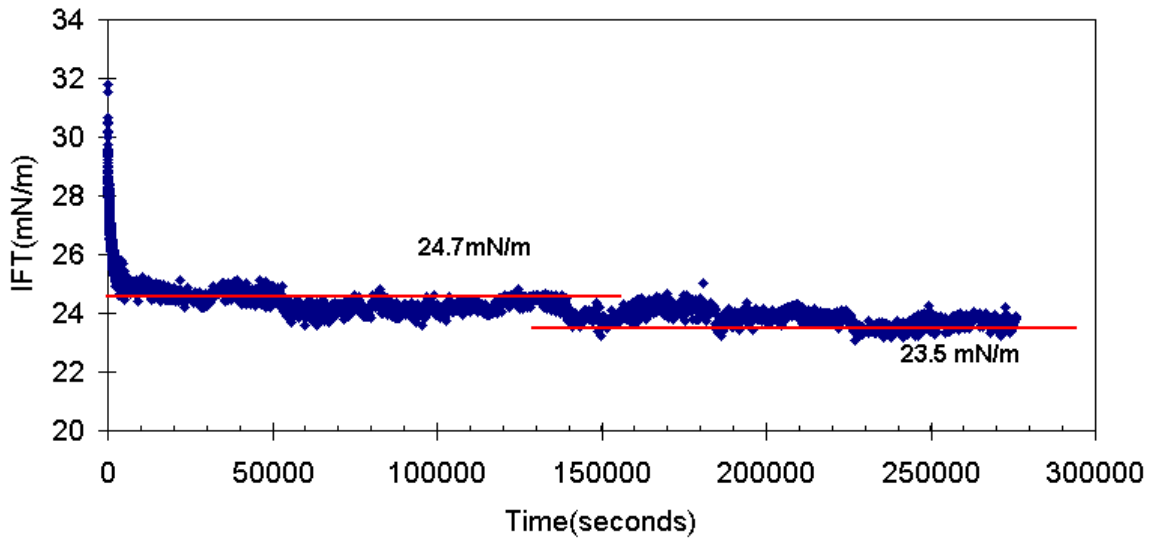


**Figure 13: Dynamic Interfacial Tension of Yates Live Oil/Yates Brine at Reservoir Conditions (82°F and 700 psi, over a time period of 10 days)**

Next, it was planned to find the optimum measuring time for IFT measurements. If the equilibrium IFT was 23.5 mN/m for Yates live oil / Yates brine at reservoir conditions, then to minimize the measuring time, the time corresponding to  $23.5 \times 1.05 = 24.7$  mN/m, which is within 5% of the equilibrium IFT, was used as the terminating time. From Figure 13, it can be seen that this value was reached at about 16000 seconds (4.5 hrs). This time was still quite long for IFT measurements. However, for getting the true equilibrium IFT data, long aging time is essential. For dynamic analysis, the trends in IFT-time plots were used to predict equilibrium IFT (when  $t = \infty$ ).

#### **4.1.1 Effect of Crude Oil Composition**

In order to find the controlling parameters of time-dependent IFT behavior, the analysis of influence of different components on IFT was necessary. Decane and toluene

were selected to represent saturates and aromatics. Asphaltenes fraction separated from the Yates crude oil using standard procedure (Chapter 3) was used to represent polar components (asphaltene and resin). The other liquid was degassed de-ionized water. First, the time-dependent behavior of each pure component was studied, and then the time-dependent IFT behavior of multi-component mixture was studied by mixing the pure components. By comparing these results with the crude oil case, the influential component was identified (Table 3).

**Table 3: Interfacial Tension of Different Oil Components**

Fluid-Fluid System	IFT <sub>0</sub>	IFT <sub>e</sub>	condition
decane /water	56	55	ambient
Toluene/water	36.9	36.1	ambient
50%decane+50%toluene(volume)/water	39.8	39.5	ambient
Toluene+3g/100ml asphaltene/water	25	21	ambient
Toluene+0.27g/100ml asphaltene/water	31.5	25	ambient
Deasphalted oil /brine	33.23		ambient
Stocktank oil /brine	26.66	20.5	ambient
Stocktank oil/brine	32.43	15.2	82°F700psi
Live oil /brine	34.8	23.5	82°F700psi

IFT<sub>0</sub>: The first contact IFT, IFT<sub>e</sub>: Equilibrium IFT

From Figure 14, it can be seen that the IFTs of toluene, decane and their mixture were nearly stable with time. The pure hydrocarbons had stable behavior and attained equilibrium IFT quickly. The slight linear decrease of IFT with time was caused by drop volume decrease due to leakage through the syringe in the ambient cell. However, the IFT of toluene containing asphaltene was noticeably time-dependent. The asphaltene used here was nC<sub>5</sub>-insolubles extracted from Yates crude oil. Asphaltenes were defined as the fraction precipitated by addition of a low-boiling paraffin solvent such as normal-pentane and which was soluble in benzene. Asphaltenes were not crystallized and could not be separated into individual components or narrow fractions.

Further experiments were conducted at 700 psi pressure using HPHT cell and the results are shown in Figure 15. Pentane, Yates stocktank oil (STO) plus 40 times pentane solution, and its filtrate obtained by using 20 μm filter paper (deasphalted oil (DAO) + pentane) were the oil phases, while Yates reservoir brine was the water phase. The IFT

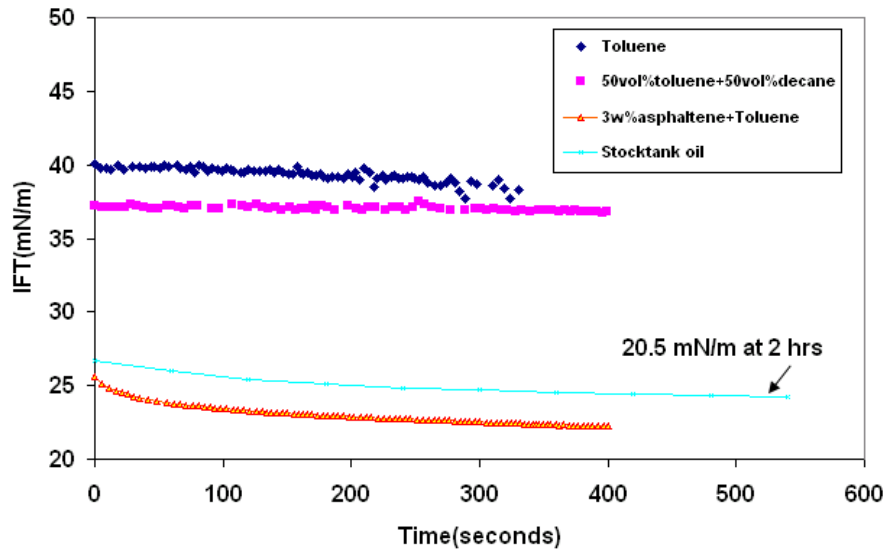


**Figure 14: Dynamic Interfacial Tension of Different Oil Components in Deionized Water at Ambient Conditions using the Ambient Optical Cell**

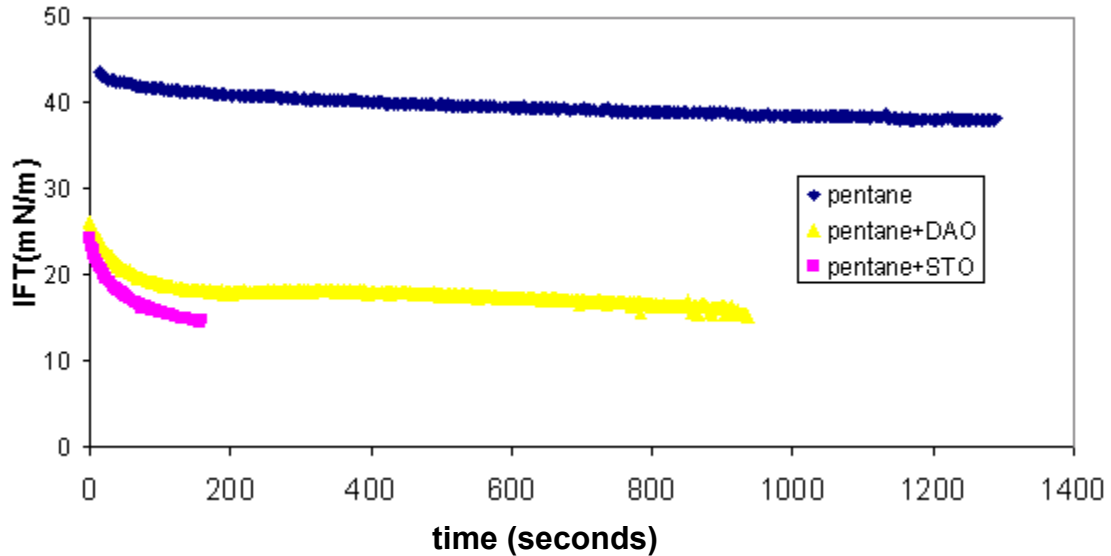


**Figure 15: Dynamic Interfacial Tension of Different Oil Components in Yates Brine using HTHP Optical Cell (700psi & 71°F)**

between pentane and brine slightly decreased with time due to impurities and solubility. The IFT of stocktank oil plus pentane solution was about half the value of pentane. It also significantly decreased with time for the first 100 seconds. While the filtrate containing less asphaltenes had almost the same IFT, it decreased with time at a slower rate. Obviously the asphaltenes seemed to be one of the components in crude oil that is responsible for the dynamic behavior of IFT. Although the deasphalting technique used

in the study is the standard technique employed by the industry, it was impossible to remove all the asphaltenes. There were also resins that could not be removed by filtration. The resins were also polar surface-active materials. This is the reason that the IFT of the filtrate (DAO+ pentane) displayed dynamic behavior. The stability of pendant drop is also represented by the staying time on the needle tip. Figure 15 shows that the STO+pentane solution could stay for only about 150 seconds on the tip.

Resins and asphaltenes are important compounds in the crude oils. There is a close relationship between asphaltenes, resins, and high molecular weight polycyclic hydrocarbons. In IFT experiments reported by others (Hirasaki and Zhang, 2004), the impurities are considered to be responsible for time-dependent behavior. Since impurity is a character of crude oil and asphaltenes exist in all reservoir crude oils, this behavior cannot be avoided. On the other hand, upon adsorption at the oil/water interface, it is believed that asphaltenes slowly form a glassy interphase, which is likely the reason for prolonged stability of crude oil - water emulsions and for the propensity of asphaltenic crude oils to alter the wettability of reservoirs. Hence the dynamic behavior of crude oil IFT is a key to understanding interfacial mechanisms occurring in oil reservoirs.

Most of the other dynamic IFT studies are focused on the surfactant-induced change. Asphaltenes can be considered as natural surfactants. The N, S, O elements in its structure distinguish it from the hydrocarbons. Being polar in nature, asphaltenes are surface-active substances. They can modify significantly the properties of interfaces by adsorption.

The light ends in crude oil also had influence on IFT. Yates live oil was prepared by adding measured amounts of lighter ends (methane to pentane) to the stock-tank oil according to the production gas-oil ratio (Table 2). Figure 16 shows the IFT behavior of live oil at reservoir conditions and stocktank oil at ambient conditions. It can be seen that the IFT of stocktank oil was much lower than that of live oil and live oil was able to reach equilibrium faster than stocktank oil. The almost linear decrease of stocktank oil IFT at the later stage represents higher activity of surface-active materials. It is also noticeable that a pendant drop of live oil at reservoir conditions could stay on the tip for a long time (at least more than one month as observed in Figure 13) where the stocktank oil couldn't due to the same reason. The general difference of IFT between live oil and

stocktank oil was due to the decrease of density in live oil but the difference of time-dependant behavior is not very clear. It is believed that the light ends may have decreased the concentration of asphaltene in the oil and hence changed the behavior of IFT. It may also have decreased the formation and the size of asphaltene aggregates. The dynamic influence of light ends on IFT needs to be further studied in the future. The mass transfer by slow diffusion of light fractions from crude oil into the brine and the consequent change in the chemical composition of both phases could indeed be one of the reasons for the observed time dependent behavior of live oil - brine IFT.

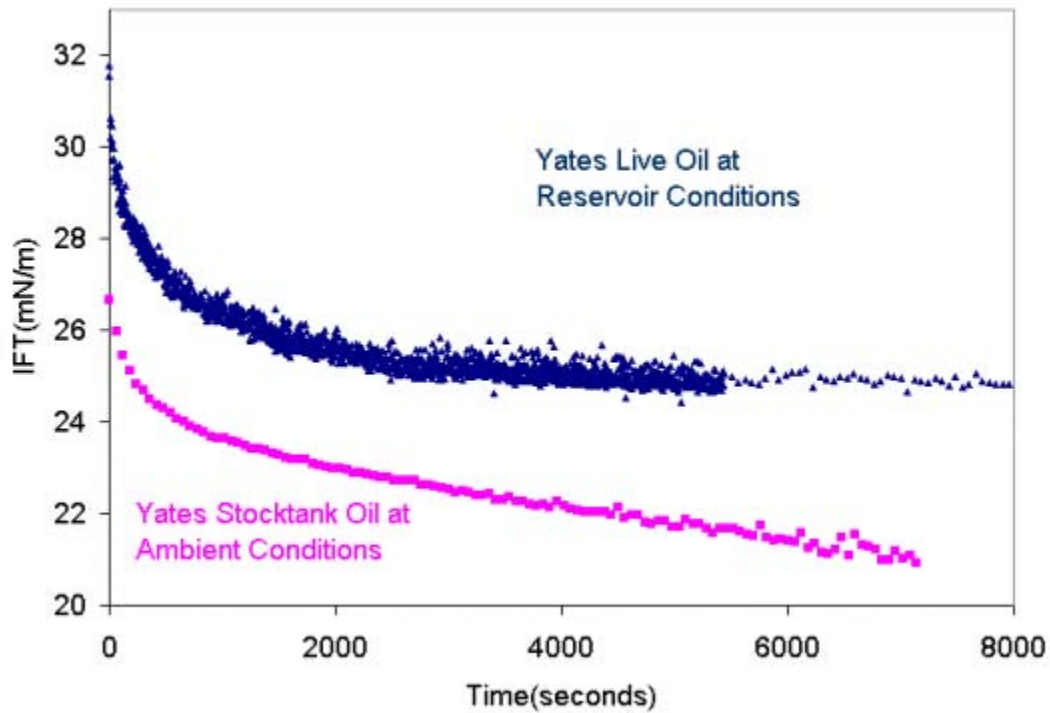


**Figure 16: Comparison of Time-dependent behavior of Interfacial Tension (Yates Live Oil and Yates Stocktank Oil)**

#### 4.1.2 Effect of Brine Composition

Using the same Yates live oil phase, the effect of brine composition was studied by changing salinity and salt composition. Figure 17 shows that dynamic IFT of deionized water, 50% Yates brine in deionized water and 100% Yates reservoir brine had similar slopes when plotted against  $\log(t)$ . The dilution did not influence IFT's dynamic behavior but it increased the value of IFT compared to IFT of Yates brine. Same compositions have same electrostatic behavior. The IFTs in the NaCl solution and  $\text{CaCl}_2$

solution displayed different slope from that of Yates brine. The IFT of live oil in the pure  $\text{CaCl}_2$  solution has the highest equilibrium IFT value.

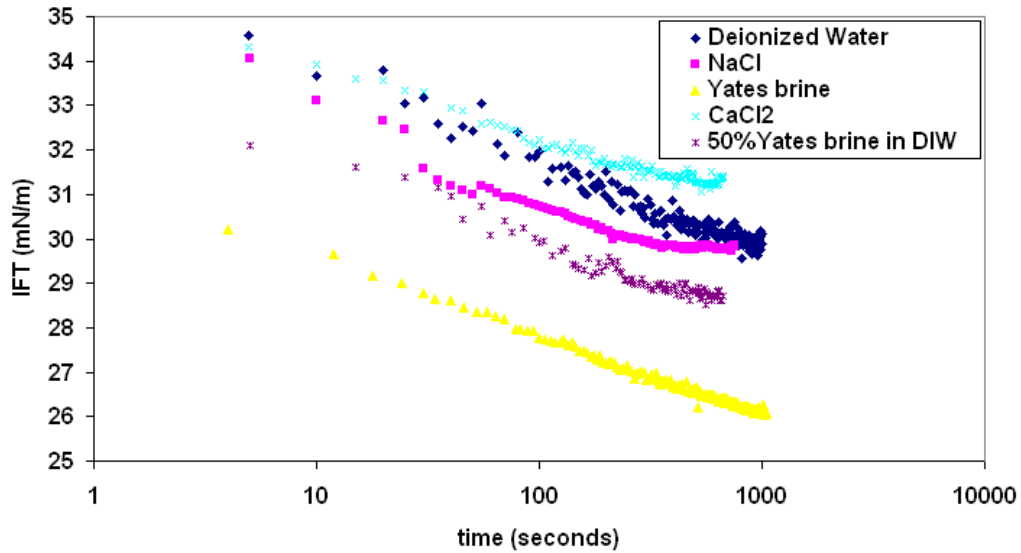


**Figure 17: Dynamic Interfacial Tension of Yates Live Oil against Different Brines at Reservoir Conditions (82°F & 700 psi)**

Optimal salinity is a useful term in EOR process. It was used to describe the salinity of the lowest IFT point at alkaline and/or surfactant flooding. For example, Bagci et al. (2001) reported the IFT decreased and then increased with the increase of salinity of NaOH and  $\text{NaSiO}_4$ . Figure 18 is a plot of the interfacial tension versus increasing sodium chloride concentration between oil-microemulsion (OM) and microemulsion-brine (MB) phases in the presence of surfactant.

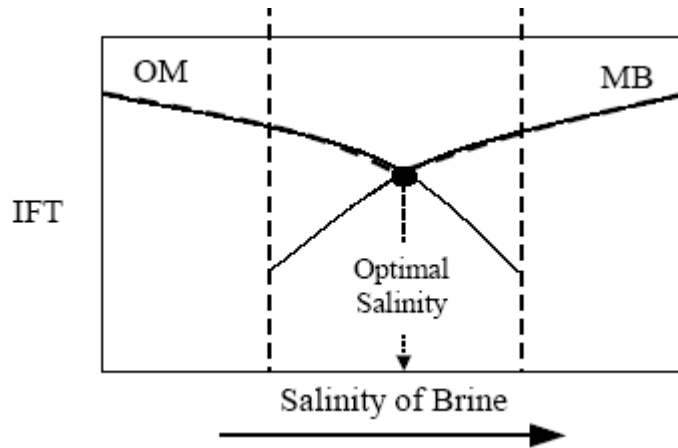


**Figure 18: Optimal salinity in oil recovery [5]**



The higher IFT of the OM or MB values was the controlling or limiting value as the surfactant solution flows in the reservoir. The IFT of OB (oil and brine) has the trend that decreases to the minimum IFT and then increases with the increase of salinity.

The dilution of Yates old brine at ambient conditions showed the similar trend as Figure 18 (Figure 19). The optimal salinity was reached at 50-50 mixtures of Yates brine and deionized water (Vijapurapu, 2002). The value of IFT decreased to about 10 mN/m from 27.9 mN/m (for 100% brine). The minimum IFT fell below Zisman-type critical spreading tension.

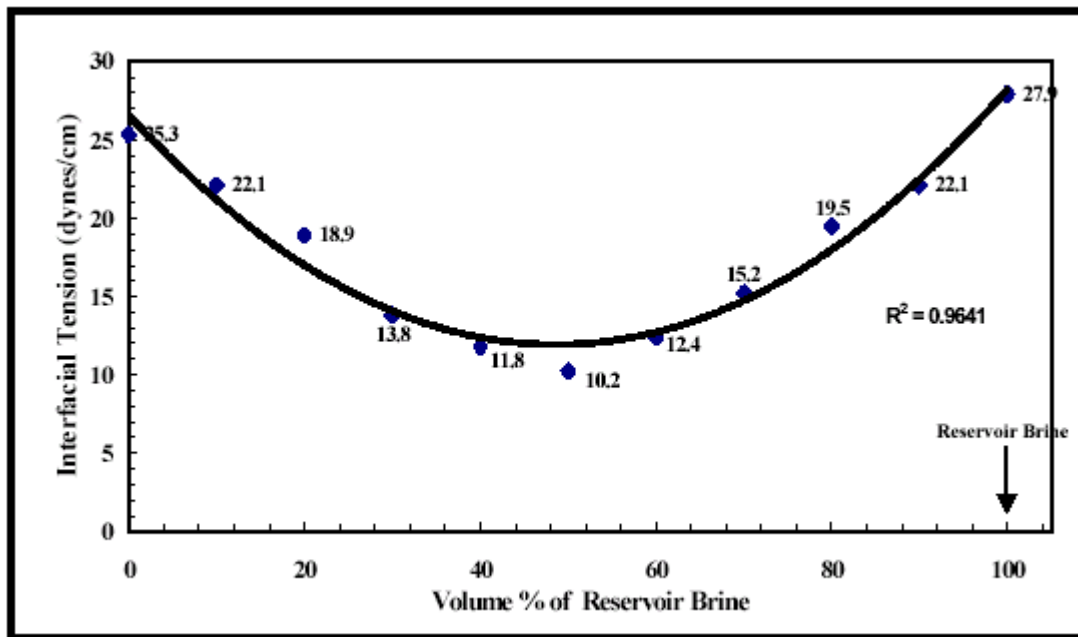


**Figure 19: Effect of brine dilution on Interfacial Tension between Yates Reservoir brine and Yates stocktank oil at Ambient Conditions (Vijapurapu, 2002)**

However, in contrast with stocktank oil, for Yates live oil, dilution of Yates new brine only caused the increase of IFT. The main difference between the two brines is that the old one had  $\text{NaHCO}_3$ , which is an alkaline. It caused microemulsion during dilution. Hence the IFT behavior of Yates stocktank oil during dilution of Yates old brine adapted the model described in Figure 18. It fell in the region of “optimal salinity” alkaline surfactant flooding category. However, the Yates live oil had a relatively higher IFT value than stocktank oil and the Yates new brine has no alkaline component. The optimum salinity was not observed during the experiments of Yates new brine dilution.

The increase of brine concentration caused decrease of the IFT of Yates live oil and brine. It fell in the first region (OM) in Figure 18.

#### 4.1.3 Effect of Temperature and Pressure

Much of the IFT experimental data reported in the open literature on IFT and wettability were collected under ambient conditions. However, for crude oil, the reservoir condition measurements are important in order to understand the interfacial behavior between oil, brine and rock. Therefore, it is important to make measurements at reservoir conditions in the studies of surfactant induced IFT reduction and enhanced oil recovery.

Figure 20 shows IFT of Yates live oil at a temperature of 136°F for different pressures. They have the same slope during the early time before equilibrium was reached. An IFT- $\ln(t)$  relationship was used to obtain  $IFT_0$ , the first contact IFT at zero time, and the equilibrium IFT which was calculated from the trend equation by  $IFT_e = IFT(4.5\text{hrs}) - 1$ . As shown in Figure 21, these two values have a good linear relationship with pressure. The IFT increased as the pressure increased. When the trend lines were extended to zero pressure, the  $IFT_0$  of 34.5 mN/m and  $IFT_e$  of 24.5 mN/m were obtained.

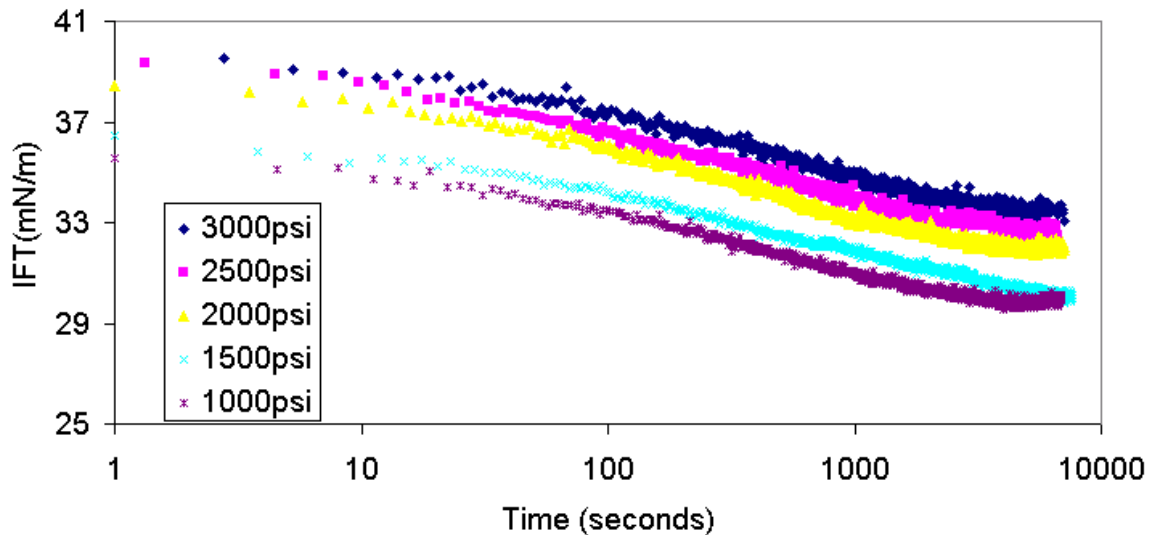


**Figure 20: Effect of Pressure on Dynamic Interfacial Tension of Yates Live Oil and Yates Brine at 136°F**

At room temperature of 74°F, also a similar linear trend of IFT versus pressure was obtained (Figure 22, and Figure 23) but with a lower slope. In Figure 22 and 23, the IFT at 500 psi was somewhat off the trend, because this pressure was lower than the measured bubble point pressure of 650 psi for Yates live oil, resulting in gas evolution from the live

oil. When the pressure continued to decline, the free gas bubbles evolved in the cell and the pendant oil drops did not stay on the tip anymore, making further measurement difficult.

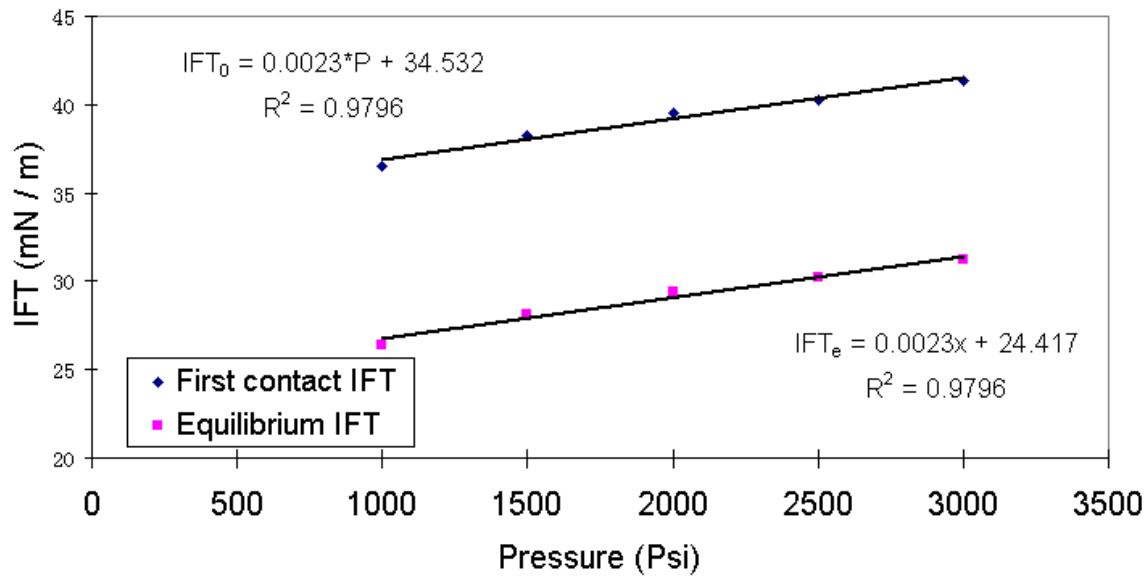


**Figure 21: Influence of Pressure on Interfacial Tension of Yates Live Oil and Yates Brine at 136°F**

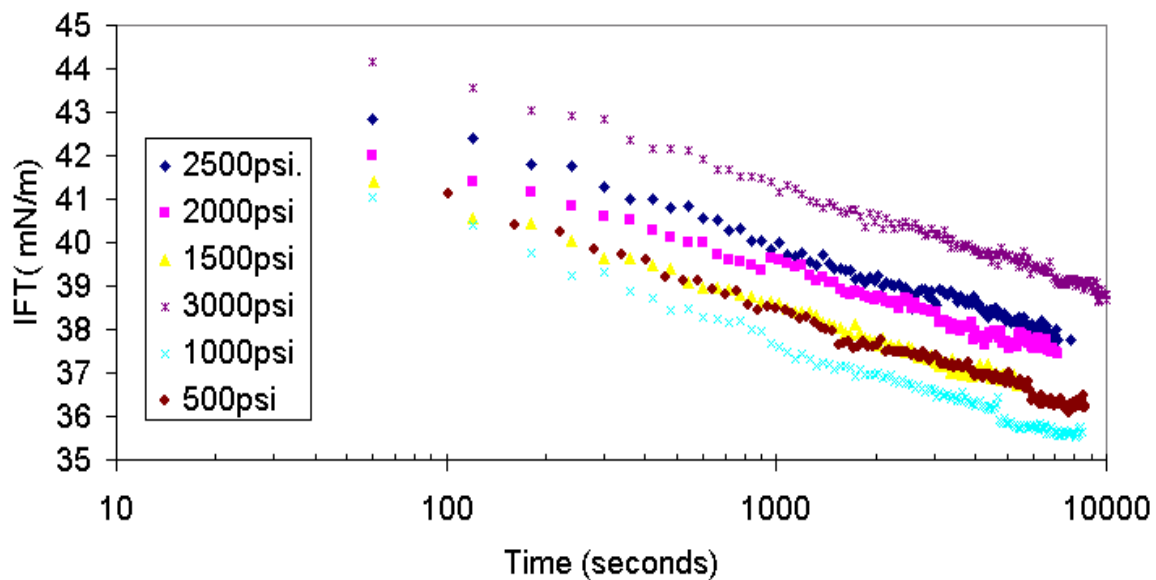


**Figure 22: Effect of Pressure on Dynamic Interfacial Tension of Yates Live Oil and Yates Brine at 74°F**

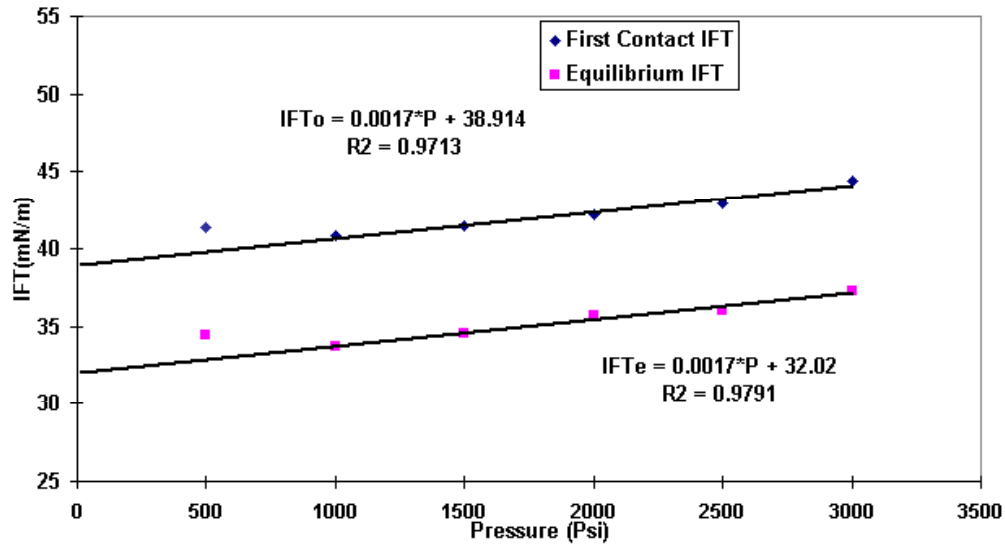


**Figure 23: The Effect of Pressure on Interfacial Tension of Yates Live Oil against Yates Brine at 74°F**

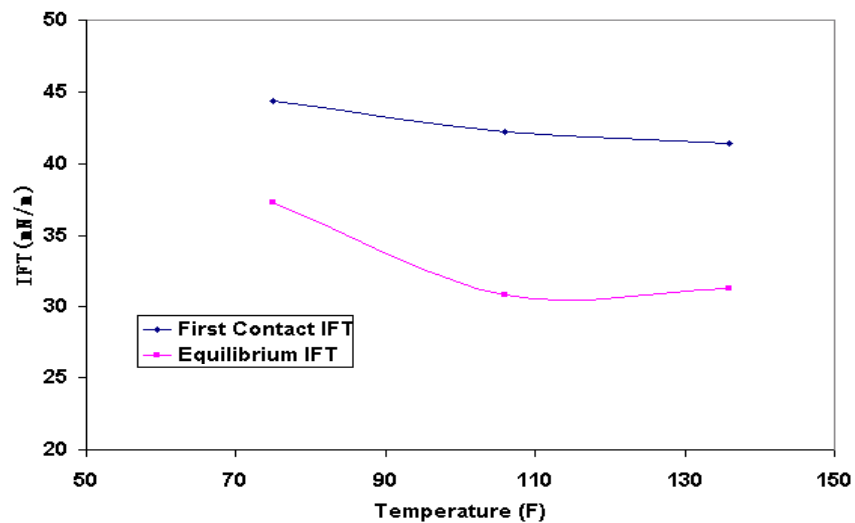


**Figure 24: The Effect of Temperature on Interfacial Tension of Yates Live Oil against Yates Brine at 3000 psi**

The above trends of IFT increasing with pressure and decreasing with temperature is in agreement with the literature review (section 2.2.4). It was also found that the dynamic behavior of IFT at different pressures (the slope of semi-log plots) is almost the same. Obviously, this time-dependent behavior is not related to pressure. This time-dependent behavior was also studied for the effect of temperature. Figure 24 is the IFT versus temperature at a constant pressure of 3000 psi. The IFT decreased as temperature increased, but it was not a strict linear relationship. This means that temperature had a remarkable influence on this time-dependent behavior. The higher the temperature, the

higher was the absolute value of slope. The reason is that the activities of surface-active materials increased with temperature. This made the equilibrium process of interfacial tension had a longer time and faster drop.

#### 4.1.4 Effect of Surfactant

Two surfactants were used in this study to evaluate their effects on IFT. One was a nonionic surfactant (Ethoxy Alcohol), the other one was an anionic surfactant (Ethoxy Sulfate). Each surfactant was mixed with Yates brine in concentrations of 500ppm, 1500ppm and 3500ppm respectively.

As the surfactant was injected into the cell, the oil-water IFT decreased. The pendant drop did not stay on the tip. For extra-low IFT, the spinning drop method is perhaps the best method but it cannot be used at high pressures. Therefore, the IFT was measured by DSA – pendant drop method in the present study. The IFT decreased with increasing surfactant concentration. It was also observed that it decreased with time, displaying a dynamic nature.

Figure 25 shows the dynamic IFTs of Yates live oil at different concentrations of Ethoxy alcohol (surfactant A). Figure 26 shows the dynamic IFT of Yates live oil at different concentrations of Ethoxy Sulfate (surfactant B). Table 4 shows the change of IFT at different concentrations.

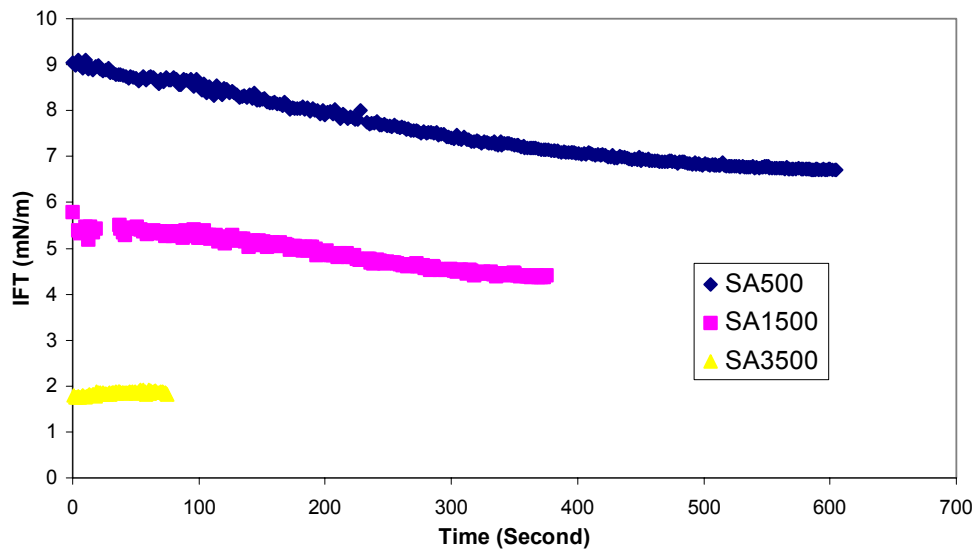


**Figure 25: The Effect of Nonionic Surfactant on Interfacial Tension of Yates Live Oil against Yates Brine at Reservoir Conditions (82°F & 700 psi)**

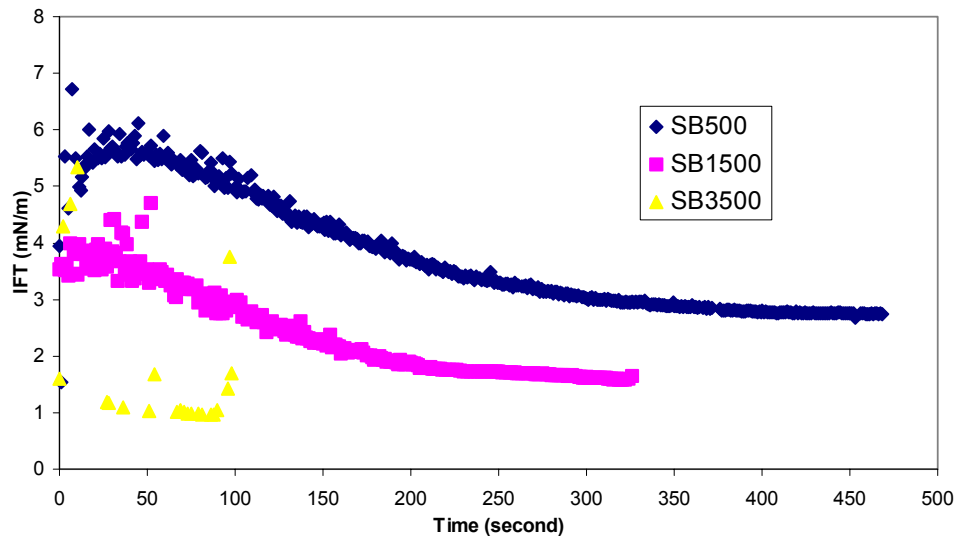


**Figure 26: The Effect of Anionic Surfactant on Interfacial Tension of Yates Live Oil against Yates Brine at Reservoir Conditions (82°F & 700 psi)**

Dynamic behavior of the two surfactants used is different. IFTs of surfactant A - oil system continuously decreased with time. While IFTs of surfactant B and oil increased with time first, and then decreased with time. This behavior influenced the time that the pendant drop stayed on the needle tip. Although the surfactant B system had lower IFT than surfactant A system, the pendant drop in surfactant B solution stayed on the needle much longer than surfactant A system. The dynamic behavior of IFT with the surfactant is an important indicator of the characteristics of surfactant. The charged behavior of surfactant B makes it more likely to be adsorbed than surfactant A. The surfactant adsorption induced adhesion of oil on the needle tip makes the pendant drop stay on the tip longer. However, the continuous decrease of IFT caused by interactions of surfactants finally resulted the detachment of the oil drop.

Table 4 shows the decrease of IFT with the increase of surfactant concentration. The IFT of live oil was only lowered one to two orders of magnitude by surfactant from the 25 mN/m to nearly 1 mN/m. The influence of IFT reduction on enhanced oil recovery caused by these two surfactants is not significant. IFT reduction can be effective in enhancing recovery only when it reduced by four to six orders of magnitude (Klins, 1984).

**Table 4 Effect of Surfactants on Dynamic Interfacial Tension of Yates Live Oil / Yates Brine at Reservoir Conditions (82°F & 700 psi)**

Surfactant	Surfactant concentration (ppm)	First contact IFT (mN/m)	Extended contact IFT (mN/m)	The drop staying time on needle (seconds)
A (nonionic)	500	9.05	6.7	605
	1500	5.79	4.41	375
	3500	1.79	1.82	75
B (Anionic)	500	3.94	2.47	1075
	1500	3.53	1.59	326
	3500	1.6	0.97	90

#### **4.1.5 Dynamic IFT Model of Crude Oil**

The experimental measurements were presented in the previous sections. Here an attempt is made to seek correlation between our measurement results with theoretical models in the literature.

- **Crude Oil**

In the published literature, there are two different theories to describe the dynamics of adsorption at liquid interfaces. The diffusion controlled model assumes the diffusional transport of interfacially active molecules from the bulk to the interface to be the rate-controlling process, while the so-called kinetic controlled model is based on transfer mechanisms of molecules from the solution to the adsorbed state and vice versa. The experimental verification of existing theoretical models of adsorption dynamics and the development of new correlations for more complex systems are discussed here.

For crude oil – brine system, the relaxation time of interface is much longer than that of oil – surfactant solution system. Existing models fail when the relaxation time of an adsorption layer (the interface) exceeds the characteristic time of surfactant transport. This situation occurs quite often because both the parameters change in a wide range of time. Systematic experimental investigations are necessary to cover the application range of the adsorption dynamic models. Further progress towards understanding the physical

mechanisms of so-called kinetic-controlled adsorption dynamics also requires special experimental studies (Dukhin et al., 1995). The application of the theoretical and experimental foundation of adsorption dynamics at liquid/fluid interfaces involving a live crude oil is therefore one of the objectives of this study.

It appears that the difference between crude oil and the other surfactant induced dynamic IFT behavior is that the crude oil needs a longer time to reach equilibrium. Some surfactant induced IFT changes cannot reach equilibrium and they can only attain minimum IFT in a certain time (Figure 5). The reason is that upon adsorption at the oil/water interface, asphaltenes slowly form a glassy interphase. This robust, asphaltene-rich interphase is likely the possible reason for prolonged stability of crude oil/water emulsions and for the propensity of asphaltenic crude oils to alter the wettability of reservoirs. Freer and Radke (2004) compared classical viscoelastic models with the measured rheologic data and found that the frequency response of the dilatational moduli fits a combination of diffusion-exchange and surface-rearrangement mechanisms. The combined relaxation model was verified by solvent washing of asphaltenes from the interface and measuring the dilatational response of the resulting irreversibly adsorbed species. After washout, the oil-phase diffusion component of the frequency response disappeared, and the relaxation time of the adsorbed film increased by an order of magnitude. They also found that most of the surface-active asphaltenic molecules were irreversibly adsorbed from the oil phase. In our case, it appears that the asphaltenes only existed on the periphery of oil drops, and could not diffuse into the surrounding brine phase. The conventional surfactant diffusion model (IFT versus  $1/\sqrt{t}$ , as in Figure 27 ) could not be simply used here. Figure 27 shows that the results display good linear relationships at several different time spans, which indicate the role of different mechanisms of interfacial interactions.

Models other than the approximate IFT –  $\log(t)$  linear approach, are discussed below. IFT versus  $\text{Sqrt}(t)$ : For diffusion control, if diffusion occurs at a short time, the IFT should be linear with  $\text{sqrt}(t)$  (Figure 28). A dimensionless form of IFT, based on the Lankveld and Lyklema's model (Lankveld and Lyklema, 1972) that adsorption was limited by the activation energy barrier, is shown in Figure 29. For this kind of mechanism, the dimensionless IFT should be linear with  $\log(t)$  below unit 1.



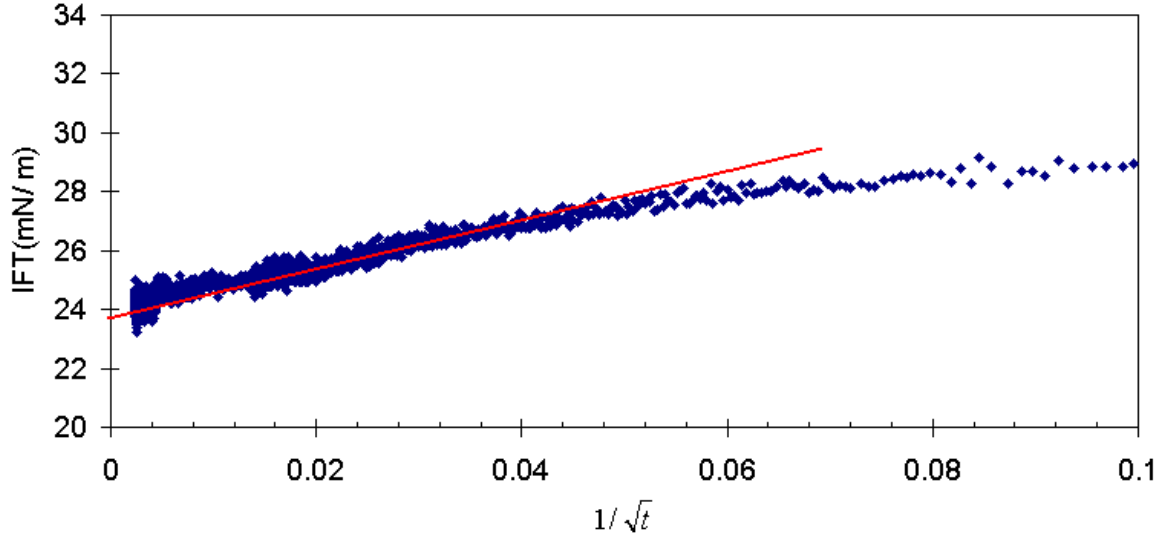


**Figure 27:  $IFT \sim 1/\sqrt{t}$  (Yates Live Oil against Yates brine at 82°F and 700psi), unit of t is second, Extrapolation of trend to 0 should indicate equilibrium IFT**

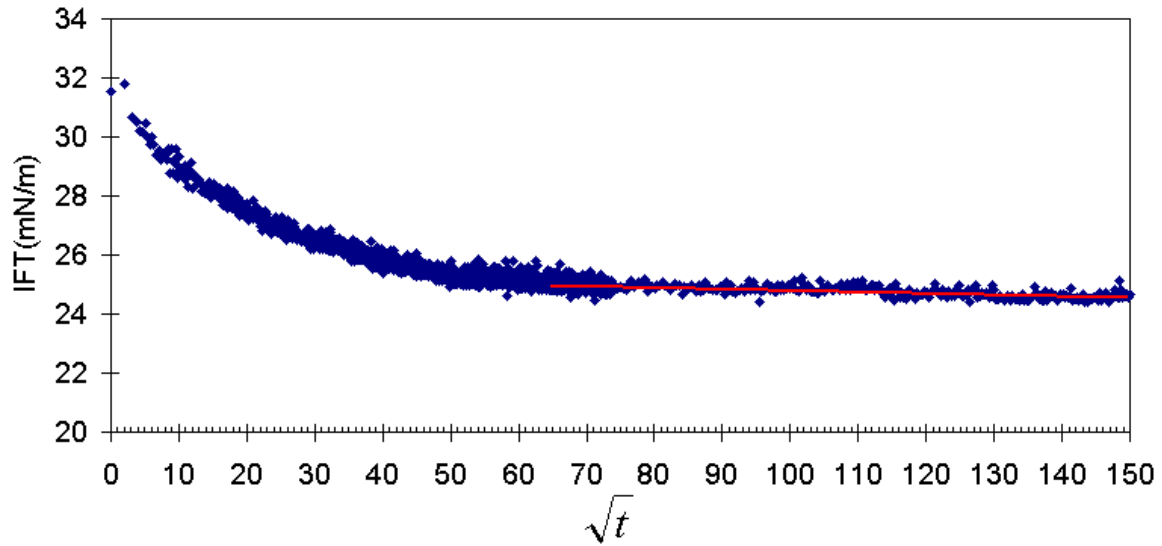


**Figure 28: Dynamic Interfacial Tension, IFT versus  $\sqrt{t}$**   
(Yates live oil against Yates brine at 82°F and 700 psi, t is second)

No single linear relationship was found in those figures. Hence, none of the dynamic IFT models proposed in the literature for pure oil component -surfactant solution systems can explain the measured IFT behavior of crude oil – brine system used in the current study. The difference is that the surface-active materials in those models came from solution fluid (water), in this case the surface active materials (asphaltene) came from the oil drop. Another difference is the asphaltenes were almost insoluble in water, and the

surfactant was soluble in water. Hence, a four-stage dynamic IFT model proposed by Hua and Rosen (1988) and discussed in section 2.2.2, was used in this study and shown in Figure 30. This model appears to explain the dynamic IFT behavior of Yates live crude oil against Yates brine.

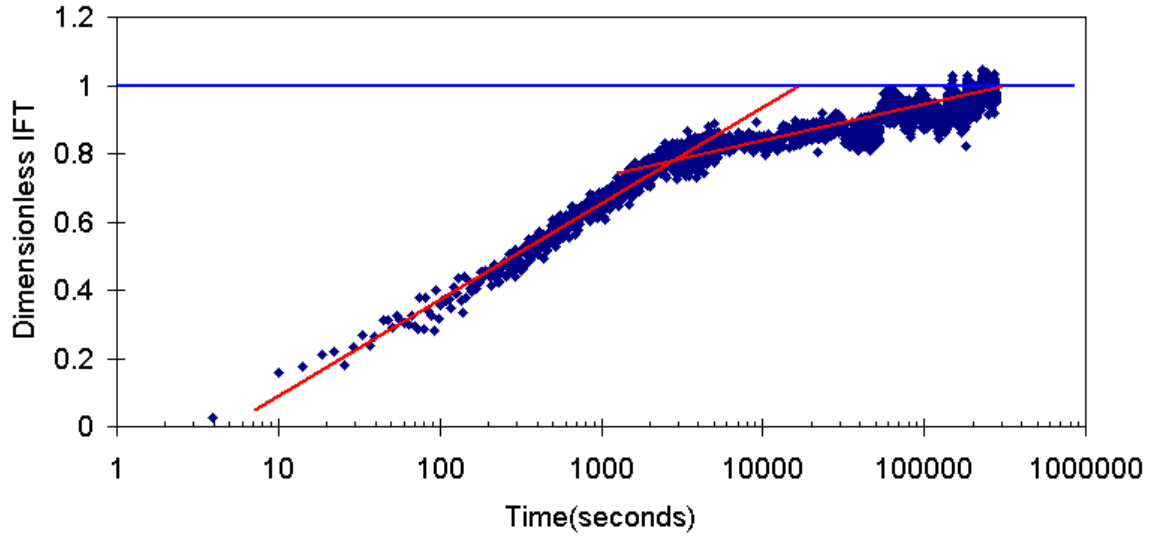


**Figure 29: F (IFT) ~ log(t) Model, (Yates Live Oil and Yates brine, 700psi and 82°F)**

$$\text{Dimensionless IFT} = \frac{(IFT_0 - IFT_t)}{(IFT_0 - IFT_e)}$$

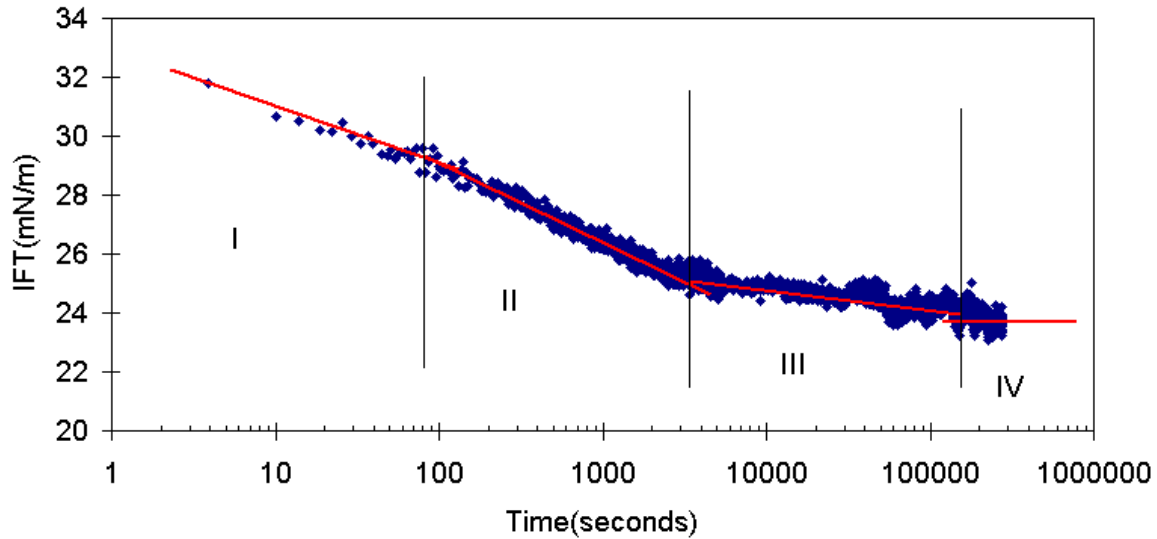


**Figure 30: Multi-stage Model for Dynamic Interfacial Tension of Yates Live Oil against Yates Brine at Reservoir Conditions**

I: Induction Region, elastic control; II: Diffusion Region, III: Pseudo-equilibrium Region, Kinetics barrier control; IV: Equilibrium Region

The first stage is due to the method used, that is, when the oil drop was squeezed into the brine, the drop needed several seconds to respond to plastic – elastic deformation before becoming stable. So, it was named as the induction stage. The second stage was due to diffusion-control. The components in one phase are free to diffuse into the other phase. The slope of this stage in Figure 30 was large enough to be explained by traditional diffusion theory. The third stage was due to the insolubility of asphaltenes in brine, when the asphaltenes concentrated on the interface and could not diffuse into the water phase easily. This phenomenon is called kinetics barrier, so the diffusion became restricted, hence the slope decreased as shown in Figure 30. The fourth stage was called the equilibrium stage, where the interface became stable after the migration and accumulation of surface-active materials at the interface came to a stop.

- Surfactant Model

There are many dynamic IFT models proposed for surfactants, but most of them have been developed for low concentrations of surfactant in fresh water and are not applicable to crude oil systems. The multi-component crude oil - brine system may not be amenable to simple explanations by either diffusion or kinetic theory. Although the model developed from the crude oil – brine system discussed previously can be used for natural surfactant (most likely asphaltenes), considering that the equilibrium of IFT in surfactant A and B solution was not achieved by pendent drop method, the dynamic IFT model of Yates crude oil – surfactant bearing Yates brine system may be only a part of the complete crude oil model. Hence, the crude oil model is also applicable for a real surfactant – crude oil system. The relatively long induction stage in Figure 25 and 26 was caused by the drop volume increase since the measurement started from a relatively small volume, and then the volume increased as the drop rose due to surfactant activity on the neck. Hence, the final value was not the equilibrium value. The shape of the sessile drop on the crystal changed after aging overnight, which indicates the long-time decrease of IFT in surfactant solutions. However, an attempt to calculate the equilibrium IFT using sessile drop method failed. The accuracy of the sessile drop method for IFT is larger than 0.1 mN/m theoretically (Table 1). The estimated equilibrium IFT of the crude oil – surfactant system in this study is lower than 0.5 mN/m. The IFT in the live oil –

surfactant B (3500ppm) system calculated by sessile drop method was 0.9 mN/m, which was higher than the estimated equilibrium IFT of 0.5 mN/m.

Diamant et al. (2001) summarized that for common non-ionic surfactants, not hindered by high adsorption barriers, the adsorption process can be roughly divided into three temporal stages. At extremely early times (usually less than microseconds), the surface coverage and surface tension change linearly with time because of interfacial kinetics. Due to this fast adsorption stage, the sub-surface layer becomes nearly empty, which in turn drives a second, diffusion-limited stage, where the surfactant diffuses from the bulk with a  $t^{1/2}$  time dependence. The final relaxation towards equilibrium is usually diffusion-limited, exhibiting an asymptotic  $t^{-1/2}$  behavior. This surfactant IFT model is almost the same as the crude oil model (Figure 30) in the early stages, but the final stage was not observed in this study. The reason is that pendant drop method was used in this study instead of spinning drop method. The oil drop could not stay that long. However, the dynamic measurement of spinning drop method is doubtful because the equilibrium IFT could not be obtained due to the increase of IFT after a minimum IFT was reached (Figure 5).

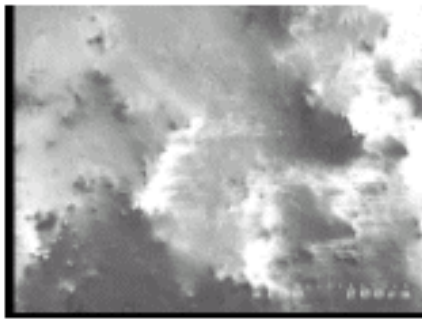
## **4.2 Wettability and Dynamic Contact Angles**

The conventional techniques used to measure dynamic contact angles in solid-liquid-vapor (S-L-V) systems have failed to yield meaningful results when applied to solid-liquid-liquid systems. Rao (2003) clarified the use of the concept of contact angles to characterize wettability of petroleum reservoirs. If the correct measurement technique is used, the adhesion on a rock surface is well characterized by the water-advancing contact angle and the spreading along the rock surface is characterized by the water-receding angle. DDDC technique can attain reproducible contact angles with shorter aging time when compared to other conventional techniques (Rao 2003). The detailed measurement procedure of this technique was discussed in Chapter 3.

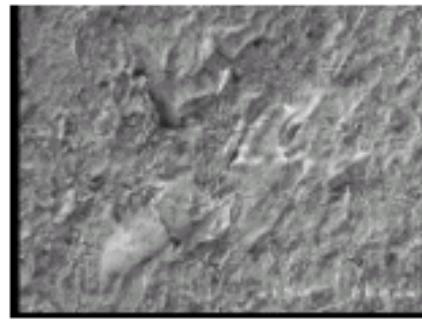
### **4.2.1 Effect of Rock Characteristics**

This study focuses on the dolomite reservoir, the rock itself is a kind of chemical deposit with infinite small particles. The smoothness was easy to attain. To avoid contamination and oxidation, the rock (mineral) surface is polished by diamond sandpaper and cleaned by deionized water before use. Fresh cleaned and polished rock

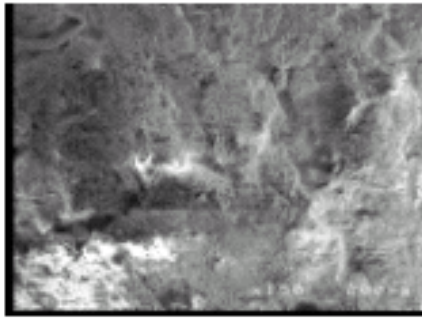
crystal was put into brine immediately for use in the same day. Used or stocked samples were not used in experiments. Two common minerals, pure crystallized transparent quartz and calcite were also used in the study to represent sandstone and carbonate rock surfaces. Berea is used to study the influence of pores on wettability measurement. Figure 31 shows the surface roughness of the crystal samples used in this study.



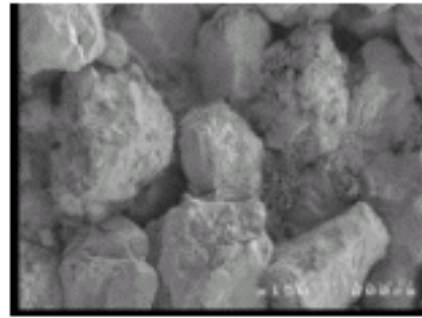
(a) Calcite (single crystal)



(b) Quartz (single crystal)



(c) Dolomite (rock)



(d) Berea Sandstone (rock)

**Figure 31 Rock Surface Roughness Analysis Using SEM (Magnified 150 times)**

The sample surface have been magnified 150 times. Obviously the calcite crystal has the highest smoothness, and then quartz and dolomite. The dolomite sample has slight roughness because it is a rock sample, not a single crystal. The dolomite is formed by kind of chemical precipitation or alteration. The “grain size” of dolomite is infinitely small, so the roughness of dolomite rock would not cause a major problem. Another noticeable phenomena during SEM scanning is, the carbonate (calcite and dolomite) has some reflection to electrons, but the silica (quartz and Berea) can adsorb and transfer the electrons very rapidly. The difference of electronic characteristics probably results in the

difference of charge behavior of rock surface in brine, which is one of the main reasons for wettability difference of carbonates and sandstones.

The dynamic contact angles of Yates live oil – Yates brine system on different rock substrates was summarized in Table 5. When comparing the contact angle of Yates live oil on different rock surfaces, the initial receding angle (the angle measured as soon as the oil was put on the crystal, no aging) angles are almost the same (25°-30°). This is because at the beginning, the thin film between rock surface and fluids has not been disturbed. This angle most likely represents the spreading between brine and oil while it has not been influenced by the rock characteristics. The receded angles after 24 hrs were almost same as the first contact angle except for the calcite case. The advancing contact angles that represent the wettability on different rock surfaces were different. The Berea surface had the lowest advancing angle (26°), which was most likely completely water-wet. Its advancing angle was the same as the receding angle. This is because of the obvious influence of pores or in other words, roughness. It does not represent the real wettability of sand particles. Hence, sandstone should not be used as material of this contact angle measurement technique. The calcite had the highest value of 85°. Considering the calcite crystal is a pure high quality single crystal and has relatively high smoothness, their wettability characteristic was similar to that of dolomite (60°) because dolomite used here is not a single crystal but an aggregate. The smoothness of quartz was also near perfect, so it had a relatively higher advancing contact angle (65°) than expected. However, its spreading behavior on the solid surface differed from carbonates. The diameter of the oil drop on the quartz crystal surface did not change for 24 hours while it did increase on the calcite and dolomite surfaces. Hence, the true wettability of carbonate for the Yates live oil – brine system is weakly water-wet to intermediate-wet with an advancing angle in the range of 55° to 85°. The wettability of sandstone for the same fluids system is water-wet to weakly water-wet with an advancing angle in the range of 26° to 65°. Wettabilities of different rocks in Yates stocktank oil – brine system at ambient conditions have been studied by Vijapurapu (2002). Strong oil-wet on carbonate (160°) and intermediate-wet (97°) on quartz have been reported.

Unlike the generally expected oil-wet behavior of calcite widely mentioned in the literature, the intermediate-wet of calcite-Yates live oil – brine system observed in this study provides more evidence for the influence of light ends in live oil on wettability.

**Table 5: Dynamic Contact Angles of Yates Live Oil at Reservoir Conditions**

Substrate	Brine	Pressure and temperature	Contact Angles (degrees)				Spreading On rock surface D/Di*
			Initial receding 0 hr	Receded 24 hrs	DDDC Advancing 24hrs	DDDC Receding 24hrs	
dolomite	Yates	700psi&82°F	27	26	55-60	22	1.101
berrea	Yates	700psi&82°F	26	26	26	26	1
quartz	Yates	700psi&82°F	29	27	65	25	1.001
quartz	Yates	2500psi&82°F	27	25	60	24	1
calcite	Yates	700psi&82°F	25	36	85	20	1.085
calcite	Yates	100psi&82°F	30	30	120	30	
dolomite	50% Yates	700psi&82°F	28	23	105	12	1.045
dolomite	CaCl <sub>2</sub>	700psi&82°F	25	28	140	15	1.467
dolomite	NaCl	700psi&82°F	16	17	22	13	1.040
dolomite	DIW	700psi&82°F	27	27	77	10	1.263

\* The ratio of oil drop diameter on the rock surface at 24 hours and 0 hour.

#### 4.2.2 Effect of Brine Composition

Wettability is a three-phase interaction between rock, oil and brine. The salinity and pH of brine strongly affect the surface charge on the rock surface and the fluid-fluid interfaces in turn affects the adsorption of surfactants (Anderson, 1986). Since most reservoir brines have nearly neutral pH behavior and the measured pH of Yates brine is 7.3, only neutral pH characteristics are discussed here. The silica is negatively charged and the calcite is positively charged near neutral pH (Anderson, 1986).

The influence of salinity on Yates stocktank oil at ambient conditions has been described by Vijapurapu (2002). The dilution of brine at ambient conditions had significant effect on IFT and contact angle. The lowest IFT was reached at 50% dilution. It also caused spreading on the rock surface with a large receding angle (140°), which

was much higher than in other concentrations. Rao (2003) explained this behavior based on the concept of the critical spreading tension. Dilution of brine also caused the contact angle change using live oil at reservoir conditions. The water-advancing contact angle of Yates live oil at 50% brine increased to 105° from 55° (100% brine). The water-advancing contact angle of Yates live oil at 0% brine was 77° (Table 5). However, no oil spreading characteristics were observed with brine dilution. The receding angle and receded angle were only 15° and 23°. This is because the critical IFT had not been reached as explained in section 4.1.2. The change of advancing angle was related to the stability of the thin wetting film of water through brine salinity and pH.

Many researchers have reported the wettability alteration caused by multivalent metal cations in brine in silica/oil/brine systems, even at very low concentrations (Anderson, 1986). However, it appears that no investigations are reported in the current literature with a dolomite system. To investigate the influence of cation type on wettability in a dolomite/oil system, two typical salts were added to deionized water in the salinity of the same molar equivalent weight as Yates brine. The tests with deionized water were also done as a reference. Like the results in the silica system reported in the literature, Table 5 shows that the calcium chloride solution had influenced the wettability of dolomite compared with pure water. The receded angles were the same and the advancing angles increased from 77° for the pure water case to 140° of the CaCl<sub>2</sub> solution case. The addition of divalent calcium cations into solution resulted in more positive charges on the rock surface. Those positive charges made the thin film more easily ruptured by the polar materials in the oil. The sodium chloride solution also had a surprising effect on the wettability of dolomite. The initial receding angle in NaCl system (16°) was much lower than in other cases (25°-30°). The advancing angle (22°) and receding angle (13°) indicated the completely water-wet behavior instead of intermediate-wet of pure water cases. The active Na<sup>+</sup> ions covered the rock surface and prevented the divalent cations of dolomite to contact with the oil phase. It also kept the interface neutrally charged, so the thin film could not be ruptured or even disturbed by the organic acids or bases. The wettability alteration in the Yates brine or 50% brine cases were less than that of CaCl<sub>2</sub> solution case but higher than the NaCl case. It was reasonable because the Yates brine has both Ca<sup>+</sup> and Na<sup>+</sup>. This means that not only divalent, but also monovalent cations had



influence on the adsorption and electrostatics of the thin wetting film. The adsorption of divalent cations on the dolomite surface enhanced the positive charge behavior while the existence of monovalent cations diluted the charges or even erased the charges by occupying the contact region of thin film.

#### 4.2.3 Effect of Crude Oil Composition

Which component(s) in the crude oil is (are) responsible for establishing non-water wet conditions in the reservoir? The answer found in literature indicates that the polar components, especially the asphaltenes, are believed to be the main reason. However, these evidences in literature are based on ambient condition experiments. To further study the influence of different components on wettability, several experiments were conducted to answer this question. The results are presented in Table 6.

**Table 6: Dynamic Contact Angles of Different Oil Components at Ambient Conditions**

Oil phase	Aqueous phase	Solid phase	Does drop stay when crystal turned over?	DDDC	
				$\theta_a$	$\theta_r$
Yates stocktank oil	Yates brine	Dolomite	Yes	154-156	25
Yates Deasphalted oil	Yates brine	Dolomite	Yes/Partly	152	25
Yates De-resined oil	Yates brine	Dolomite	Partly	148	17
Yates crude oil	Yates brine	Glass	Yes	158	20
Yates De-resined oil	Yates brine	Glass	Yes	150	46
Decane	Water	Glass	Yes	77	31
Toluene	Water	Glass	Yes	80	31
50%Toluene+50%decane	Water	Glass	Yes	72	38
Toluene+0.27g/100mlAsphaltene	Water	Glass	Yes	130(aging5 min)-141(12hrs)	15
Toluene+3g/100mlAsphaltene	Water	Glass	Yes	133(aging5 min)-162(12hrs)	15

The mechanism of wetting in porous media is more complex than non-porous substrates. On imperfect solids, the spreading barrier may exist due to roughness. To avoid the influence of rock characteristics (roughness and mineralogy), smooth glass substrates were used instead of real rock surfaces. Well-cleaned glass had been aged in

the aqueous phase before being installed into crystal holders. Another advantage of glass is that it needs a relatively short aging time to reach equilibrium. Table 6 shows the result of contact angle tests at ambient conditions for different hydrocarbon components. The results obtained using deasphalted and de-resined oils indicate that the asphaltene and resin did not have a significant effect on wettability ( $\theta_a > 148^\circ$  on dolomite and  $\theta_a > 150^\circ$  on glass). This seems to contradict the general practice in the literature which attributes wettability effects mostly to asphaltenes. However, for pure fluids (Decane and Toluene) on glass, the addition of asphaltenes altered the wettability from weakly water-wet ( $\theta_a$  of  $77^\circ$  and  $80^\circ$ ) to weakly oil-wet ( $\theta_a$  of  $130^\circ$ ). Obviously, the asphaltene was one reason for the oil-wet nature. The concentration of asphaltene in the oil was also a factor in altering wettability. The advancing contact angle of toluene with 0.27g/100ml asphaltene ( $141^\circ$ ) was much lower than that of the toluene with 3g/100ml asphaltene ( $162^\circ$ ) at an aging time of 12 hours.

For live oil and stock-tank oil at the same reservoir conditions, the contact angle on dolomite was significantly different, from  $55^\circ$  to  $154^\circ$ , respectively. The live oil system was water-wet while the stock-tank oil system displayed a strong oil-wetting tendency. It appears that, not only the asphaltenes, but also the lighter ends in the live oil influenced the wettability characteristics of Yates dolomite. To confirm this water-wet behavior of live oil, several experiments were conducted. Instead of the traditional 24 hours aging period, live oil – dolomite experiments were conducted using one week and two -week aging periods. The contact angles did not change and they still showed weakly water – wet behavior. By increasing pressure to 2700 psi and after aging one week, the contact angle was about 85 degrees.

How the light ends influence the wettability is unclear. The light ends may peptize the asphaltene molecules by surrounding them, thereby preventing their agglomeration and migration to interface.

#### **4.2.4 Effect of Pressure and Temperature**

Since the actual reservoir conditions are totally different from ambient conditions, the experiments were conducted with live oil, reservoir rock and brine at reservoir temperature and pressure. The simulation of reservoir conditions was accomplished in the newly built high-pressure high-temperature cell. The dynamic contact angle

measurements were also made for stock-tank oil at reservoir conditions. This is the first time that dynamic contact angles of live oil have been measured under reservoir conditions at LSU Petroleum Engineering laboratory.

For Yates stocktank oil and dolomite system, the contact angles measured at ambient condition and reservoir conditions were the same ( $\theta_a=154^\circ$  to  $156^\circ$ ). However the adhesion characteristics were slightly different. Only a part of oil drop stayed on the lower crystal when turning over at reservoir conditions while the whole oil drop stayed on the crystal at ambient conditions. As mentioned in literature review (section 2.3.4), increase of temperature tends to make the oil-wet system more water-wet. The temperature of reservoir conditions was about  $10^\circ\text{F}$  higher than that of ambient conditions, which made the stocktank oil at reservoir conditions less oil-wet comparing with the same oil at ambient conditions.

A test was run by decreasing the pressure of live oil system to below bubble point pressure. By dropping the pressure from reservoir pressure (700psi) to 200 psi, gas was released in the form of bubbles from the oil. An oil drop was captured by the crystal and the contact angle was measured. The value was much higher than at reservoir pressure based on visual observation. This means that the oil became less water-wet as the light ends partly came out and the live oil composition tended toward that of stocktank oil. However, since the system was very unstable due to continuous formation of bubbles, the reproducible and stable contact angles could not be measured.

Another test was conducted using calcite crystal. After measuring the wettability of live oil at reservoir pressure of 700 psi, the pressure in the cell was brought to 100 psi, which was much lower than the bubble point pressure of 650 psi. The gas and oil drops came out from the needle tip separately due to the depressurization. By shifting the side crystal arm on purpose, an oil drop was captured on the calcite surface. This oil drop had less light ( $C_1$ - $C_5$ ) components than the live oil at reservoir pressure, but more than the stocktank oil. It represented the live oil phase at 100 psi. To avoid the further release of gas in the system, pressure was soon increased to 700 psi. After one day of aging as the usual procedure, the contact angle was measured by the DDDC technique. The advancing angle of this special oil drop was  $120^\circ$ , which was much higher than the contact angle of Yates live oil on the same crystal ( $85^\circ$ ) but lower than the stocktank oil case ( $160^\circ$ ). This

test was a firm evidence of the influence of light gaseous ends on wettability. The oil with higher content of light ends displayed a stronger water-wet tendency.

To investigate the effect of pressure above bubble-point pressure, the wettability of quartz and dolomite were measured at 2500 psi. Comparing with the results at 700psi, the advancing angle on dolomite increased to 85° from 55°, while the advancing angle on quartz slightly decreased to 60° from 55°.

When live crude oils at the reservoir pressure and temperature were used, the solubilities of the wettability-altering compounds had their corresponding reservoir values. The use of dead crude at ambient or reservoir pressure may change the wettability because the properties of the crude were altered. Light ends are lost from the crude, while the heavy ends are less soluble, which may make the core more oil-wet (Anderson, 1986). However, the effects of pressure are not known at present. The two reported experiments found that pressure is much less important than temperature (Mungan 1972, Hjelmeland and Larrondo 1986). However, in our study, a clear evidence of the effect of pressure on wettability was observed indicating the need to use live reservoir fluids and actual reservoir conditions in wettability measurements.

#### **4.2.5 Wettability of Subsurface Reservoir**

All reservoirs were once believed to be water-wet because water was the original occupant and the oil came into the reservoir by migration. Even today, much simulation efforts still assume complete water-wet conditions in their calculations. Then some people found that several carbonate reservoirs are oil-wet. The earliest oil-wet report is by Nutting in 1934 (Anderston, 1986). Around the 1980s to 1990s, some authors argued that there are more oil-wet reservoirs than water-wet reservoirs (Anderson, 1987). Recently, more researchers believe that most of the reservoirs are mixed-wet (Morrow, 1990). However, this term, mixed-wettability, proposed by Salathiel (1973), can be, and has been, easily misinterpreted. The oil reservoirs cannot be simply water-wet or oil-wet because all reservoirs have both oil-wet and water-wet fractions. Let us consider the real picture of a subsurface reservoir. The pores under oil-water contact are filled only by water. No matter what rock properties they have, they are completely water-wet. In the case of dead pores, small pores in the oil zone that never have oil flowed in, they kept the original wettability of water wet too. On the other hand, the wettability of oil occupied

pores might have been changed to weakly water-wet or even oil-wet. However, not all so-called mix-wet reservoirs have high oil recovery as mentioned by Salathiel. This is because the most important part for this term is the continuity. Does the oil keep a continuous oil flow in and only in the oil-wet pores? If so, high oil recovery can be achieved since the oil is only trapped in oil-wet fractures and large pores. Therefore, some mixed-wet cases in the literature actually may be just fractional-wet.

In the field scale, the results from fundamental studies of wettability are also helpful for comparison. The oil, brine and rock in this study were from Yates Field, West Texas, which was discovered in 1926. The main reservoir is a classic naturally fractured dolomite reservoir (Campanella et al., 2000).

A field evidence to support the wettability conclusion of this study is the oil recovery. Estimates of the original oil in place vary from 3.7 to 4.3 billion barrels (Christiansen, 1990). Cumulative oil production from the field reached 1 billion barrels in early 1985 and 1.3 billion barrels in 1999. Pressure maintenance by gas injection to the gas cap started from 1976. The oil recovery by 1999 was about 30%-35%. However, the general recovery for fractured oil-wet carbonates is typically less than 10% (Xie et al., 2004). It is doubtful for oil-wet carbonates to yield such high oil recovery. Hence, the wettability of the Yates reservoir cannot be simply oil-wet. The mixed-wet characteristic reported by several researchers (Chen et al., 2001, Freedman et al., 2003) is reasonable but questionable due to the misinterpretation of the mixed-wet definition, as we mentioned earlier. Considering the weakly water-wet behavior of the Yates live oil system at reservoir conditions, the oil-wet behavior of stocktank oil and the wettability alteration due to depressurization, the wettability of the Yates oil reservoir in field scale can be summarized as follows: The Yates reservoir is preferably weakly water-wet in origin. The production in past years might have changed the wettability of the area in main flow paths or near-well area to more oil-wet, but those oil occupied pores which were not on the main flow paths are weakly water-wet as indicated by laboratory results in this study. Not all oil occupied pores are large and connected together due to the heterogeneity of carbonate. So, current wettability in the field scale appears to be imperfect mixed-wet, or preferably weakly water-wet.

### 4.3 Surfactant Injection

#### 4.3.1 Stocktank Oil at Reservoir Conditions

Yates synthetic brine (prepared according to the composition supplied by Marathon Oil Company), Yates stock tank crude oil, dolomite rock substrate and the two surfactants (Surfactant A: Ethoxy Alcohol; Surfactant B: Ethoxy Sulfate) were used in these experiments.

Table 7 shows the experimental results for the two surfactants at different concentrations. The results indicate the dynamic drop behavior before, during and after surfactant injection and observed changes in advancing and receding contact angles as well as the oil-water interfacial tension. The results were divided into the following three sections for better analysis.

**Table 7: Interfacial Tension and Dynamic Contact Angle Measurements for Yates Stocktank oil/Brine/Dolomite System at Reservoir Conditions (700psi and 82°F)**

Surfactant		Before injection				During injection				After injection				
Type	ppm	IFT (mN/m)	Receding angles (0 - 24 hrs)	Advancing angles (24 hrs)	Drop dynamics upon turning lower crystal?	Drop behavior	$\Delta$ Injection time for equilibrium drop to float away	TPCL movement	Advancing angles	Advancing angles		Upper drop height (mm)	Receding angles of new drop	IFT (mN/m)
										0 hrs	16 hrs			
A	500	32.43	23-26	154	Partly	Shape changed	24 hrs	No	154	154	154	3.56	23	
	1000	32.10	23-26	156	Partly	Floated	11 mts	No	154	154	154	2.48	23	4.70
	3500	32.05	23-26	154	Partly	Floated	8 mts	No	154	154	154	1.96	23	2.88
B	500	31.83	23-26	154	Partly	Floated	3.5 mts	Yes	138	*	139	1.41	23 +	0.22
	3500	33.54	23-26	156	Partly	Floated	4.7 mts	Yes	141	*	*	1.07	23 +	0.08

#### (A) Drop Behavior Before Surfactant Injection

The interfacial tension measured between Yates synthetic brine and Yates stocktank oil for all the experiments using the Drop Shape Analysis matched well with each other (about 33 mN/m average with a standard deviation of 1 mN/m). The sessile drop receding angles measured initially on both the upper and lower crystal surfaces were nearly the same, 23-26 degrees for all the experiments conducted. After 24 hours of aging, the equilibrium sessile drop receding angles were either almost unchanged or just increased slightly, but the drop contact diameters increased by about 20 %. Once the lower surface was turned upside down, part of the oil drop floated away leaving 20-30 % of oil on the surface. After the two oil drops were mingled, the lower crystal was shifted laterally to measure the dynamic advancing and receding angles. The advancing angle was about

154-156 degrees for all experiments conducted using Yates reservoir rock and fluids at reservoir conditions, showing a strong oil-wet nature of the reservoir. The position of the three phase contact line (TPCL) was monitored throughout the experiment and there was hardly any visual movement of it since the oil was strongly adhering to the dolomite rock surface. By capturing the pictures using a video recorder, the changes in TPCL movement were analyzed later for estimation of true advancing angles (Figure 32). The definition of L and Ri of TPCL movement was described in Figure 12. Upon further shift of the lower surface, the drop sheared in the middle and the drop remained as an adhering film on the lower crystal surface. The two sections of oil were mingled again into one by adjusting the positions of crystals to repeat the measurement before injecting the surfactant-containing brine into the cell.

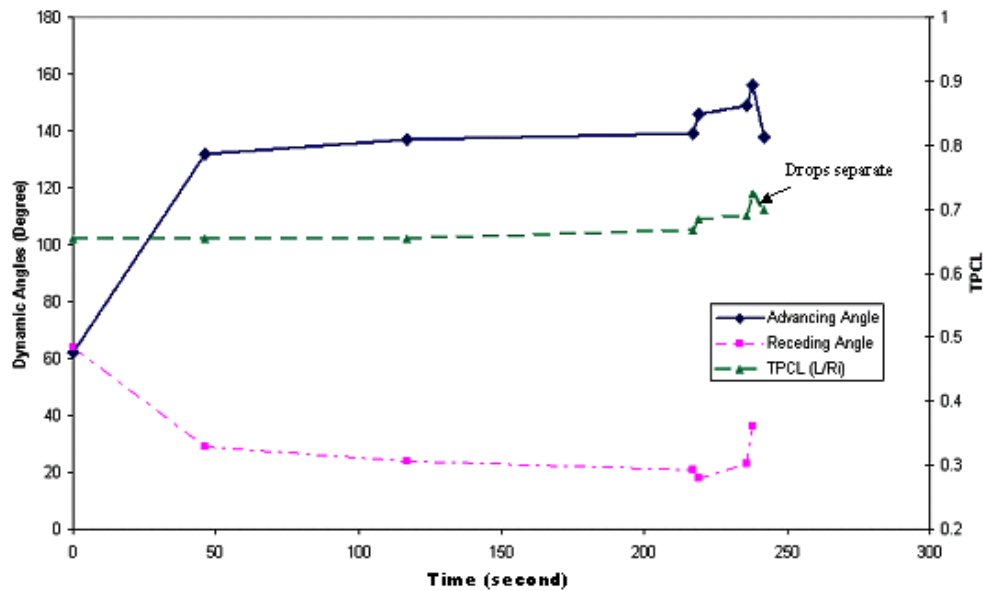


**Figure 32: DDDC Contact Angle Measurements and Three Phase Contact Line Movement** (Yates Stocktank Oil/Brine/Dolomite System Before Surfactant Injection at Reservoir Conditions of 700 psi and 82 °F)

#### (B) Drop Behavior During Surfactant Injection

With the drop in the equilibrium position, surfactant-containing brine at a specified concentration was injected into the cell at reservoir conditions of temperature and pressure (700 psi and 82 °F). Sufficient volume of surfactant containing brine was injected to make sure all the old brine was completely replaced. This step was carried out to simulate the flow of surfactant from the fracture into the matrix.

At high concentrations of surfactant A (3500 ppm, Figure 33; and 1000 ppm, Figure 34), the equilibrium drop between the two crystals moved and floated to the upper surface, thus increasing the volume of the upper drop and flattening it. The advancing dynamic angle and TPCL movement were measured using the drop dimensions on the lower crystal. The current angles between oil drop and lower crystal in both sides were advancing angles because the water was invading along the TPCL due to the surfactant flooding. No change in advancing angles was observed for these two cases. These angles were similar to those obtained before the surfactant injection. There were no significant changes observed in TPCL movements too. Hence, the nonionic surfactant A influenced IFT, but it did not result in significant wettability alteration.

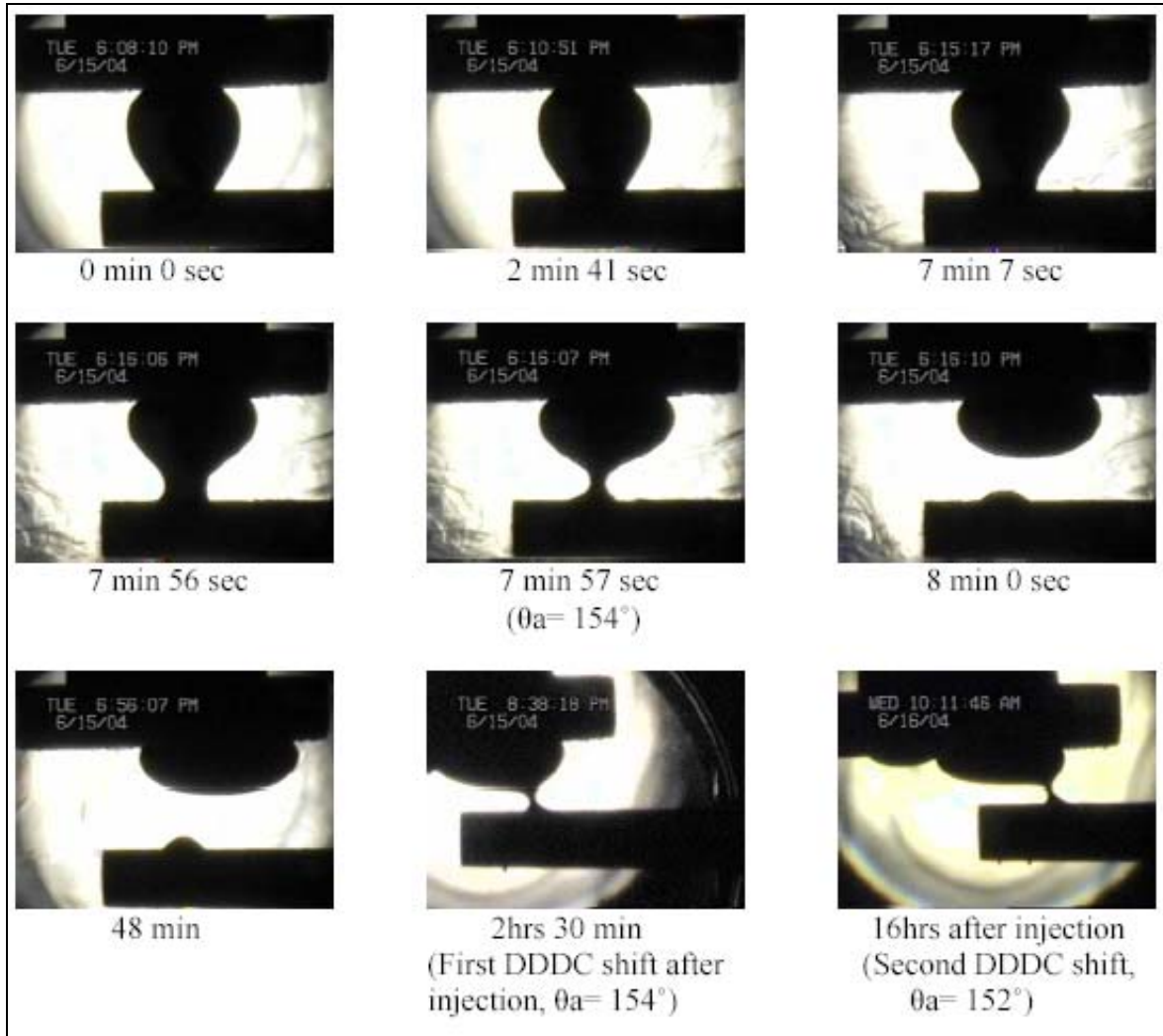


**Figure 33: Depiction of Drop Movement During and After Surfactant Injection (Nonionic Surfactant A at 3500 ppm, 700 psi and 82 °F, Yates stocktank oil)**



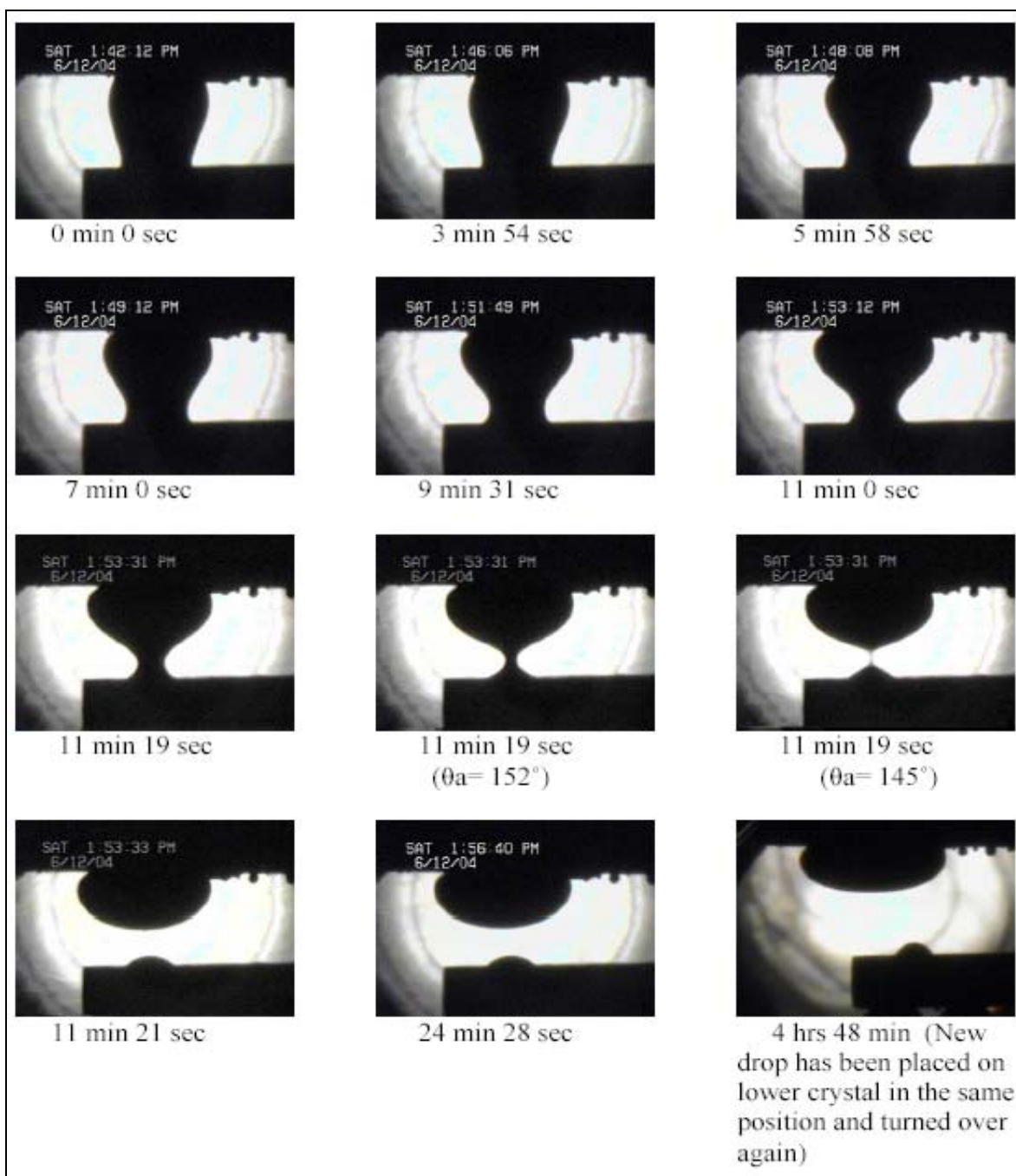


**Figure 34: Depiction of Drop Movement During Surfactant Injection (Nonionic Surfactant A at 1000 ppm, 700 psi and 82°F, Yates stocktank oil)**

At lower concentrations of nonionic surfactant A (500 ppm), the equilibrium drop between the upper and lower surfaces was not significantly affected. The shape of the drop changed slightly due to IFT change. After 24 hours, the equilibrium drop became flattened and separated.

During the injection of anionic surfactant B, the equilibrium drop moved and floated to the upper crystal very soon even at the low concentration of 500 ppm. Significant TPCL movement with a constant advancing angle was observed during the drop movement (Figures 35 and 36). The TPCL movement here was described according to the decrease of drop diameter on lower surface (Figure 35). The advancing angle (135-139 degrees) during injection was lower than the initial advancing angle (154 degrees) measured before surfactant injection, indicating wettability alteration by surfactant B. For Surfactant B injection at 3500 ppm, the same characteristics as observed at 500 ppm concentration were seen (Figure 37). The measured advancing angle during the injection was 141 degrees. For both these cases, there was about a  $16^\circ$  decrease in the advancing contact angles when compared with the initial advancing angle before injection. This indicates reservoir wettability alterations from strongly oil-wet to weakly oil-wet state by the anionic surfactant B and hence has potential to increase oil recovery by wettability alteration.

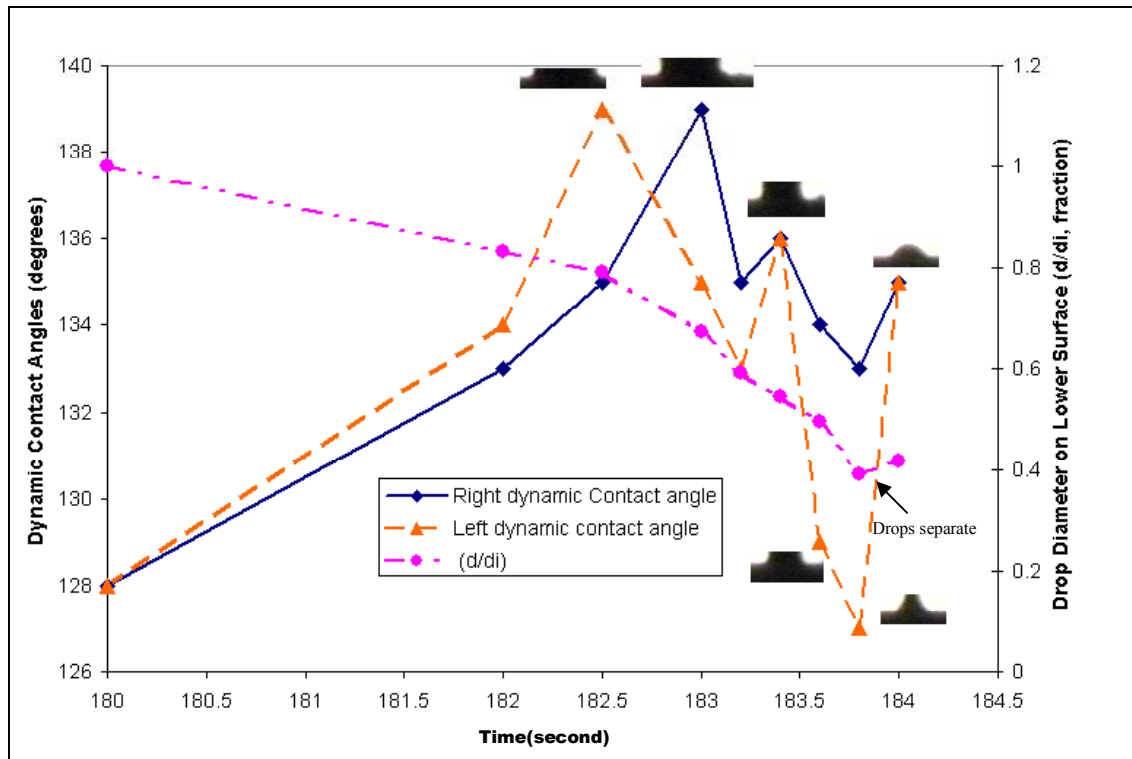


**Figure 35: Dynamic Contact Angle Measurements and Three Phase Contact Line Movement in Yates Stocktank Oil/Brine/Dolomite System During 500 ppm Anionic Surfactant B Injection at Reservoir Conditions of 700 psi and 82 °F**

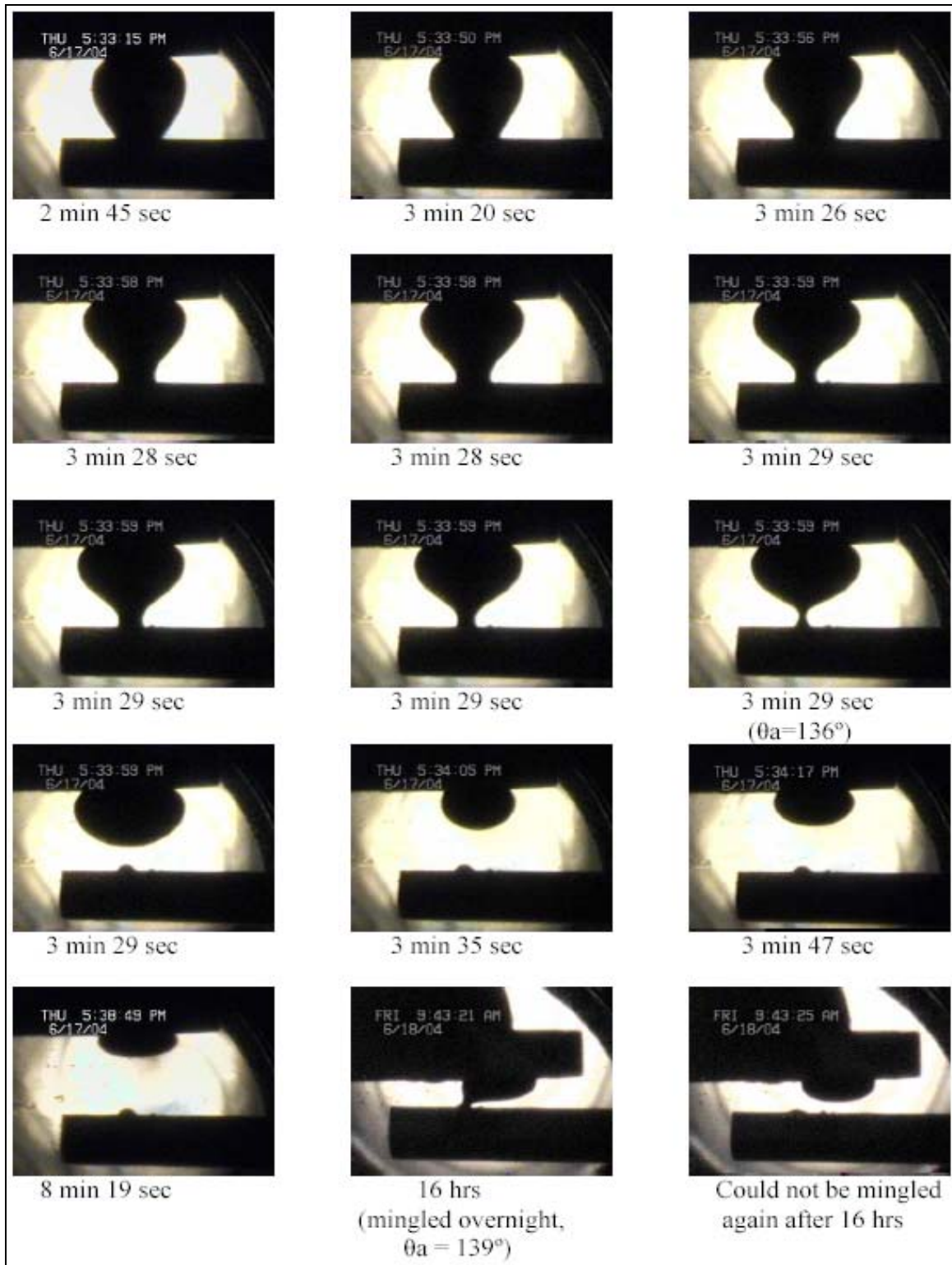


**Figure 36: Depiction of Drop Movement During and After Surfactant Injection  
(Anionic Surfactant B at 500 ppm, 700 psi and 82 °F, Yates stocktank oil)**



**Figure 37: Depiction of Drop Movement During Surfactant Injection (Anionic Surfactant B at 3500 ppm, 700 psi and 82 °F, Yates stocktank oil)**

### (C) Drop Behavior After Surfactant Injection

About more than one hour after surfactant injection, two crystals were moved closer to mingle the two oil drops at the equilibrium position. For surfactant A, two drops were mingled within ten minutes. For surfactant B, overnight or longer times were needed to mingle the drops. Advancing angle was measured by shifting the lower crystal. For all concentrations of surfactant A, the advancing angles measured immediately after injection and 16 hours after injection were the same as initial values (154 degrees). For surfactant B, the advancing angle after surfactant injection was 139 degrees for 500 ppm, almost the same as that obtained during the surfactant injection (Figure 38). For surfactant B at 3500 ppm, the oil on the upper crystal was too flat to merge it with lower crystal, but the visual observations indicated that the value of the advancing angle was the same as that obtained during the surfactant injection.

Due to IFT change by one to two orders (Table 7), changes in drop shapes were observed for both the surfactants at different concentrations. Most of the oil drop became flattened and stayed under the upper crystal. It became easier for the drop to move under gravity. The oil remaining on the lower surface was about 5-10 % of the initial oil drop. This oil can be considered as residual oil in the subsurface reservoir and hence cannot be removed at any concentration of surfactants. This residual oil was not observed in ambient condition experiments, which provides evidence that the high pressure and high temperature experiments were valuable to understand the behavior of subsurface reservoir rock-fluids interactions in the laboratory.

The lower crystal surface #1 (where oil previously occupied) was turned towards the tip of the needle to place a new drop of crude oil in the same place where oil was previously occupying it. But the drops repelled each other at 3500 ppm surfactant A concentration and at both concentrations of surfactant B (500 ppm and 3500 ppm). Surfactant molecule orientation mechanisms appeared to be the reason for this repulsion between the oil drops.

Oil drops were also placed on the surface of the lower crystal not exposed to oil before (surface #2). For surfactant A at 500 ppm and 1000 ppm, the oil drops stayed overnight, but when the crystal surface was turned over, the oil drops floated away without leaving even a trace. At surfactant A concentration of 3500 ppm, the oil drop

stayed for about 30 minutes and then floated away. For surfactant B at 500 ppm and 3500 ppm, the oil drops did not stay at all. These observed different drop dynamics on this rock surface due to surfactants could be inferable based on sufficiency of surfactant molecules and their relative distribution between oil-rock and oil-brine interfaces.

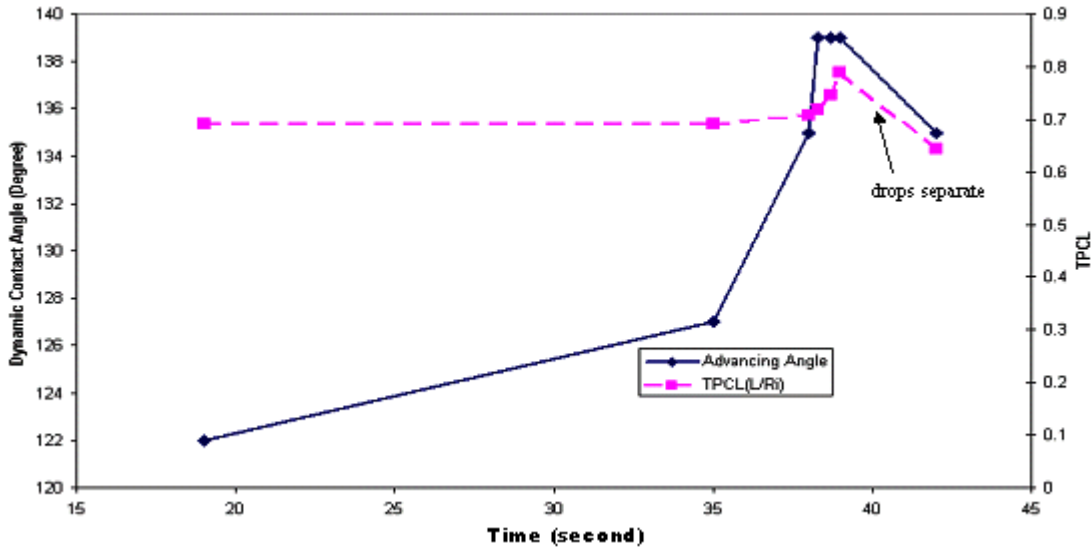


**Figure 38: DDDC Contact Angle Measurements and Three Phase Contact Line Movement in Yates Stocktank Oil/Brine/Dolomite System, 16 hours after 500 ppm Anionic Surfactant B Injection at Reservoir Conditions of 700 psi and 82 °F**

From the above discussion, it can be concluded that no significant wettability alterations were obtained with the surfactant A (nonionic) for Yates reservoir rock-fluids system at reservoir conditions at concentrations of 500 ppm, 1000 ppm and 3500 ppm. Wettability alterations from a strongly oil-wet to a weakly oil-wet state were obtained in Yates reservoir rock-fluids system with the surfactant B (anionic) at reservoir conditions at concentrations of 500 and 3500 ppm.

#### **4.3.2 Live oil at Reservoir Conditions**

Yates Live oil was recombined by adding lighter ends (methane to pentane) to Yates stocktank oil according the composition provided by Marathon Oil Company (Table 2).

Yates synthetic brine, dolomite and surfactants used here are the same as described in section 4.3.1.

##### **(A) Drop Behavior Before Surfactant Injection**

The interfacial tension measured between Yates synthetic brine and Yates live oil has been described in Section 4.1. The sessile drop receding angles measured initially on both



the upper and lower crystal surfaces were nearly the same, 25-28 degrees for all the experiments conducted. After 24 hours of aging, the equilibrium sessile drop receded angles were either almost unchanged or just increased slightly, but the drop contact diameters increased by about 5 %. Once the lower surface was turned, the oil drop completely floated away when the arm of the crystal holder was rotated about 30°. Then the lower crystal was turned fully upside down. The oil drop on the upper crystal was brought down to contact with the initial oil occupied area on the lower crystal. The lower crystal was shifted laterally to measure the dynamic advancing and receding angles. The advancing angle was about 55°-60° for all experiments conducted using Yates live oil/brine/dolomite system at reservoir conditions, showing a weakly water-wet nature of the reservoir. After several repeatable measurements of the advancing and receding angles, the lower crystal was shifted back to the original place where the oil drop was held between two previously oil-occupied areas of crystals before injecting the surfactant-containing brine into the cell.

#### (B) Drop Behavior During and After Surfactant Injection

As in the stocktank oil case, with the drop in the equilibrium position, surfactant-containing brine at a specified concentration was injected into the cell at reservoir conditions of temperature and pressure (700 psi and 82 °F).

At lower concentrations of nonionic surfactant A (500 ppm), the equilibrium drop between the upper and lower surface was not significantly affected during injection. The shape of the drop changed slightly due to IFT change. After injection, DDDC contact angle measurements were made. The contact angle was seemed to be decreased 1-3° (Figure 39).

At higher concentrations of surfactant A (1500 ppm, Figures 40 and 3500 ppm, Figure 41), the equilibrium drop between the two crystals moved and floated to the upper surface, thus increasing the volume of the upper drop and flattening it. The advancing dynamic angle was measured. During injection, the advancing angle caused by the invading surfactant increased by 17°-23°. The wettability was altered from weakly water-wet (55°) to intermediate-wet (85°). After injection, the advancing angle decreased to 40°-50°, even lower than the initial advancing angle of 55°. This behavior made the oil detach from the solid more easily during surfactant injection (a higher capillary number caused

by lower value of cosine of contact angle) and flowed more freely after injection (more strongly water-wet).

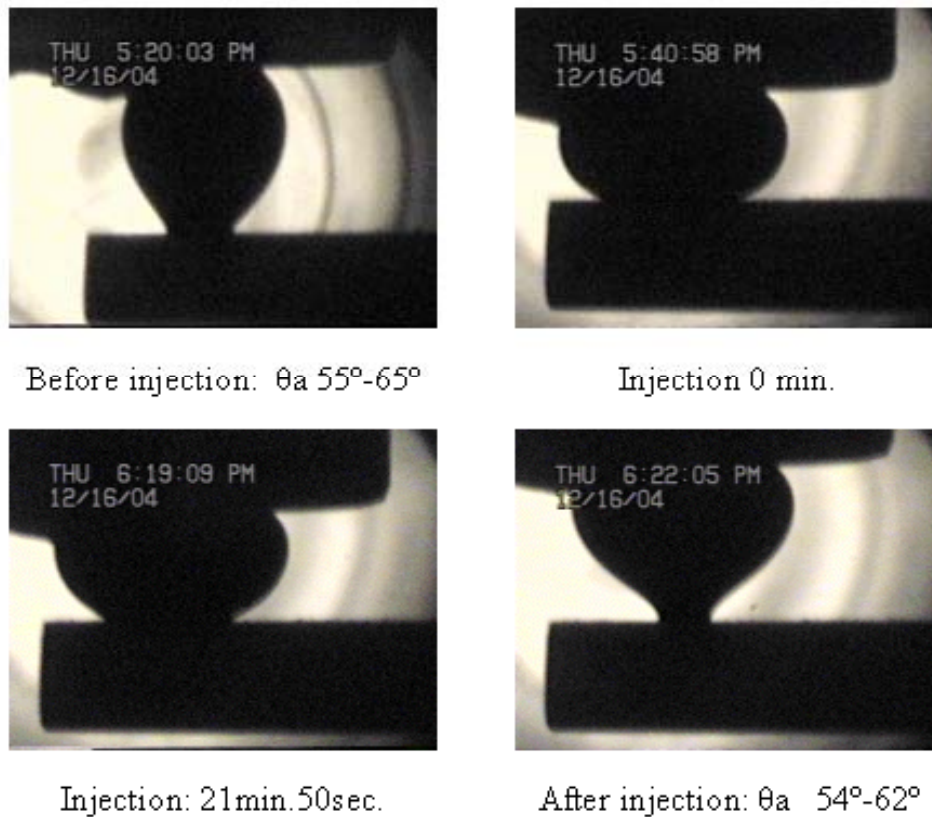


**Figure 39: Depiction of Drop Movement During Surfactant Injection (Nonionic Surfactant A at 500 ppm, 700 psi and 82 °F, Yates Live Oil/Brine/Dolomite)**

During the injection of anionic surfactant B, the equilibrium drop moved toward the upper crystal due to a lowering of the IFT at low concentration of 500 ppm. However, the significant wettability alteration (from water-wet to oil-wet) with a continuous increasing of advancing angle and TPCL movement was observed (Figure 42). The advancing angle increased from 58° to a value larger than 140° with time.

To further investigate this significant wettability alteration, a new experiment was conducted with a completely water-wet dolomite (without aging by oil drop). The oil drop on the upper crystal was brought down to contact with the completely water-wet lower crystal at 900 ppm surfactant B concentration at reservoir temperature and pressure. After aging one night, this advancing angle was measured by shifting the lower crystal. Even without the advantage of any buoyancy during the initial aging of the oil



drop, the lower crystal still became strongly oil-wet with a contact angle at larger than  $160^\circ$ , indicating significant wettability alteration by surfactant B (Figure 43).

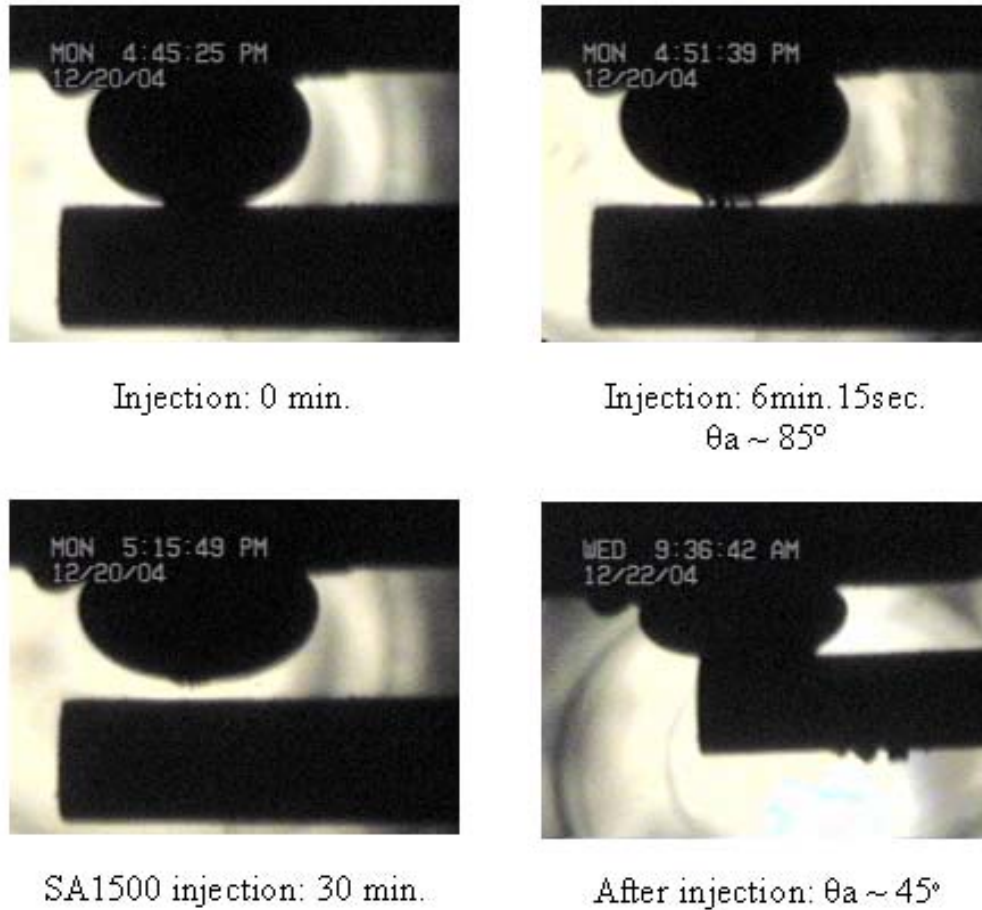


**Figure 40: Depiction of Drop Movement During Surfactant Injection (Nonionic Surfactant A at 1500 ppm, 700 psi and  $82^\circ\text{F}$ , Yates Live oil/Brine/Dolomite)**

For surfactant B injection at 1500 ppm, the same characteristics as observed at 500 ppm concentration, were seen (Figure 44) but with a slightly lower contact angle. The measured advancing angle during the injection was  $110^\circ - 120^\circ$ , and  $100^\circ$  after injection. A tiny residual drop was stuck on the lower surface after injection. At 3500 ppm surfactant B injection, the oil drop floated more quickly due to lower IFT. The advancing angle increased to  $140^\circ$  and then decreased to  $100^\circ$  during injection (Figure 45). This could be due to the rapid concentration change along the surface during injection.

For the weakly water-wet live oil system, the nonionic surfactant A slightly increased the contact angle to intermediate wet, while the anionic surfactant B altered the wettability to strongly oil-wet even at relatively low concentrations and weakly oil-wet at

higher surfactant concentrations. This surfactant induced wettability alteration has good potential to increase oil recovery as will be discussed later.

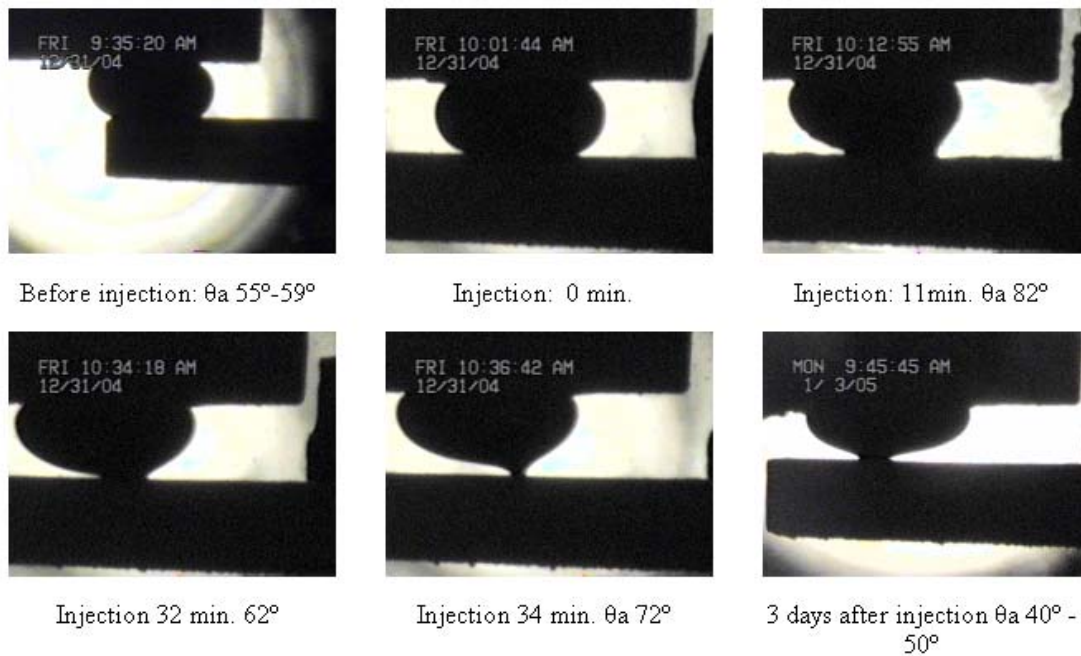


**Figure 41: Depiction of Drop Movement During Surfactant Injection (Nonionic Surfactant A at 3500 ppm, 700 psi and 82 °F, Yates Live oil/Brine/Dolomite)**

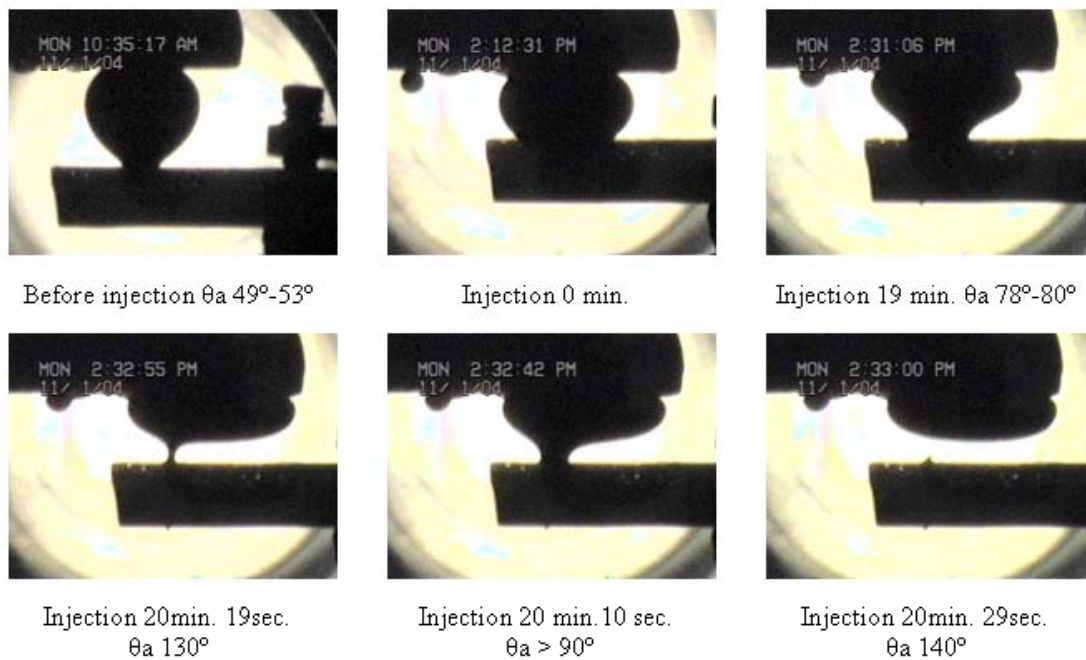
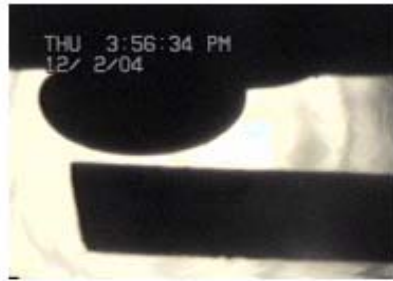
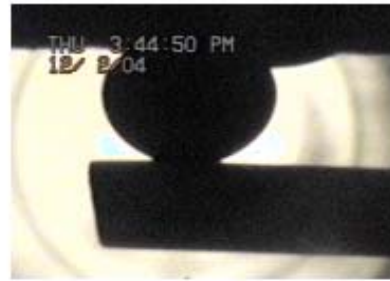


**Figure 42: Depiction of Drop Movement During Surfactant Injection (Anionic Surfactant B at 500 ppm, 700 psi and 82 °F, Yates Live oil/Brine/Dolomite)**



(a) SB900 solution, without aging, complete water-wet dolomite



(b) SB900 solution, oil drop was brought to contact with dolomite surface



(c) SB900 solution, aging overnight, DDDC  $\theta_a > 160^\circ$ , complete oil-wet



(d) SB900 solution, after shifting, residual oil left on dolomite surface

**Figure 43: Depiction of Dynamic Contact angle at Anionic Surfactant B Solution (900 ppm, 700 psi and 82 °F, Yates Live oil/Brine/Dolomite)**



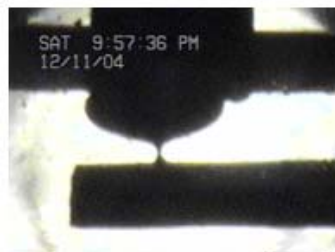
Injection: 0 min.



Injection: 4 min.10 sec.  
 $\theta_a 95^\circ\text{--}105^\circ$



Injection: 4 min.13 sec.  
 $\theta_a 110^\circ\text{--}115^\circ$



Injection: 4min.13sec.  
 $\theta_a 120^\circ$



Injection: 4 min. 14 sec.  
A small residual drop left on surface



1 day after injection, DDDC  $\theta_a=100^\circ$

**Figure 44: Depiction of Drop Movement During Surfactant Injection (Anionic Surfactant B at 1500 ppm, 700 psi and 82 °F, Yates Live oil/Brine/Dolomite)**

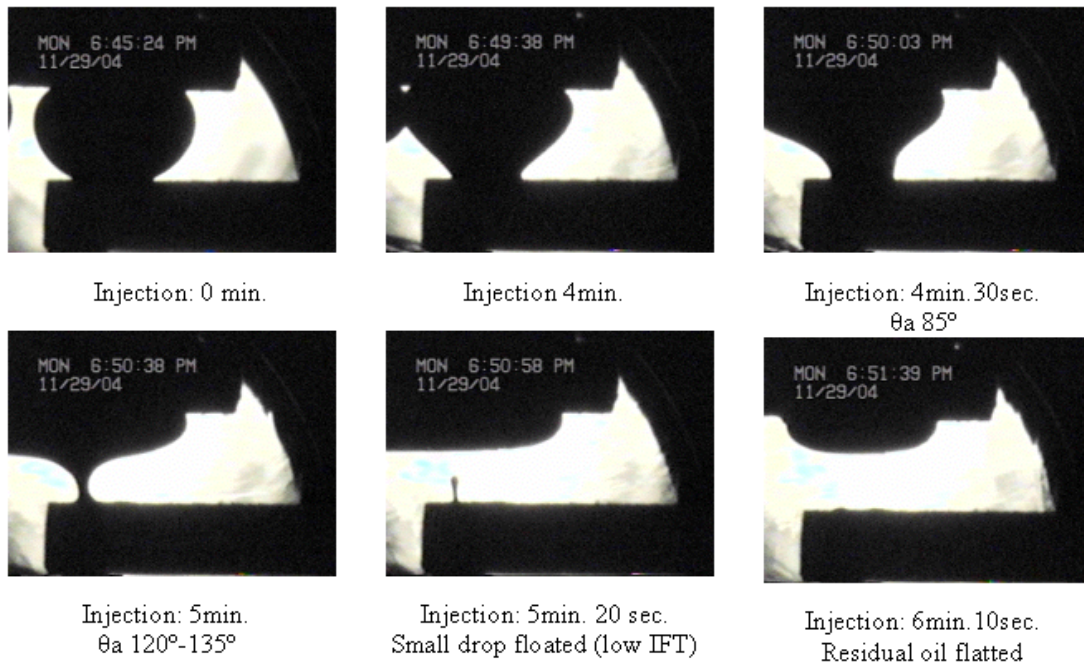


**Figure 45: Depiction of Drop Movement During Surfactant Injection (Anionic Surfactant B at 3500 ppm, 700 psi and 82 °F, Yates Live oil/Brine/Dolomite)**

The significant differences in wettability and wettability alteration mechanism between live oil and stocktank oil systems as observed in this study, clearly indicate that oil reservoir wettability experiments must be conducted at reservoir conditions using live crude oil. The experiments at ambient conditions using stocktank crude oil may lead to wrong characterization of reservoir wettability.

#### **4.3.3 Mechanism of Surfactant-induced Wettability Alteration**

A number of factors affect the interaction of surfactants with the solid surface of porous rock and consequently affect wettability. Some of the more obvious items include: surfactant structure, surfactant concentration, kinetics, pore surface composition, surfactant stability, electrolytes and pH, temperature, rock roughness and reservoir structure (Spinler and Baldwin, 2000).

- Anionic surfactant (Figure 46)

The anionic surfactant had more influence on wettability alteration compared with nonionic surfactant. Figure 46 shows that for strongly oil-wet Yates stocktank oil case, the addition of anionic surfactant altered the wettability to less strongly oil-wet, while for



the weakly water-wet Yates live oil case, the addition of anionic surfactant altered the wettability to strongly oil-wet at low concentrations and less oil-wet at high concentration.

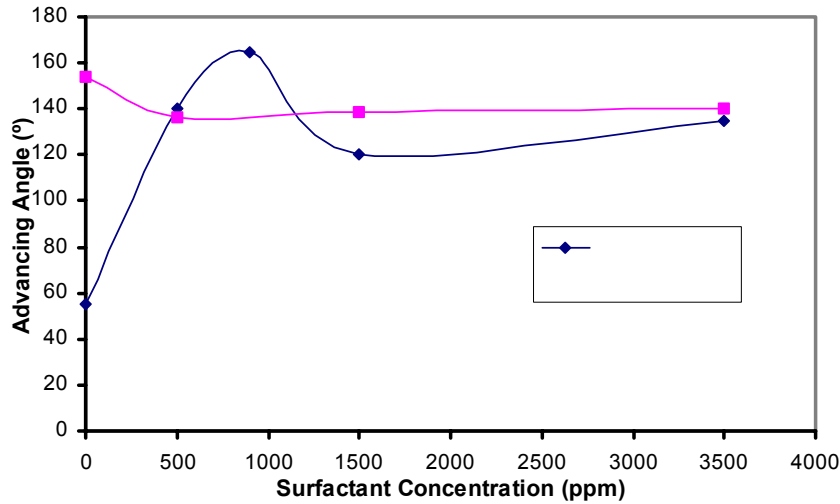


**Fig. 46: The Effect of Surfactant Concentrations on Water-Advancing Angles (Anionic Surfactant B, Yates Live oil/Brine/Dolomite System, 82°F & 700 psi)**

These phenomena can be well explained by the typical ionic surfactant adsorption isotherm. The model built by Somasundaran and Zhang (2004) was introduced here (Figure 48). This is a typical ionic surfactant adsorption isotherm for an oppositely charged substrate, which has been accepted and described by many researchers (Somasundaran and Fuerstenau, 1966; Spinler and Baldwin, 2000). Since the anionic surfactant is negatively charged and dolomite substrate used here is positively charged, they are oppositely charged hence this adsorption model can be well applied here.

In Region I, the surface was water-wet and in Region II it was oil-wet while in regions III and IV it began to become less oil-wet. The adsorption of surfactant on the rock surface between oil and rock caused this alteration. For the water-wet case (Yates live oil), the thin water film was replaced by surfactant-containing brine gradually. Region I corresponds to low surface coverage by individual surfactant molecules with an absence of surfactant aggregate, showed weakly water-wet behavior. In Region II, with the increase of surfactant concentration, the surfactant aggregates (called admicelles or hemimicelles) formed and produced the sharp increase in the slope of the isotherm. The hydrophilic head group adsorbed on the rock surface and the hydrophobic tail connected

with the oil drop. Oppositely charged behavior of surfactant and substrate made the random adsorption become well arranged. The system became strongly oil-wet. In region III, sufficient accumulation of aggregates resulted in the aggregates attracted each other and hydrophobic head of one surfactant molecular connected with the hydrophobic tail of the other. This caused the electrostatic repulsion of further surfactant molecules. A potential decrease of oil-wetting was observed in this region. Region IV begins at the CMC and is described as completion of bilayer coverage of the surface. The wettability should return to the initial status, which in this case, weakly water-wet. However, region IV has not been reached in our study.

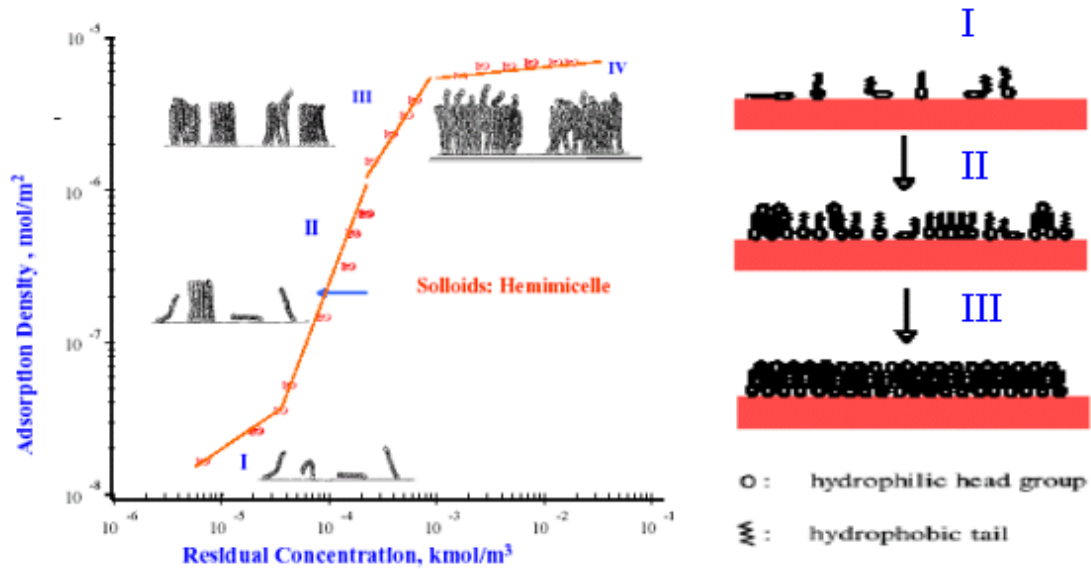


**Figure 47: Schematic Representation of the Growth of Aggregates for Various Regions of the Adsorption Isotherm (Somasundaran and Zhang, 2004)**

For oil-wet stocktank oil case, region I was absent since the surface was already covered by natural surfactant (asphaltenes, for example). It started from the region II directly. At low surfactant concentrations, it was strongly oil-wet. At higher concentrations, it became less oil-wet (region III). Above CMC, it should return to the initial oil-wet. Therefore, anionic surfactant may not be suitable in wettability alteration in strongly oil-wet cases.

- Nonionic surfactant (Figure 48)

For strongly oil-wet case (Yates stocktank), the nonionic surfactant has no effect or only slightly decreased the advancing angle by less than 10°. For weakly water-wet case

(Yates live oil), the nonionic surfactant altered the wettability to intermediate wet with an advancing angle in a range of 82° to 85°. The wettability alteration caused by nonionic surfactant was largely different with that of anionic surfactant (Figure 48).

The wettability alteration mechanism of nonionic surfactants is less understood than that of anionic surfactant. Nonionic surfactants are described as having Langmuir type adsorption isotherms on charged substrates with the surfactant lying prone on the surface and at higher concentrations with the hydrophobic group displaced from the surface (Rosen, 1978, Spinler and Baldwin, 2000). For concentrations at or above the CMC, either a monolayer or a bilayer may form. Although the model in Figure 47 may not be suitable for nonionic surfactant case, the same four regions are used here to represent the surfactant concentration. In region I, at very low nonionic surfactant concentration there is no wettability alteration. The surfactant molecules randomly adsorb on the surface. At higher concentrations (region II and III), it becomes more oil-wet. Above CMC, it may become strongly oil-wet (monolayer) or return to the initial wetting state (bilayer).

For the water-wet case (Yates live oil), it was water-wet at low concentrations (region I), and more oil-wet (intermediate wet) at region II and III. Region IV, above CMC, it should return to initial status of weakly water-wet. For the oil-wet case (Yates stocktank oil), it was oil-wet at the beginning. The further increase of surfactant concentration could not increase the oil-wet anymore. So the measured advancing angles almost have no change (145° to 154°) during surfactant injection (Figure 48).

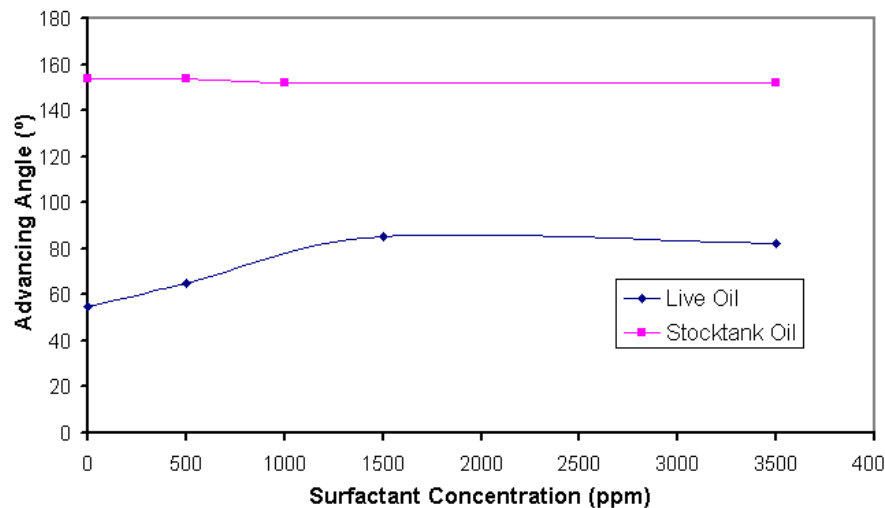


**Figure 48: The Effect of Surfactant Concentrations on Water-Advancing Angles (Nonionic Surfactant A, Yates Live oil/Brine/Dolomite System, 82°F & 700 psi)**

#### 4.4 Enhanced Oil Recovery

Wettability affects the distribution of fluids in the reservoir. Accurate measurement of wettability is important for any EOR process. The results of wettability experiments conducted using Yates oil/brine system at reservoir conditions helped us better understand the phenomena during core flooding and reservoir IOR procedures.

The differences of wettability between live oil and stocktank oil, reservoir conditions and ambient conditions, and nonionic and anionic surfactants gave us a full picture of wetting behavior of Yates oil reservoir. The results of these laboratory experiments were able to explain the oil recovery data obtained from the previous and ongoing core flooding experiments as well (Yates stocktank oil coreflooding results: Rao et al, 2004: Yates live oil coreflooding results: Adebola, ongoing thesis, 2005).

For Yates stocktank oil/brine/dolomite system at reservoir conditions, which has oil-wet characteristics as inferred from contact angle measurements, its oil recovery increased with nonionic surfactant A concentration but only by marginal increments of up to 6% OOIP. This can be attributed to the slight wettability alterations from the initially strongly oil-wet to that of less oil-wet due to the surfactant. Similar results are obtained with anionic surfactant B, where the wettability is altered from original oil-wet to strongly oil-wet at low surfactant concentrations and then to less oil-wet at high surfactant concentrations. The maximum oil recovery increment observed in corefloods with anionic surfactant B was also about 6% OOIP. These results indicate that the initial strongly oil-wet behavior of stocktank oil may not have been restored during the corefloods. Hence, the weakly oil-wet core became strongly oil-wet at low concentrations (500 ppm, region II of surfactant adsorption isotherm proposed by Somasundaran and Zhang, 2004) with reduced oil recovery, and then became less oil-wet at high concentrations (region III of surfactant adsorption isotherm proposed by Somasundaran and Zhang, 2004) with increased oil recovery.

For Yates Live oil/brine/dolomite system, which is weakly water-wet as indicated by contact angle measurements, the core-flooding results corroborated well with contact angle measurements. Contact angle measurements with nonionic surfactant A showed that the contact angles at 1500 ppm and 3500 ppm surfactant concentrations increased to intermediate-wet (about 80°-85°) from the original water-wet characteristics (about 55°).



The oil recoveries in corefloods at these surfactant concentrations also showed a significant increase. This behavior can be explained using the definition of capillary number. The cosine of contact angle decreases significantly as the contact angle becomes closer to  $90^\circ$  and hence the capillary number increases, which in turn resulted in significant oil recovery enhancements. However, for anionic surfactant B, the surfactant-induced wettability alterations observed could be again well explained using the adsorption isotherm model in Figure 47. The wettability is altered from initial weakly water-wet state to oil-wet at low concentrations (the contact angle increased to  $160^\circ$  at 900 ppm). The further increase of concentration lowered the strongly oil-wet contact angle to that of less oil-wet. These wettability alterations resulted in lower oil recoveries at all surfactant concentrations when compared to 0 ppm concentration in coreflooding experiments.

Although anionic surfactant B was more effective in altering wettability than nonionic surfactant A, it was less effective in oil recovery enhancement in Yates reservoir. The reason is that anionic surfactant appears to change the native weakly water-wet wettability to strongly oil-wet at low concentrations, and then to less oil-wet at higher concentrations. Contrarily, there is a possibility of increasing oil recovery with the anionic surfactant B if the native wettability state of the system is very strongly oil-wet.

However, the development of a special kind of heterogeneous wettability known as “mixed-wettability” due to these surfactants makes the anionic surfactant B the potential EOR choice. Salathiel (1973) first explained the phenomenon of mixed-wettability development in crude oil reservoirs. According to Salathiel, strongly oil-wet paths are generated in the reservoir at those parts of the pore surface in contact with crude oil, while the remainder stays strongly water-wet. The oil would flow continuously through these well-connected oil-wet paths resulting in very high oil recoveries. Sometimes, the strongly oil-wet characteristics rendered on the pore surface due to the surfactants may result in continuous oil-wet paths for mixed-wettability development. The corefloods conducted by Ayirala (2002) in Berea sandstones using Yates stocktank oil and synthetic brine substantiated the ability of these surfactants to develop mixed-wettability for significant oil recovery enhancements (94% OOIP).

The decrease of oil recovery observed in corefloods with anionic surfactant B and Yates fluids-dolomite system was due to wettability alterations to oil-wet at all surfactant concentrations used. The brine-oil interfacial tension measurements conducted with both the surfactants explained the effect of wettability alteration on oil recovery. The oil-water IFT observed with anionic surfactant B at all surfactant concentrations was much lower when compared to that at the same concentration of nonionic surfactant. However, more oil was recovered by the nonionic surfactant A in core flooding tests. This indicates that the favorable wettability alteration, beneficial to oil recovery, has occurred with the nonionic surfactant A. However, at field scale, it is sometimes possible to develop mixed wettability by anionic surfactant B. Wettability alteration due to surfactants can become a very effective EOR process if mixed-wettability is developed.

Now, this imposes an important question. Is it possible to develop mixed-wettability in Yates reservoir? Salathiel (1973) pointed out that the pore geometry and mineral composition of the rocks can affect the formation of continuous oil-wet paths and hence the oil recovery. He reported a 20-26% residual saturation limit below which oil saturation cannot be reduced for a limestone core and a calcite cemented sandstone core. He explained this by assuming the deposited oil-wet film to be less stable on carbonate surface than on silicate surface. It is a well-known fact that the carbonates are more heterogeneous and oil-wet in most cases. Irregular fractures, enlarged pores, vugs and cavities are difficult to be organized for the continuous oil phase flow. Hence, any attempt to alter the wettability of a carbonate reservoir into mixed-wet may result into a worse heterogeneous oil-wet case. Hence, for the carbonates, perfect mixed-wettability is much difficult to attain due to surfactant. However, although the anionic surfactant B altered the wettability of core-sized rock to strongly oil-wet, in field scale, certain volume of anionic surfactant B injection and the consequent partial wettability alteration may result in mixed-wettability. Thus, by careful selection of surfactant and its concentration, it is possible to develop mixed-wettability in a fractured carbonate reservoir like Yates for significant oil recovery enhancements.

Wrong information on original reservoir wettability can lead to poor decisions for improved oil recovery field applications using surfactants. This can be well understood with the explanation provided here. If a water-wet reservoir was misunderstood as oil-

wet, the flooding of anionic surfactant at low concentrations may render strongly oil-wet characteristics and hence can significantly reduce the oil recovery. Hence, an accurate in-situ reservoir wettability characterization is essential for success of any improved oil recovery process in the field.

## CHAPTER 5. CONCLUSIONS AND RECOMMENDATIONS

### 5.1 Summary and Conclusions

High-Temperature and High-Pressure Optical cell as well as an ambient cell were used to measure dynamic interfacial tension and dynamic contact angles at reservoir and ambient conditions using the computerized drop shape analysis method and dual-drop-dual-crystal techniques. We were able to evaluate the effects of temperature and pressure, oil components especially light ends, brine composition, rock characteristics and the addition of surfactants on interfacial properties.

The main findings of this study are:

1. The interfacial tension between crude oil and brine has time-dependent behavior even after prior mixing. This is caused by the polar components such as asphaltenes in the oil. A four-staged model has been adapted to describe this behavior using induction stage, diffusion-control stage, kinetic barrier-control stage and equilibrium stage.
2. The interfacial tension is largely influenced by the oil and brine compositions. Live oil has higher and stable IFT than that of stocktank oil. Dilution of brine caused an increase in live oil/brine IFT. The IFTs of Yates live and stocktank oil increased with pressure and decreased with temperature.
3. Time-dependent behavior of IFT of Yates live oil in diluted surfactant A and B solution are different. Surfactant B first caused an increase and then a decrease in IFT with time, while surfactant A caused continues decline of IFT. Both surfactants were able to lower the IFT of Yates live oil by two orders of magnitude.
4. High degree of smoothness of rock substrates is required for contact angle measurements. Different rock or minerals have different charge behavior in brine. The spreading of oil on rock surfaces is related to mineral type as well as brine composition. Multivalent cations tend to increase oil-wet behavior while monovalent cations tend to increase the water-wet behavior for Yates oil-dolomite system.
5. Below bubble point pressure, depressurization caused the release of light ends from crude oil and hence increased oil-wet behavior. Above the bubble point pressure,

increase of pressure tended to increase the live oil contact angle and change the water-wet behavior to intermediate wet.

6. The Yates live oil-Yates brine-Yates dolomite system is weakly water-wet ( $\theta_a = 55^\circ$ ) at reservoir conditions, while Yates stocktank oil-Yates brine-Yates dolomite system is oil-wet ( $\theta_a = 154^\circ$ ) at reservoir and ambient conditions. The difference is caused by the dilution and change of polar component characteristics in the crude oil due to the addition of gaseous light ends.
7. For the oil-wet Yates stocktank oil – Yates brine- dolomite system at reservoir conditions, the injection of a nonionic surfactant (ethoxy alcohol) at different concentrations had no significant influence on wettability, while the injection of an anionic surfactant (ethoxy sulfate) decreased the contact angle from  $154^\circ$  to  $135^\circ$ .
8. For the water-wet Yates live oil –Yates brine – dolomite system at reservoir conditions, the injection of the nonionic surfactant increased the contact angle from  $55^\circ$  to  $85^\circ$ , while the injection of anionic surfactant increased the contact angle from  $55^\circ$  to more than  $160^\circ$ .
9. The wettability alteration caused by surfactants indicates the ability of these surfactants to develop intermediate wettability by the nonionic surfactant or mixed-wettability by the anionic surfactant in field scale. Both these surfactant-induced wettability alteration can result in significant oil recovery enhancements. The adsorption of surfactant and its concentration on rock surfaces are the key factors that control wettability.

## **5.2 Recommendations for Future Work**

1. The correlation of receding angle and oil spreading need further studied since the rapid spreading is important in building a continuous oil paths needed in the development of mixed-wettability.
2. Determine the Zisman-type spreading and critical spreading tension for different reservoir mineralogies for a priori determination of spreading of wettability characteristics.
3. Simulate the development of mixed-wettability in field scale by anionic surfactant flooding (resulting oil-wet in lab) using reservoir simulators.

4. Other types of surfactants need to be used in future for further experiments to find out the most effective surfactant for favorable wettability alteration.
5. Stability of thin wetting films is an integral part of any wettability alteration process. Further experimental work at actual reservoir conditions and attempts to correlate these results with the theory of wetting films would be of immense help in furthering on understanding of reservoir wettability.

## REFERENCES

1. [http://www.ksvinc.com/surface\\_tension1.htm](http://www.ksvinc.com/surface_tension1.htm).
2. [http://www.ksvinc.com/contact\\_angle.htm](http://www.ksvinc.com/contact_angle.htm).
3. [http://www.ksvinc.com/contact\\_angle.htm](http://www.ksvinc.com/contact_angle.htm).
4. [http://www.ksvinc.com/powder\\_wetting.htm](http://www.ksvinc.com/powder_wetting.htm).
5. [http://www.engr.pitt.edu/chemical/undergrad/lab\\_manuals/optimal\\_salinity.pdf](http://www.engr.pitt.edu/chemical/undergrad/lab_manuals/optimal_salinity.pdf).
6. Adebola, A.A., Thesis Proposal, Department of Petroleum Engineering, Louisiana State University, 2004
7. Al-Hadhrami, H.S.; Blunt, M.J. "Thermally Induced Wettability Alteration to Improve Oil Recovery in Fractured Reservoirs, SPE 71866, SPE Reservoir Evaluation and Engineering, June 2001.
8. Al-Maamari, R.S.H. and Buckley, J.S., "Asphaltene Precipitation and Alteration of Wetting: The Potential for Wettability Changes During Oil Production", SPE 84938, SPE Reservoir Evaluation & Engineering, August 2003.
9. Akkurt, R.; Merkel, R.H.; Coates, G. R.; Stever, R. C. "Remaining Oil Saturation from NMR in a Mixed-Wet, Three-Phase Carbonate Reservoir", SPE 63216, SPE ATCE (2000).
10. Anderson, W.G., "Wettability literature survey-part 1: Rock/Oil/Brine Interactions and the Effects of Core Handling on Wettability", SPE 13932, JPT, October 1986.
11. Anderson, W.G., "Wettability literature survey-part 2: Wettability Measurement", SPE 13933, JPT, November 1986.
12. Anderson, W.G., "Wettability literature survey-part 5: the Effect of Wettability on Relative Permeability", JPT (Nov. 1987) 1453-1465.
13. Ayirala, S.C., "Surfactant-induced Relative Permeability Modifications for Oil Recovery Enhancement", Master's Thesis, Louisiana State University, December 2002.
14. Ayirala, S.C., Vijapurapu, C.S. and Rao, D.N.: "Beneficial Effects of Wettability Altering Surfactants in Oil-Wet Fractured Reservoirs," Paper Presented at the Proceedings of 8<sup>th</sup> International Symposium on Evaluation of Reservoir Wettability and its Effect on Oil Recovery, Houston, TX (2004).

15. Babadagli, T., "Analysis of Oil Recovery by Spontaneous Imbibition of Surfactant Solution", SPE 84866, SPE International IOR Conference, 2003.
16. Bagci, S.; Kok, M.V., "Effect of Brine Composition and Alkaline Fluid on the Permeability Damage of Limestone Reservoirs", SPE 65394, SPE International Symposium on Oilfield Chemistry, Houston, Texas, 2001
17. Basu, S. and Sharma, M.M. "Investigating the Role of Crude-Oil Components on Wettability Alteration Using Atomic Force Microscopy", SPE 57466, SPE Journal 4 ~3!, September 1999
18. Blunt, M.J., "Effects of Heterogeneity and Wetting on Relative Permeability Using Pore Level Modeling", SPE 36762, SPE Journal, Volume 2, March 1997.
19. Brown, J.B. and Radke. C. J.: "Area Effects in Spinning-drop Dynamic Interfacial Tensions", Chem. Eng. Sci. (1980) 35.1458, 1460.
20. Buckley, J.S., Liu, Y., Xie, X., Morrow, N.R., "Asphaltenes and Crude Oil Wetting - The Effect of Oil Composition", SPE 35366, SPE Journal, Vol 2, Number 2, June, 1997.
21. Busoni, L. "An axisymmetric drop shape apparatus for the study of insoluble films", PhD thesis, UNIVERSIT` DEGLI STUDI DI FIRENZE, April 2003.
22. Campanella, J.D.; Wadleigh, E.E.; Gilman, J.R. "Flow Characterization – Critical for Efficiency of Field Operations and IOR", SPE 58996, 2000 SPE IPCE, Mexico.
23. Campanelli, J.R. and Wang, X. "Dynamic Interfacial Tension of Surfactant Mixtures at Liquid-Liquid Interfaces", Journal of Colloid and Interface Science 213, 340-351 (1999).
24. Chen, H.L.; Lucas, L.R.; Nogaret, L.A.D.; Yang, H.D.; Kenyon, D.E. "Laboratory Monitoring of Surfactant Imbibition with Computerized Tomography", SPE 69197, SPE Reservoir Evaluation & Engineering, Feb. 2001.
25. Cheng, P.; Li, D.; Boruvka, L.; Rotenberg, Y. and Neumann, A. W., "Automation of Axisymmetric Drop Shape Analysis for Measurements of Interfacial Tensions and Contact Angles", Colloids and Surfaces, 43 (1990) 151 –167.
26. Christiansen, R. L.: "Gas Flooding Experiments for the East Side of the Yates Field Unit," SPE 16986, SPE Res. Eng., 5 (No. 1) (February 1990) 14-18.
27. Cooke Jr., C.E., Williams, R.E., Kolodzie, P.A., "Oil Recovery by Alkaline Waterflooding", SPE 4739, JPT, 1365-1374, December 1974.



28. Diamant, H.; Andelman, D. "Kinetics of Surfactant Adsorption at Fluid/Fluid Interfaces: Non-ionic Surfactants", *Europhysics Letters*, 34(8), pp. 575-580(1996).
29. Diamant, H.; Andelman, D. "Adsorption kinetics of surfactants at fluid-fluid interfaces", *Progress in Colloid and Polymer Science* 103, 51 (1997)
30. Diamant, H., Ariel, G. and Andelman, D., "Kinetics of surfactant adsorption: the free energy approach (review article)", *Colloids and Surfaces A* 183-185, 259 (2001)
31. Drelich, J. and Miller, J.D. "Surface and Interfacial Tension of the Whiterocks Bitumen and Its Relationship to Bitumen Release from Tar Sands During Hot Water Preprocessing", *Fuel*, 1994, V. 73, N. 9, pp. 1504-1507.
32. Drelich, J., Fang, Ch., White, C.L., "Measurement of Interfacial Tension in Fluid-Fluid Systems", *Encyclopedia of Surface and Colloid Science*, Marcel Dekker, Inc. 2002, P3152-3166.
33. Dukhin, S.S.; Kretzschmar, G.; Miller, R. *Dynamics of Adsorption at Liquid Interfaces: Theory, Experiment, Application*; Elsevier, Amsterdam, 1995.
34. England, D.C. and Berg, J.C., "Transfer of Surface-active Agents Across a Liquid-Liquid Interface", *AIChE J.* 312-22, March 1971.
35. Evans, G.M., Habgood, M.G. and Galvin, K.P., "A description of Dynamic Interfacial Tension", 9<sup>th</sup> APCCChE, 2002.
36. Freedman, R.; Heaton, N.; Flaum, M.; Hirasaki, G.L.; Flaum, C.; Hurlimann, M. "Wettability, Saturation, and Viscosity From NMR Measurements", SPE 87340, *SPE Journal*, December 2003.
37. Freer, E.M. and Radke, C.J., "Relaxation of Asphaltenes at the Toluene/Water Interface: Diffusion Exchange and Surface Rearrangement", *J. of Adhesion*, 80:481-496, 2004.
38. Gao, T., and M. J. Rosen. 1994. "Dynamic surface tension of aqueous surfactant solutions". *J. Am. Oil Chem. Soc.* 71:771-776.
39. He, Y.; Howes, T.; Litster, J. D., "Dynamic Interfacial Tension of Aqueous Solutions of PVAAAs and its Role in Liquid-Liquid Dispersion Stabilisation", 9<sup>th</sup> APCCChE, 2002.
40. Hiemenz, P.C.; Rajagopalan, R. "*Principles of Colloid and Surface Chemistry*", 3<sup>rd</sup> edition, Dekker, New York, 1997.
41. Hirasaki, G.; Zhang, D.L. "Surface Chemistry of Oil Recovery From Fractured, Oil-Wet, Carbonate Formations", SPE 88365, *SPE Journal*, June 2004.

42. Hjelmeland, O.S.; Larrondo, L.E. "Experimental Investigation of the Effects of Temperature, Pressure, and Crude Oil Composition on Interfacial Properties", SPE 12124, SPE Reservoir Engineering, July 1986.
43. Hocott, C.R., "Interfacial Tension between Water and Oil under Reservoir Conditions", Petroleum Technology, November 1938.
44. Hough, E.W., Rzasa, M.J. and Wood, B.B., "Interfacial Tensions at Reservoir Pressure and Temperatures: Apparatus and the Water-Methane System", Petroleum Transactions, AIME, Vol.192, 1951.
45. Hua, X.Y.; Rosen, M.J. "Dynamic Surface Tension of Aqueous Surfactant Solutions: 1. Basic Parameters", Journal of Colloid and Interface Science 1988, 124, 652-659.
46. Hua, X.Y.; Rosen, M.J. "Dynamic Surface Tension of Aqueous Surfactant Solutions: 3. Some Effects of Molecular Structure and Environment", Journal of Colloid and Interface Science 1991, 141, 180-190.
47. Hunsel, V. J., Joos P., "Study of the dynamic interfacial tension at the oil/water interface", Colloid Polym. Sci., 267, 1026–1035. 1989
48. Jennings, H. J., "The effect of temperature and pressure on the interfacial tension of benzene-water and normal decane-water", J. Colloid Interf. Sci., 24 (1967) 323–329.
49. Jennings, H.J., Johnson, C.E., McAuliffe, C.D., "A Caustic Waterflooding Process for Heavy Oils", SPE 4741, JPT, December 1974.
50. Kaminsky, R. and Radke, C.J., "Asphaltenes, Water Films, and Wettability Reversal", SPE 39087, SPE Journal, Volume 2, December 1997.
51. Klins, M.A., "Carbon Dioxide Flooding – Basic Mechanisms and Project Design", International Human Resources Development Corporation, Boston, 1984.
52. Kokal, S.; Al-Dokhi, M.; Al-Zubail, M.; Al-Saeed, S., "Asphaltene Precipitation in a Saturated Gas-cap Reservoir", 2004 SPE ATCE, SPE 89967.
53. Kumar, K.; Dao, E.K.; Mohanty, K.K., "Atomic Force Microscopy Study of Wettability Alteration", SPE 93009, SPE 2005 International Symposium on Oil Field Chemistry. Feb., 2005
54. Lakatos, I.; Bauer, K. et al. "Injection of Lean Gases into Light Oil Reservoirs: Interfacial Aspects". SPE 56605, SPE ATCE 1999.

55. Lankveld, J. M. G.; Lyklema, J. L. "Adsorption of Polyvinyl Alcohol on the paraffin-Water Interface", *Colloid Interface Sci.* 1972, 41, No.3, 475-483, December 1972.
56. Li, J.; Wang, W.; Gu, Y.; "Dynamic Interfacial Tension Phenomenon and Wettability Alteration of Crude Oil-Rock-Alkaline-Surfactant Solution Systems", SPE 90207, SPE ATCE 2004.
57. Lucassen J., van den Tempel M., "Dynamic measurements of dilational properties of a liquid interface", *Chem. Eng. Sci.*, 271 (1972) 1283.
58. Monroy, F.; Ortega, F.; Rubio, R.G., "Rheology of a Miscible Polymer Blend at the Air-Water Interface. Quasi-Elastic Surface Light Scattering Study and Analysis in Terms of Static and Dynamic Scaling Laws", *J. Phys. Chem. B* 103(12), 2061-2071 (1999).
59. Morrow, N.R. "Wettability and Its Effect on Oil Recovery", SPE 21621, JPT, December 1990.
60. Morrow, N.R., "physics and Thermodynamics of Capillary Action in Porous Media", *Ind. Eng. Chem* (June 1970) 62, No.6, 32-56)
61. Mungan, N., "Relative Permeability Measurements Using Reservoir Fluids", SPE 3427, SPE Journal, October 1972.
62. Rao, D.N, Vijapurapu, C., Abe, A., Ayirala, S., Busireddy, C., Kulkarni, M., Sequeira, D., Sharma, A., Xu, W., "Enhancement of Oil Recovery by Reservoir Wettability Alteration", Fourth Year Progress Report, June 2004.
63. Rao, D. N. "The Concept, Characterization, Concerns and Consequences of Contact Angles in Solid-Liquid-Liquid Systems", *Contact angle, Wettability and Adhesion*, Vol. 3, pp. 191 –210 (2003).
64. Rao, D.N., "Measurements of Dynamic Contact Angles in Solid-Liquid-Liquid Systems at Elevated Pressures and Temperatures", *Colloids and Surfaces A*, 206 (2002) 203-216.
65. Rao, D. N., Girard, M. G. "A New Technique for Reservoir Wettability Characterization", *JCPT*, Jan 1996, V. 35, No1.
66. Reisberg, J., and Doscher, T. M.: "Interracial phenomena in Crude-Oil-Water Systems," *Prod. Monthly* (1956) 21,43.
67. Rosen, M.L., "Surfactants and Interfacial Phenomena", A Wiley-Interscience publication, 1978.

68. Rubin, E. and Radke, C. J. , “Dynamic Interfacial Tension Minima in Finite Systems”, Chem. Eng. Sci. ( 1980) 35.1129-38.
69. Rusanov, A.I; Prokhorov, V.A. *Interfacial Tensiometry*, Elsevier, Amsterdam, 1996.
70. Salathiel, R.A., “Oil Recovery by Surface Film Drainage in Mixed-wettability Rocks”, SPE 4104, JPT, October 1973.
71. Seethepalli, A.; Adibhatla, B.; Mohanty, K.K. “Wettability Alteration During Surfactant Flooding of Carbonate Reservoirs”, SPE 89423, SPE/DOE 14<sup>th</sup> Symposium on IOR, 2004.
72. Schramm, L.L. “*Surfactants: fundamentals and applications in the petroleum industry*”, New York, Cambridge University Press, 2000.
73. Sharma and Filoco, “Effect of Brine Salinity and Crude-Oil Properties on Oil Recovery and Residual Saturations”, SPE 65402, Volume 5, Number 3, September 2000.
74. Sharma, M.M and Filoco, P.R. “Effect of Brine Salinity and Crude-Oil Properties on Oil Recovery and Residual Saturations”, SPE 65402 SPE Journal 5 (3), September 2000.
75. Spinler, E.A.; Baldwin, B.A., “Surfactant Induced Wettability Alteration in Porous Media”, *Surfactants: Fundamentals and Applications in the Petroleum Industry* by Schramm, L.L., p176-179, Cambridge, 2000.
76. Somasundaran, P.; Zhang, L. “Adsorption of Surfactants on Minerals for Wettability Control in Improved Oil Recovery Processes”, 2004.
77. Tang, G. Q. ; and Morrow, N.R. “Oil Recovery by Waterflooding and Imbibition – Invading Brine Cation Valency and Salinity”, SCA 9911
78. Taylor, K.C. and Nasr-El-Din, H.A., “The Effect of Synthetic Surfactants on the Interfacial Behaviour of Crude Oil/Alkali/Polymer Systems”, Colloids and Surfaces: A, 108(1996) 49-72.
79. Touhami, Y., V. Hornof and G.H. Neale. “Dynamic interfacial tension behavior of acidified oil/surfactant-enhanced alkaline systems: Part 2. Theoretical studies”. Coll. and Surf. A - Physicochem. & Eng. Aspects, 133, 211-231 (1998).
80. Trujillo, E.M., “The Static and Dynamic Interfacial Tensions Between Crude Oils and Caustic Solutions”, SPE 10917. SPE Journal, Aug. 1983.
81. Vijapurapu, C.S. “The Effect of Rock and Fluids Characteristics on Reservoir Wettability”, Master’s Thesis, Louisiana State University, December 2002.

82. Wang, W., Gupta, A., "Investigation of the Effect of Temperature and Pressure on Wettability Using Modified Pendant Drop Method", SPE 30544, ATCE, 1995.
83. Wang, J.X., Buckley, J.S., Creek, J.L., "A Practical Method for Anticipating Asphaltene Problems", SPE 87638, SPE Production & Facilities, Volume 19, Number 3, August, 2004
84. Ward, A. F. H., and Tordai, L., " Time-dependence of boundary tensions of solutions. I. The role of diffusion in time-effects", J. Chem. Phys. 14:453-461, 1946.
85. Webb, K.J. ; Black C.J.J "Resolving Wettability in a Giant Carbonate Reservoir", SPE 36257, 7<sup>th</sup> ADIPEC, UAE, 1996.
86. Xie, X., Weiss, W.W., Tong, Z. and Morrow, N.R., "Improved Oil Recovery from Carbonate Reservoirs by Chemical Stimulation", SPE 89424, SPE/DOE Symposium on Improved Oil Recovery, 2004.
87. Yang, D.Y.; Tontiwachwuthikul, P. and Gu, Y.G. "Interfacial Interactions between Reservoir Brine and CO<sub>2</sub> at High Pressures and Elevated Temperatures", Energy & Fuels 2005, 19, 216-223.
88. Zekri, A.Y.; Ghannam, M.T.; Almehaideb, R.A. "Carbonate Rocks Wettability Changes Induced by Microbial Solution", SPE 80527, SPE 2003 Asia Pacific Oil and Gas Conference, April 2003.
89. Zhang, P. and Austad, T. "The Relative Effects of Acid Number and Temperature on Chalk Wettability", SPE 92999, SPE 2005 International Symposium on Oil Field Chemistry. Feb., 2005
90. Ziegler, V.M. ""Laboratory Investigation of High-Temperature Surfactant Flooding", SPE 13071, SPE Reservoir Engineering, May 1988.

## **VITA**

Wei Xu, son of Chenggong Xu and Deju Zhou, was born in Dangyang, Hubei, China, on March 4, 1973. He obtained a bachelor's degree in petroleum geology in 1993, and a master's degree in oilfield geology and exploration in 1996, both from University of Petroleum, China. He then worked as an instructor and research geologist at the University of Petroleum of China until 2002. In June 2003, he enrolled the Graduate School of Louisiana State University, Baton Rouge, Louisiana, USA, in the Department of Petroleum Engineering. The degree of Master of Science in Petroleum Engineering will be conferred in May 2005.